University of Southampton

Rat liver fatty acid binding protein structure and function: The targeting of FABP-bound ligands to anionic interfaces

Joanna Kay Davies, BSc. (Hons.)

A thesis submitted for the degree of Doctor of Philosophy

Division of Biochemistry and Molecular Biology

September 2001

UNIVERSITY OF SOUTHAMPTON

ABSTRACT

FACULTY OF SCIENCE
DIVISION OF BIOCHEMISTRY AND MOLECULAR BIOLOGY

Doctor of Philosophy

Rat Liver Fatty Acid Binding Protein Structure and Function – The Targeting of FABP-bound Ligands to Anionic Interfaces

By Joanna Kay Davies

Liver fatty acid binding protein (LFABP) belongs to a family of small (14kDa) intracellular lipid-binding proteins, which have a characteristic β-barrel structure. The physiological role of FABP's within the cell remains unclear but a targeting role for the protein would provide an attractive mechanism for ligand (fatty acid) transfer to membrane sites for further metabolism and requires an interaction between the FABP and the membrane. In preliminary studies it was shown that LFABP released the fluorescent fatty acid 11-(5-dimethylaminonapthalenesulphonylamino) undecanoic acid (DAUDA) in the presence of anionic phospholipid vesicles under conditions that indicated a direct interaction between the LFABP and the anionic phospholipid interface. This interaction was investigated in more detail in order to identify the parameters that affect binding and ligand release.

The ligand release that was observed with anionic vesicles was sensitive to the ionic strength of the assay conditions and the anionic charge density of the phospholipid at the interface, indicating that non-specific electrostatic interactions play an important role in the process. The stoichiometric relationship between anionic phospholipid and LFABP suggests that the LFABP coats the surface of the phospholipid vesicle. The most likely explanation for ligand release is that interaction of LFABP with an anionic membrane interface induces a rapid conformational change, reducing the affinity of DAUDA for the protein. The nature of this interaction involves both electrostatic and non-polar interactions as maximal release of LFABP from phospholipid vesicles with recovery of ligand binding cannot be achieved with high salt and requires the presence of a non-anionic detergent.

Lysine residues in the α-helical region of adipocyte and heart FABP had previously been identified as important for interactions between these proteins and the phospholipid interface. Therefore, the charge reversal mutants, K20E, K31E and K33E of the α-helical regions of LFABP were produced and investigated. The results of these studies suggested that α-helix II, in particular, residue K31 of LFABP are involved in interactions with the anionic phospholipid interface. In contrast, two other charge reversal mutants, K125E and R126E, did not affect the binding of LFABP to anionic vesicles. The stability and ligand-binding characteristics of all charge reversal mutants was also studied.

For the interaction of LFABP with phospholipid vesicles to result in ligand release from the protein there must be a considerable conformational change. In order to investigate this change the F3W, F18W and C69W tryptophan mutants of LFABP were produced. A significant conformational change was detected at position 3, but not position 18 or 69, that paralleled DAUDA release from LFABP upon interaction with anionic phospholipid vesicles. Fluorescence resonance energy transfer studies established that position 3 came in close proximity to the anionic phospholipid interface.

For my wonderful husband,

John

Acknowledgements

I would like to thank Dr David Wilton for providing the opportunity to work on this project and for his continual encouragement, patience, guidance and support in his supervisory role. I am also grateful to the Heads of Biochemistry and Molecular Biology, Prof. Anthony Lee and subsequently Dr David Wilton, for providing laboratory space. A School of Biological Sciences studentship is also gratefully acknowledged.

Thanks also have to go to the members of the DCW laboratory over the past four years, Isabel Lobo, Steve Beers, Rob Hagan, Alisan Foyle, Jane Gibbs and, most importantly, Andy Buckland for seeing me through the duration and Susie Edwards for being the best PhD lab-mate. Loads of thanks also have to go to Mel Logan-Smith, Aisling O'Keeffe and Sue Twine for their alcohol-based support, I think the world has just about been set to rights over the last few years, what a team!

Special thanks go to my Mum and Dad and to Jenny and Paul for their constant support throughout my studies.

Now to the man that is my rock, my husband John, without whom this thesis would never have been finished. I cannot thank him enough for his unwavering support, encouragement, patience and love even though he's played second fiddle to the computer for the last year. Thank you.

Contents

Figures

Tables

Abbreviations

LFABP	-Recombinant rat liver fatty acid binding protein
HFABP	-Heart (muscle) FABP
IFABP	-Intestinal FABP
AFABP	-Adipocyte FABP
WT	LFABP wild-type
DAUDA	-11-(5-dimethylaminonapthalenesulphonylamino) undecanoic acid
DOPG	-(Dioleoyl)-phosphatidylglycerol
DOPC	-(Dioleoyl)-phosphatidylcholine
DOPE	-(Dioleoyl)-phosphatidylethanolamine
DOPS	-(Dioleoyl)-phosphatidylserine
DOPA	-(Dioleoyl)-phosphatidic acid
CL	-Cardiolipin
PI	-Phosphatidylinositol
Dansyl DHPE	-Dansyl-dihexadecyl-phosphatidylethanolamine
E.coli	*-Escherichia coli*
FRET	-Fluorescence resonance energy transfer
LB	-Luria Bertani medium
SUV	-Small unilamellar vesicle
MLV	-Multi-lamellar vesicle
NBD-PE	-N-(7-nitro2,1,3-benzoxadiazol-4-yl)-phosphatidylethanolamine
AOFA	-Anthroyloxy-labelled fatty acids
Hepes	-(N-[2-Hydroxyethyl]piperazine-N'-[2-ethanesulfonic acid]

EGTA	Ethyleneglycol-bis(β-aminoethyl ether)-N,N,N',N'-tetraacetic acid
Oleoyl CoA	-Oleoyl Coenzyme A
LPA	-Lysophosphatidic acid
ER	-Endoplasmic reticulum
PPAR	-Peroxisome proliferator activated receptor

Standard one and three letter codes for amino acids are used

Chapter One:

Introduction

1.1. Fatty acids and Phospholipids

1.1.1. Fatty Acids

Fatty acids are physiologically important molecules that are major components of phospholipids and glycolipids. The primary role of fatty acids is as a major fuel molecule. However, fatty acids also play minor but important roles as the precursors of signalling molecules while, in addition, many membrane associated proteins are acylated. Cells take up long chain free fatty acids *in vivo* from the non-protein bound ligand pools in extracellular fluid and plasma [1] where the physiological concentration of unbound free fatty acids is <1μM. In addition, fatty acids are synthesised in the cell in response to various stimuli including, for example, high levels of carbohydrate and low levels of fatty acids or a high concentration of citrate within the cell. Intermediates in the synthesis are linked to acyl carrier protein throughout the process of fatty acid chain elongation. The acetyl CoA required for fatty acid synthesis is obtained from mitochondria with citrate acting as a carrier for acetyl CoA from the mitochondrial inner membrane to the cytosol.

Fatty acids are stored in the form of triacylglycerols primarily in adipose cells, these triacylglycerols are then hydrolysed by adipose cell lipase to release the fatty acids in response to various stimuli. Hormones such as adrenalin and glucagon regulate the enzyme and as a result this enzyme is also known as hormone sensitive lipase.

Fatty acid degradation occurs in the mitochondrial matrix via the β-oxidation pathway. Fatty acids are first activated to acyl CoAs and transported across the

inner mitochondrial membrane as a carnitine derivative. Degradation continues in the mitochondrial matrix by repeated cycles of oxidation linked to FAD (flavin adenine dinucleotide), hydration, oxidation linked to NAD^+ (nicotinamide adenine dinucleotide) and thiolysis by CoA.

Important functional roles of long chain fatty acids reveal the need for highly regulated and efficient selective uptake and retention. Long chain fatty acids and their CoA derivatives have been shown to be either directly or indirectly involved in the regulation of the activity of many cellular processes including membrane receptors, enzymes, ion channels, cell differentiation, cellular development and gene expression [2]. Metabolites of long chain fatty acids, such as, prostaglandins, leukotrienes, and thromboxanes, which are derived from arachidonic acid, are important signalling molecules. It is not known, at present, whether the mechanism of long chain fatty acid transport across cellular plasma membranes is by simple diffusion, by membrane-protein mediated translocation, or both [2].

1.1.2. Phospholipids

Phospholipids are the major class of membrane lipids. The main phospholipids, phosphoglycerides, are derived from glycerol and consist of a glycerol backbone, two fatty acid chains and a phosphorylated alcohol. The major phosphoglycerides are derivatives of phosphatidate, in which the phosphate group of phosphatidate is esterified to the hydroxyl group of one of several alcohols, for example; choline, ethanolamine, serine or glycerol.

Phospholipids containing long chain fatty acids readily form bilayers in which hydrophobic interactions are the main driving force. In addition, there are Van der Waals forces between the hydrocarbon tails with electrostatic and hydrogen bonding between the polar headgroups and H_2O. The presence of anionic phospholipids in a membrane produces a negatively charged interface owing to the fact that, with the exception of sphingosine, there are no natural occurring positively charged membrane lipids to neutralise the anionic effect [3]. The introduction of anionic phospholipid into a predominantly phosphatidylcholine bilayer results in lipid packing perturbations owing to the differing headgroup sizes and effects of headgroup repulsion [3].

The majority of phospholipids are synthesised in association with the smooth endoplasmic reticulum membrane (ER). The biosynthesis occurs at the interface of the ER membrane and the cytoplasm with the fatty acyl CoA partially embedded in the membrane. All other components for synthesis are soluble constituents of the cytoplasm.

There are two generally accepted models for the movement of newly synthesised phospholipids from the ER to other organelles. The first model is that of membrane budding and involves the formation of a membrane vesicle that buds off from the ER and fuses with the membrane of another organelle. The second model involves phospholipid exchange proteins to transport phospholipids between membranes. There is also transport of newly synthesised phospholipids, triglycerides and cholesterol esters between tissues and this is via specific lipoproteins. Such

transport is primarily from the gut in the form of chylomicrons as a result of fat digestion and from the liver as VLDL during lipogenesis [2].

Overall it is the insolubility of long chain fatty acids and their derivatives (phospholipids, triacylglycerols and cholesterol esters) that dominate their metabolism requiring the formation of stable aggregates such as lipoproteins or specific binding proteins to allow the necessary flux of these compounds through the aqueous compartments of the body.

1.2. Fatty Acid Binding Protein

1.2.1. Discovery

Fatty acid binding proteins (FABPs) are a family of 14-15 KDa monomeric proteins that were discovered in 1972 by Ockner *et al.* [4]. FABP was first identified as a protein that bound long-chain fatty acids (C_{16}-C_{20}) within the cytosol of many different tissues, including intestinal mucosa, myocardium, liver, kidney and adipose tissue. It has since been realised (see below) that there is not just one FABP that is found in many tissues but that there are many different types of FABP with significant sequence homology.

1.2.2. Distribution of Fatty Acid Binding Proteins

Fatty acid binding proteins were initially isolated and purified from rat tissue [4, 5] but later from a variety of mammalian tissues, which enabled characterisation of the

protein. These characterisation studies have shown that the purified FABPs were not one and the same protein, as was first thought, but several distinct forms of the protein expressed from distinct genes that vary in their ligand binding properties. As a result, FABPs are now classified by the tissue that they are predominantly found in, such as liver FABP (LFABP), heart FABP (HFABP), adipocyte FABP (AFABP) and intestinal FABP (IFABP). Different FABP types can be found in a variety of tissues and not exclusively in the tissue dictated by classification. For example, the enterocytes of the small intestine contain not only IFABP but also LFABP, although to a lesser extent. IFABP has only so far been detected in the intestine but HFABP has been found in a variety of different tissues, such as cardiac and skeletal muscle, kidney, brain and reproductive tissues [6].

1.2.3. Structure

FABPs have an amino acid chain length of between 126 and 137 (LFABP is 127 amino acids) and all have the same basic structure consisting of a β-barrel comprising 10 β-strands which is topped by a helix-turn-helix motif at one end between two of the β-strands [7].

Figure 1.2.3.1. Structure of Native LFABP

β-strands are shown in light blue and α-helices in red.

Hydrogen bonding between β-strands 1 and 10 force the structure into the β-barrel conformation with the 2 α-helices, orientated between β-strands 1 and 2, forming a 'lid' across one end of the barrel (Figure 1.2.3.1). There is a visible gap between β-strands 4 and 5 which is only linked by one backbone hydrogen bond but, in the case of LFABP, this is filled with atoms from the amino acid residues K57, I59, N61, F63, C69, L71 and E72, some of which are in direct contact with each other [8]. It has also been demonstrated that there are four highly ordered water molecules on the surface of LFABP in the region of β-strands 4 and 5, three of which form

hydrogen bonds that help bridge the gap between the side-chains [8]. It is thought that as the fatty acid molecule enters the cavity through the portal region the interior solvent is released through the 'secondary opening' between β-strands 4 and 5 [9]. There is a second gap present in the β-barrel structure between β-strands 6 and 7 that is unique to LFABP and results in the formation of a salt bridge between residues E77 and K96 [8]. Solvent access through the gap is prevented by bordering residues (Figure 1.2.3.2).

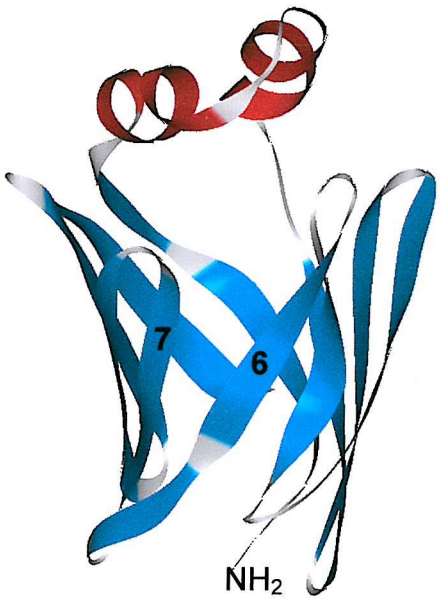

Figure1.2.3.2. Structure of Native LFABP Showing Gap Region Between β-strands 6 and 7

Contained within the β-barrel structure is a water-filled cavity whose surface is lined by both polar and hydrophobic residues [10]. This is the ligand binding site of FABP. Most FABPs can bind just one fatty acid molecule within the binding cavity, in which the fatty acid is orientated with the carboxylate group facing inwards and is solvent

inaccessible [11]. Electrostatic interactions involving arginine residues are responsible for the orientation of the fatty acid within the binding cavity of the protein. Studies using ^{13}C NMR of the dynamics of palmitic acid complexed with rat IFABP have shown that the fatty acid bound within the structure is not rigidly anchored and can, therefore, move relatively freely within the cavity [12].

LFABP is known to bind two fatty acid molecules within the cavity, which is a property unique to the liver form of the protein. In the LFABP binding cavity one fatty acid is orientated with the carboxylate group facing inwards in a similar manner to the other types of FABP and the other fatty acid carboxylate is orientated facing outwards and is solvent exposed (Figure 1.2.3.3). The inward facing carboxylate has been found to interact with a network of amino acids including arginine-122, which is likely to be one of the residues responsible for the orientation of this fatty acid. As yet interactions involving the outward facing carboxylate have not been determined [13].

From the structure of the FABPs and the nature of the binding cavity one would expect that conformational changes in the protein would be necessary to allow ligand entry into the cavity. There is evidence to suggest that the portal region of the protein exhibits some conformational flexibility. Results from multidimensional NMR studies by Hodsdon and Cistola of apo and holo IFABP show an 'open' portal in the apo structure and a 'closed' portal in the holo structure [14].

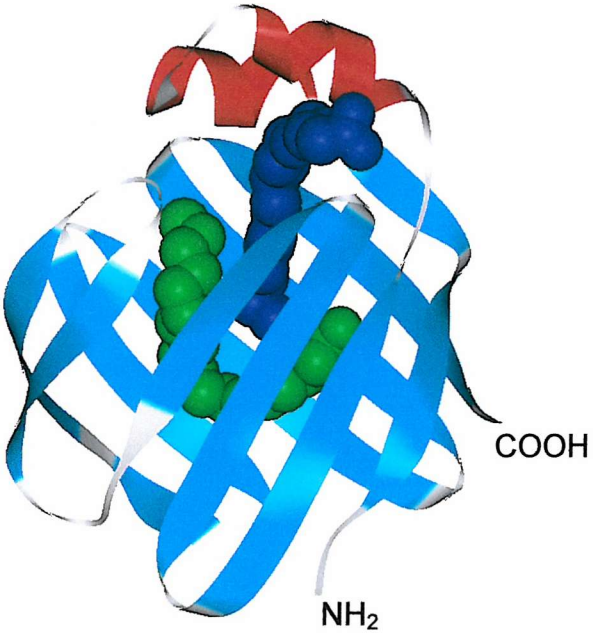

Figure 1.2.3.3. Structure of Native LFABP with Two Bound Oleates

The two oleate molecules are shown in green and in dark blue. The primary site is occupied by the green oleic acid while the blue oleic acid is in the secondary site with the carboxyl group exposed through the portal region (Thompson *et al.* 1997).

Work carried out by Richieri *et al* on IFABP has used engineered mutants to propose a pathway for the entering and exiting of fatty acids from the protein. Their work has suggested that arginine-56 on β-strand 4, orientated on the surface of IFABP, is involved in an initial electrostatic interaction with the fatty acid prior to the insertion into the binding cavity. They have proposed that the dissociation of the ligand is a reversal of these steps [15]. LFABP has a serine at position 56 but there is a lysine present on the surface at position 57.

1.2.4. Ligands

Most FABPs can only bind fatty acids at the binding site located within the binding cavity of the protein but LFABP has been shown to be unique in that it can bind a variety of different ligands including haem, fatty acyl CoAs and lysophospholipids. The specificity of LFABP for fatty acids has been investigated. Binding studies have shown that LFABP binds very poorly to saturated fatty acids of chain length C_{14} or less and that the binding of saturated fatty acids is preferential to the binding of the corresponding unsaturated fatty acids [16, 17]. Richieri *et al.* (1997) have presented data to show that fatty acid solubility governs the binding affinity of FABPs for their ligand. They have suggested that the higher the fatty acid aqueous solubility the lower the affinity the FABP has for the ligand although IFABP is an exception to this rule. This proposal has been used to explain the differences between the affinity of FABPs for saturated and their affinity for unsaturated fatty acids, [17]. It is thought that the second fatty acid binding site in LFABP is only available once the first site has been occupied and that the binding affinities of the two long chain fatty acid sites are approximately equivalent for saturated fatty acids. However, these sites differ by approximately 10-fold for unsaturated fatty acids with the first site having the higher affinity [18]. The LFABP binding cavity is a high affinity binding site for haem and also a binding site for long chain fatty acyl CoAs, although with a lower affinity than haem and the corresponding fatty acid. It has been proposed that LFABP has two binding sites for fatty acyl CoAs with a K_d = 3-14 μM [19] however only one molecule has been modelled into the crystal structure of LFABP [8] in which the bulky ADP derivative extends outward beyond the portal and is thus solvent exposed.

It has been demonstrated that lysophospholipids bind to LFABP with a 1:1 binding stoichiometry and with K_d values of 1-2 μM [20]. Displacement studies have indicated that lysophosphatidic acid has the highest affinity for LFABP [20]. LFABP will also bind certain bile salts with the highest affinity being seen for lithocholate and taurolithocholate 3-sulphate [21]. A photoaffinity analogue of taurolithocholate 3-sulphate has been shown to exclusively label a hepatic protein subsequently identified as LFABP [22]. LFABP also bind cholesterol sulphate with an affinity similar to lithocholate based on displacement studies [21] however such displacement studies were unable to identify cholesterol as a potential ligand [21].

The fact that LFABP can bind such a variety of ligands compared to other forms of FABP could possibly be attributed to the presence of the 'gap' regions within the β-barrel structure of the protein. It may be that these regions allow a greater conformational flexibility in LFABP than can be seen in the other forms of FABP as other forms only contain the gap region between β-strands 4 and 5 and not the region between β-strands 6 and 7.

1.2.5. Functions of FABP

1.2.5.1. General Functions of FABPs

The physiological functions of FABP are not clear and as of yet it has not been possible to assign a specific function to the protein. There are, however, many suggestions based on experimental evidence, none of which is conclusive. It is clear that the different types of FABPs must have different roles within the cell as cells

such as the enterocytes of the small intestine have been shown to contain both IFABP and LFABP. If IFABP and LFABP were performing the same function then the presence of both proteins in the same cell would be unnecessary. The differences in ligand binding in the FABP family, for example LFABP is clearly different to other members of the family, are also highly suggestive of individual functions. It has been proposed that FABPs act as regulators of fatty acids within the cell, preventing the concentration reaching levels toxic to the cell. This is known as a buffering role and does not obviously require different forms of FABP but there is a correlation between high levels of an FABP in a cell and the flux of fatty acids into or out of that cell. Thus hepatocytes, enterocytes and adipocytes, which are all exposed to high concentrations of fatty acids, also express high concentration of the appropriate FABP consistent with a buffering role.

FABPs have been considered as transporters for long chain fatty acids, allowing transfer between bilayers at a rate greater than any spontaneous movement. The fact that certain types of cells exposed to high fatty acid flux express high levels of a particular FABP is an argument for both a buffering and a transport function. A number of characteristics of FABPs have been used as indirect arguments for a transport function [23] including (i) ligand binding characteristics, (ii) the selective labelling of the protein in cells using photo-affinity probes, (iii) the facilitation of the activity of fatty acid requiring enzymes, (iv) the correlation between FABP levels and cellular functions, (v) dietary modulation and (vi) FABP levels during development. However none of this evidence could be regarded as supporting a transport role as opposed to a simple buffering role. It could be argued that transport in a cell really

means targeting i.e. the uptake of fatty acid from one site and the release at another site in the cell.

This idea of fatty acid targeting has been investigated further by Storch *et al* using more direct methods that are discussed in detail in a later section (1.3.1). In summary, their work investigated the rate at which anthroyloxy-labelled fatty acid (AOFA) moved from FABPs to model membranes that contained a fluorescence quenching agent, *N*-(7-nitro2,1,3-benzoxadiazol-4-yl)-phosphatidylethanolamine (NBD-PE) [24]. The general conclusion of these studies by Storch *et al* has been that HFABP, AFABP and IFABP all appear to bind fatty acids and deliver them to membranes via a direct collisional interaction with the membrane itself [24-30]. They have also concluded that LFABP does not behave in the same manner as the other FABPs studied. LFABP does bind fatty acids within the cell but it would appear that the fatty acids are released into the aqueous phase with no apparent direct interaction with any membrane interface [28, 31, 32]. This data is more consistent with a buffering role for LFABP, maintaining low cytosolic free fatty acid levels.

It should be remembered that FABP is present in the cytosol at a concentration of approximately 0.2–1 mM, which is representative of approximately 2-5% of the total cytosolic protein in tissues active in long-chain fatty acid metabolism. Such high concentrations would promote the partitioning of long chain fatty acids from membranes to the protein although this in itself does not imply that there are protein-membrane interactions.

1.2.5.2. Functions of LFABP

Many different roles have been discussed for the presence of LFABP within the cell. This issue has resulted in considerable debate because of the broad ligand binding capacity of the protein. In particular the ability of LFABP to bind lysophospholipids, acyl CoAs and ligands that bind to the PPAR receptors requires an explanation in terms of cell function.

In the case of lysophospholipids, studies on the regulation of phospholipid synthesis have found LFABP to stimulate mitochondrial and microsomal glycerophosphate acyltransferase (GAT) and the export of lysophosphatidic acid (LPA) from both of these organelles [33]. GAT is the enzyme which catalyses the acylation of glycerol-3-phosphate to LPA. Mitochondrially synthesised LPA exported by LFABP can be converted to phosphatidic acid (PA) by the microsomes. In the absence of LFABP the mitochondria predominantly synthesise PA [33]. This is suggestive of a major role in the mitochondrial and microsomal phospholipid metabolism by regulating both the synthesis and the utilisation of LPA by these organelles. In another experiment, 20% of the PA content of PA loaded mitochondria was shown to leave the organelles in the presence of LFABP.

In terms of acylCoA binding, LFABP binds this type of ligand with lower affinity than long chain fatty acids [19]. In addition, liver cells contain a high affinity acyl CoA binding protein (ACBP). Therefore, the precise role, if any, of LFABP in acyl CoA metabolism is not clear.

Khan and Sorof have published work that associates LFABP with mitogenesis in hepatocytes. It has been demonstrated that the level of LFABP expression in rat liver hepatocytes is increased during mitosis and also throughout the cell cycle when rats are fed with carcinogens known to induce hyperplastic hepatocytes and hepatocarcinomas [34]. One study conducted by Khan and Sorof reveals that mitogenesis induced by peroxisome proliferators requires the presence of LFABP for the process to occur [34]. It was also found during liver carcinogenesis that the LFABP present interacts with some of the metabolites of the genotoxic carcinogens and together with unsaturated fatty acids, especially linoleic acid, it promotes the growth of cultures of transfected hepatoma cells [35]. The behaviour of LFABP described is consistent with that of a protein involved in the regulation of hepatocyte multiplication.

Peroxisome-proliferator activated receptors (PPARs) are a family of ligand activated transcription factors that have been shown to be activated by long-chain fatty acids [36]. PPARs bind to DNA in the promoter regions of several genes involved in lipid metabolism, including LFABP and AFABP [6, 36]. Ligands of PPARα have been found not only to bind to LFABP but they have also been observed to increase levels of LFABP expression within the cell [37]. It is possible that the relationship between LFABP and PPARα is linked to the involvement of LFABP in hepatocyte mitogenesis and peroxisomal proliferation. It remains to be established in this system whether LFABP targets ligands to PPARα, thereby inducing a mitogenic effect. PPARα induces the expression of LFABP [6, 36] and PPARγ has been shown to induce the expression of AFABP [38]. Recently, evidence has been presented for a

direct interaction between PPAR and LFABP; these important observations are discussed in 1.3.2.

1.3. Fatty Acid Targeting

1.3.1. Membrane-Protein Interactions

Extensive work has been carried out by Storch *et al* investigating interactions between various types of FABPs and model membranes. The studies were based around a fluorescence resonance transfer assay whereby the rate of transfer of anthroyloxy-labelled fatty acids (AOFA) from FABP to model membranes was monitored [25]. The model membranes used were composed of 90 mol% egg phosphatidylcholine with 10 mol% *N*-(7-nitro2,1,3-benzoxadiazol-4-yl)-phosphatidylethanolamine (NBD-PE). The NBD-PE moiety is present in the model membrane as a non-exchangeable fluorescence quencher. Once associated with the NBD-PE containing membrane the fluorescence of the AOFA is quenched and this loss of fluorescence is a measure of the rate of transfer of AOFA from FABP to the membranes. This method has been used to examine the mechanisms involved in the transfer of AOFA from LFABP [39], HFABP [27], AFABP [24] and IFABP [26] to model membranes. Possible factors involved in the transfer, such as acceptor membrane concentration, ionic strength of the medium and membrane composition, were investigated.

Variation of the concentration of acceptor membranes present in the assays was examined. This was found to have an effect on the transfer rate of AOFA from

IFABP, HFABP and AFABP but had no visible effect on the rate of transfer from LFABP to model membranes. In all except LFABP, the increasing concentration of acceptor membrane resulted in significantly increased rates of transfer of AOFA from the proteins. There was no visible change in the rate of transfer from LFABP. If there were a direct interaction with the membrane, such as a collisional mechanism, responsible for the transfer of AOFA to the model membranes then the rate of transfer would be increased with increasing acceptor membrane concentration, as collisions would become more frequent. If an aqueous diffusion mechanism was responsible for the transfer of AOFA then changing acceptor membrane concentration would have no effect as no direct interaction between the protein and the membrane would be occurring.

Increasing NaCl concentration of the assays would reduce the solubility of the AOFA in the aqueous phase. The solubility of the AOFA in the aqueous phase would have no effect on the transfer between protein and membrane via the collisional mechanism, as there would be little contact between the AOFA and the aqueous phase. The reverse of this would be true if aqueous diffusion were the mechanism, increasing the NaCl concentration would cause the AOFA to be less soluble and, therefore, would slow the rate of transfer to the membrane. The transfer of AOFA from IFABP, HFABP and AFABP to acceptor membranes was observed to be unaffected by increasing NaCl concentration, whereas, LFABP AOFA transfer was greatly affected by increasing NaCl concentration.

Storch argues that all the evidence presented so far points to a collisional mechanism for the transfer of fatty acids to membranes from IFABP, HFABP and

AFABP but an aqueous mechanism for transfer from LFABP. The effect of phospholipid charge was also examined. Direct interaction of FABP with the membrane via a collisional mechanism would be affected by the composition of the membrane. In contrast, a diffusional mechanism through the aqueous phase would not require an interaction of the protein with the membrane and so membrane composition should have no effect on the rate of transfer of AOFA from the protein to the membrane. It was observed that transfer of AOFA from LFABP to the membrane was unaffected by membrane composition. In comparison, introduction of anionic phospholipids into the membrane increased the rates of transfer of AOFA from IFABP, HFABP and AFABP and introduction of a positive charge decreased the rates of transfer.

The conclusions from the work discussed were that IFABP, HFABP and AFABP transport fatty acids to intracellular membranes via a direct, collisional interaction with the membrane. LFABP behaves differently to the other types of FABP as it appears to deliver fatty acids to membranes via an aqueous diffusion mechanism rather than via any direct interaction with membrane. This classification of FABPs has now been extended to include the lipid binding proteins in this family. Thus CRBPII, like LFABP, is proposed to operate via an aqueous diffusion mechanism whereas CRBPI uses a collisional transfer mechanism [6].

The importance of anionic phospholipid binding in a collisional transfer mechanism highlights the potential importance of electrostatic interactions involving the protein surface and hence the role of cationic residues on the protein surface. This has been has been further investigated using AFABP [28] and HFABP [40] and the strategy

has involved the modification of surface lysine residues.

Acetylating the protein with acetic anhydride to neutralise the positive charges carried by these lysine residues was used to assess the involvement of surface lysine residues on recombinant AFABP in interactions with anionic phospholipids. The native AFABP and acetylated AFABP were compared in terms of the effects of transfer of AOFA from the protein to membranes, the effect of ionic strength, acceptor membrane concentration and membrane charge density [28]. The acetylated AFABP behaved in a similar manner to LFABP. The transfer of AOFA to model membranes was affected by increasing ionic strength but was unaffected by membrane concentration and composition. This suggests that acetylated AFABP is delivering fatty acids to membranes via an aqueous diffusion mechanism rather than by the collisional transfer mechanism of the native protein. The study demonstrated that surface lysine residues are important in the interaction of AFABP with membranes and so, therefore, binding must involve electrostatic interactions [28].

The interaction of AFABP with phospholipid membranes was analysed further with the use of FTIR (Fourier transform infrared) spectroscopy [29]. The study concluded that AFABP preferentially binds anionic phospholipids and that upon interaction with phospholipid the protein structure and thermal stability is essentially unchanged. It was also observed that the degree of membrane interaction was directly related to the rate of transfer of AOFA to model membranes and therefore it would appear that the contact of AFABP with membrane is functionally related to its fatty acid transport properties [29].

The importance of surface lysine residues in the interactions between FABP and membranes was investigated further by the chemical modification and mutagenesis of HFABP [40]. Chemical modification of the protein was by acetylation using acetic anhydride and, in addition, a series of seven mutants, K33I, K10I, K59I, K113I, K22E, T28K and a double mutant, K59,22I, were made. Using anthroyloxy-labelled fatty acid (AOFA) transfer of this fluorescent ligand from HFABP to model membranes was assessed [40]. It was noted that the rate of transfer of AOFA from HFABP to membranes was considerably slower from the acetylated protein than from the native protein. The transfer from the acetylated protein was independent of membrane composition, whereas, the native protein has an increased transfer rate with increasing membrane negative charge.

Examination of the mutants of HFABP that were made revealed that the mutations of lysine at position 22 on α-helix I significantly decreased the rate of transfer of AOFA from these proteins to membranes, compared with wild-type HFABP [40]. The rate of transfer of AOFA from K22E HFABP and K22I HFABP was shown to be three-fold slower than the transfer rate from wild-type HFABP. The rate of transfer of these two mutants was also shown to be independent of acceptor membrane composition, which suggests that the protein no longer interacts directly with the membrane. For the K59I HFABP, the transfer rate of AOFA to the model membranes was found to be two-fold faster compared to wild-type HFABP. The double mutation of K22,59I presented a protein with transfer rates comparable to the wild-type protein. The substitution of a threonine residue at position 28 on α-helix II with a lysine residue increased the rate of transfer of AOFA from H-FABP four-fold. It was concluded that

the α-helical region of H-FABP may be involved in electrostatic interactions between the protein and membranes [40].

Work described above provides evidence for the importance of the α-helical region of AFABP in interactions of the protein with membranes [40]. To investigate this idea further, Corsico *et al* produced a helix-less variant of IFABP (IFABP-HL) [41] in which the region between residues 14 and 31 had been deleted and replaced with a 2 residue linker region. Studies were carried out using the AOFA quenching assay to determine the rates of transfer of AOFA from IFABP-HL to model membranes with varying acceptor membrane concentration and composition. The transfer rate of AOFA from IFABP-HL was unaffected by changes in acceptor membrane concentration or composition whereas the rate of transfer from IFABP increased with increasing acceptor membrane concentration and with increasing membrane negative charge.

A direct method of assessing binding of IFABP and IFABP-HL to membranes was also used, involving the ability of these two proteins to prevent the binding of cytochrome c to the membrane. Cytochrome c has been used in many model studies of protein-membrane interactions and is known to interact with anionic membranes. FABP was incubated with the membrane preparation, then cytochrome c was added to the system and the extent of cytochrome c binding could be monitored via a fluorescence resonance transfer assay [25]. IFABP-HL was found to be 80 % less efficient at preventing cytochrome c binding to the model membranes than was wild-type IFABP. These studies confirm proposals that the α-helical region of FABP is directly involved in membrane interactions [41].

1.3.2. Protein-Protein Interactions

An alternative to membrane-protein interactions for targeting fatty acids would be protein-protein interactions where the FABP has specificity for a membrane protein. Recently, evidence has been presented for a direct interaction between PPARα and γ and LFABP in the nucleus for the delivery of fatty acids and hypolipidemic drugs [42]. LFABP localisation in the nucleus would be possible by either diffusion through nuclear pores or it is possible that fatty acid binding by the protein may provide a recognition signal for a targeting mechanism. Evidence of LFABP and PPARα co-localisation in the nucleus of hepatocytes was provided using laser-scanning microscopy, also direct protein-protein interactions were shown between LFABP and PPARα using pull-down assays, immunocoprecipitation and a mammalian two-hybrid system. These interactions were found to be independent of ligand binding. In LFABP transfection studies, PPAR transactivation with appropriate ligands correlated with expressed LFABP levels.

In a study conducted by Shen *et al* [43] a mechanism utilising an interaction between hormone-sensitive lipase (HSL) and adipocyte lipid binding protein (ALBP) was discussed as a route for fatty acid trafficking during lipolysis. HSL is found in the cytosol of adipose cells and is the rate limiting enzyme in the mobilization of free fatty acids, it catalyses the hydrolysis of triacylglycerols. It has been shown that HSL interacts with ALBP via a region of 300 amino acids at the N-terminal, a region completely distinct from the catalytic binding domain at the C-terminal. The presence of a complex of HSL bound to ALBP was detected using immunoprecipitation with anti-HSL antibodies. The studies of a truncated HSL

missing the first 300 amino acids showed that this HSL formed no detectable interactions with ALBP. Results from this study suggest that ALBP binds HSL-derived fatty acids via a direct interaction between ALBP and the N-terminal region of HSL and acts to facilitate the efflux of these fatty acids from the cell.

1.3.3. General Comments on Membrane-Protein Interactions

There are many different proteins that bind membrane phospholipids, the majority of which appear to be driven by electrostatic interactions involving anionic phospholipids [44]. The presence of anionic phospholipids within membranes, firstly, provides an attraction for positively charged residues on the protein surface and, secondly, the presence of anionic phospholipids may promote membrane penetration by the protein due to lipid-packing perturbations [3]. Many proteins that interact with phospholipids do so via regions rich in helical structure [45, 46] while such interactions are part of the normal physiological function of the protein. A number of examples are discussed below to illustrate the phenomenon of membrane-protein interactions and the conformational changes that occur, often linked to ligand binding. The presence of anionic phospholipids is a key element in these interactions.

CTP:phosphocholine cytidylyltransferase (CT) is an enzyme which catalyses a rate limiting step in the synthesis of phosphatidylcholine (PC) in mammalian cells. It would appear that this enzyme is regulated by the PC content in the membrane via an α-helical region that acts as a lipid sensor [48]. The presence of a relatively high proportion of anionic phospholipid, and therefore a low proportion of PC, in the

membrane, results in the translocation of CT to the membrane surface. The attraction is most likely due to areas of positively charged residues in the α-helical region of the protein interacting with anionic phospholipids at the interface causing stabilisation of the helix structure [48]. It then appears that a secondary interaction occurs whereby the hydrophobic face of the helix intercalates into the membrane core [49]. The hydrophobic interactions involved in the intercalation event are a stronger driving force than the electrostatic interactions as membrane insertion still occurs when the electrostatic interactions are disrupted [50]. This is supported by the observation that mammalian CTs contain a true lipid-binding amphipathic α-helical segment [51]. More recent evidence highlights the occurrence of a dephosphorylation event in a region adjacent to the membrane binding domain of CT which increases the affinity of the protein for anionic phospholipids [52].

DnaA protein [53] is the initiator of chromosomal replication in *E. coli* and experimental evidence suggest that anionic phospholipids are required for the activation of this protein. Membrane insertion of DnaA protein into the bilayer is accompanied by membrane-mediated dissociation of ADP and the binding of ATP. It has been observed that a region of the putative amphipathic helices is essential for functional interaction with membranes [54]. The conversion of the inactive ADP-DnaA protein to the replicatively active ATP-DnaA protein *in vitro* is shown to be promoted by anionic phospholipids in a bilayer. More recently it has been observed through studies using site-directed mutagenesis that interactions between DnaA protein and anionic phospholipids are dependent on cationic residues present on the protein surface [55]. It has been proposed that the negatively charged phospholipid head group initially attracts the DnaA protein to the membrane surface where a

secondary membrane insertion event then occurs resulting in the activation of the protein.

The *triglyceride lipase* from *Thermomyces lanuginosa* binds to the anionic phospholipid interface of SUVs but not LUVs [56] with the induction of a catalytically active conformation. Studies using tryptophan mutants have shown the 'lid' region of the protein to undergo conformational change involving insertion into the interface. This has been described as a unique system where composition and physical properties of the lipid interface control enzyme activity [56]. This system in particular has interesting parallels with the interaction of LFABP with anionic SUVs described in this thesis. The presence of a minimum density of anionic phospholipid allows penetration of the "lid" region of the enzyme into the bilayer with the resulting conformational change thus exposing the active site and allowing substrate entry prior to catalysis.

Many other examples exist in the literature of non-specific interactions between protein and membranes that contain anionic phospholipids, some of which are briefly summarised:

- Pheromone-binding Protein from *Bombyx mori* has been shown to undergo conformational change upon interaction with membranes which has resulted in the release of ligand [57].
- Conformational changes have been observed with human apolipoprotein H using circular dichroism in the presence of anionic-phospholipid containing liposomes [58].

- Large changes in the secondary structure of sterol carrier protein 2 (SCP-2) have been demonstrated upon interaction of the protein with highly curved anionic phospholipid-containing SUVs [59].
- Formation of new β-structure is thought to occur in annexin molecules as a result of direct interaction with membranes [60].
- Anionic phospholipids cause the penetration of cytochrome P450 1A2 into phospholipid bilayers which results in an increased α-helical content of the protein [61].
- Recombinant parathyroid hormone shows an increase in the α-helical content in the presence of anionic phospholipid vesicles [62].
- The activity of certain enzymes is modulated by anionic phospholipid vesicles by inducing a catalytically active conformation. Examples of such enzymes are HtrA protein, a heat shock serine protease from *E.coli*, [63] and phosphatidylserine synthase, also from *E.coli* [64].

1.3.4. Summary of Protein-Membrane Interactions

There are now many examples in the literature of protein interactions with the membrane interface as part of the normal physiological function of the protein. These interactions are relatively non-specific in comparison with the highly specific interaction between particular protein domains and specific phospholipids. Such specific interactions are exemplified by the binding of PH domains to phosphoinositides.

Non-specific interactions normally require the presence of a minimum charge density of anionic phospholipids consistent with electrostatic interactions but may also involve a membrane penetration event. The interactions result in changes in protein conformation and it is these changes that are linked to the physiological response. In most cases the residues on the protein surface that are involved in binding and the nature of the conformational changes that ensue are not known.

1.4. Aims of the Project

The ability of FABPs to interact with membranes is a potentially important mechanism for the targeting of bound ligands to enzymes within intracellular organelles. It has been observed that LFABP is able to interact with anionic phospholipid vesicles. This interaction was detected by loss of fluorescence as the ligand, DAUDA, was released from the protein as a result of binding to the vesicles.

The aims of the project are to define in molecular detail the specificity of the interaction of LFABP with the phospholipid interface and the nature of the conformational changes that occur.

Chapter Two:

Materials and Methods

2.1. Materials

All chemicals were obtained from Sigma Chemical Company Limited (Poole, Dorset) unless otherwise stated. QIAprep spin plasmid miniprep kit, QIAprep spin M13 kit, QIAquick Gel extraction kit, QIAquick PCR clean up kit and QIAquick nucleotide removal kit were all obtained from Qiagen (Dorking, Surrey). DAUDA (11-(dansylamino)undecanoic acid) was obtained from Molecular Probes (OR, USA). Dioleoylphosphatidylglycerol (DOPG), dioleoylphosphatidylserine (DOPS) and dioleoylphosphatidicacid (DOPA) were obtained from Avanti Polar Lipids (Alabaster, Alabama, USA), phosphatidylinositol (PI) and dioleoylphosphatidylethanolamine (DOPE) from Sigma and dioleoylphosphatidylcholine (DOPC) from Lipid Products (Redhill, Surrey, UK). Fatty acids and oleoyi CoA were obtained from Sigma and stored as 10 mM stock solutions in methanol. Lysophosphatidic acid and lysophosphatidylcholine were obtained in solid form from Avanti Polar Lipids. Restriction enzymes were from Promega (Southampton, UK) and Boehringer Mannheim UK Limited (Lewes, E. Sussex, UK). Muta-Gene M13 In Vitro Mutagenesis kit was from BioRad (Hemel Hempstead, Herts, UK).

2.2. DNA Techniques

2.2.1. Site-directed Mutagenesis

2.2.1.1.The Kunkel Method

The Kunkel method is a classic method used for the *in vitro* site-directed mutagenesis of plasmid DNA [65, 66]. The principle of this particular method is the production of a single-stranded template of the DNA of interest, which is used for the synthesis of a strand of complementary DNA using mutated oligonucleotides as primers. This produces 50 % mutagenic DNA and 50 % parent DNA which, using the method developed by Kunkel as described below, can be specifically selected against thereby resulting purely in the mutagenic DNA .

Initially the LFABP wild-type gene was amplified and a Nde I restriction site added to the 5' end using PCR in the pUC18 vector. The PCR reaction required 20-100 ng DNA template, 10 pmoles primers, 0.2 mM dNTP's and where Taq DNA polymerase was used 8 mM $MgCl_2$ was also present. The PCR conditions were as follows:

- Initial denaturing step of 95°C, 5 min prior to the addition of either 2.5 units pfu DNA polymerase (Promega) or 2.5 units Taq DNA polymerase (Promega).

-Denaturation 95°C, 30 seconds

-Annealing 50°C, 90 seconds

-Primer extension 68°C, 180 seconds

For 30 cycles

The PCR product and M13mp19 DNA were both digested with EcoRI and Hind III to enable the ligation of the LFABP wild-type gene into the bacteriophage DNA. Ligation was set up at room temperature and allowed to cool slowly to 4°C overnight in the presence of T4 DNA ligase (Promega). The ligation product was transformed into CJ236 *E. coli* cells, which contain *dut, ung* mutations whereby the enzymes dUTPase and uracil N-glycosylase are inactivated resulting in the incorporation of uracil into the DNA. The single-stranded uracil containing DNA was purified and used as a template, along with an oligonucleotide containing the desired mutation, for the synthesis of a strand of mutagenic complementary DNA. The double stranded DNA was transformed into MV1190 *E. coli* cells containing active uracil N-glycosylase to inactivate the uracil containing strand of DNA and hence promote the replication of the mutagenic strand. A restriction digest using Nde I and Hind III was carried out on the mutated gene in M13mp19 and also on purified pET11a plasmid prior to the ligation of the FABP mutant gene into this plasmid. Ligation of the FABP mutated gene into the pET11a vector was using T4 DNA ligase (Promega) and was set up at room temperature and allowed to cool to 4°C overnight. The ligation ratio of gene:plasmid used was 3:1 in order to maximise the ligation efficiency. The ligation product was transformed into BL21(DE3) *E.coli* cells for expression.

2.2.1.2. The PCR Method

The principle of this method is to use PCR to produce two overlapping DNA fragments with the same mutation in the overlapping region [67]. A second PCR reaction is carried out on the overlapping DNA fragments in order to fuse them together (Figure 2.2.1.2).

Initially, two PCR reactions were set up, the first using primers 1 & 1* and the second using primers 2 & 2*:

Primers:	150 μg each
10X Pfu buffer:	5 μl
dNTPs:	0.8 μl
DNA Template:	100 μg
H_2O:	To 49 μl total volume
Pfu:	2.5 units (added following 94°C hot start)

The first PCR reactions were 1/1* & 2/2* and these were run simultaneously with the following conditions:

-Initial hot start of 94°C for 1 minute prior to the addition of 2.5 units pfu DNA polymerase (Promega).

-Denaturation, 94°C for 1min.

-Annealing, 50°C for 1 min.

-Synthesis, 72°C for 1 min.

For 25 cycles.

The PCR products were run on a 1 % agarose gel in the presence of ethidium bromide to confirm that the PCR reactions had been successful. Equal concentrations of each PCR reaction were mixed and the initial end primers (1&2) were added:

Primers:	150 μg each
10X Pfu buffer:	5 μl
dNTPs:	0.8 μl

PCR Products:	100 μg each
H_20:	To 49 μl total volume
Pfu:	2.5 units (added following initial 94°C hot start)

The PCR reaction was repeated using pfu DNA polymerase to obtain the complete gene containing the desired mutation. Purification of the PCR product was using QIAquick PCR purification kit (Qiagen). The PCR product and pET11a vector were then digested using Nde I & Hind III to enable sticky-ended ligation of the gene into the vector. The ligation product was transformed into BL21 (DE3) *E.coli* cells for expression.

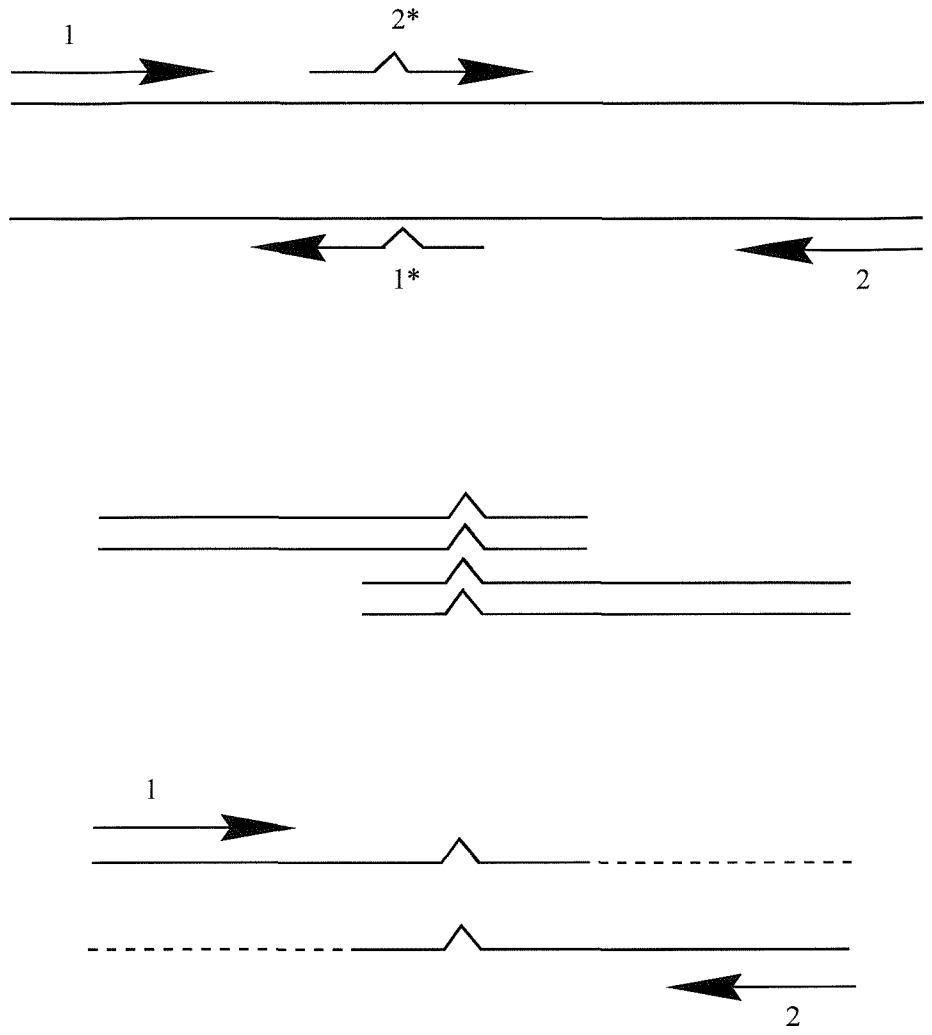

Figure 2.2.1.2. Double-stranded DNA Template with Attached Oligonucleotide Primers Showing PCR Mutagenesis

1 & 2 are LFABP forward and reverse primers, 1* & 2* are mutagenic forward and reverse primers.

2.2.1.3. Rat Liver FABP Gene Sequence

ATGAACTTCTCTGGTAAATACCAGGTGCAGTCTCAG
TACTTGAAGAGACCATTTATGGTCCACGTCAGAGTC

M N F S G K Y Q V Q S Q

GAAAACTTCGAACCGTTCATGAAAGCCATGGGTCTG
CTTTTGAAGCTTGGCAAGTACTTTCGGTACCCAGAC

E N F E P F M K A M G L

CCGGAAGACCTGATCCAGAAAGGTAAAGATATCAAA
GGCCTTCTGGACTAGGTCTTTCCATTTCTATAGTTT

P E D L I Q K G K D I K

GGTGTTTCTGAAATCGTTCACGAAGGTAAAAAAGTT
CCACAAAGACTTTAGCAAGTGCTTCCATTTTTTCAA

G V S E I V H E G K K V

AAACTGACCATCACCTACGGATCCAAAGTTATCCAC
TTTGACTGGTAGTGGATGCCTAGGTTTCAATAGGTG

K L T I T Y G S K V I H

AACGAGTTCACCCTGGGTGAAGAATGCGAACTCGAG
TTGCTCAAGTGGGACCCACTTCTTACGCTTGAGCTC

N E F T L G E E C E L E

ACCATGACCGGTGAAAAAGTTAAAGCTGTTGTTAAA
TGGTACTGGCCACTTTTTCAATTTCGACAACAATTT

T M T G E K V K A V V K

ATGGAAGGTGACAACAAAATGGTTACCACCTTCAAA
TACCTTCCACTGTTGTTTTACCAATGGTGGAAGTTT

M E G D N K M V T T F K

GGTATCAAATCTGTTACCGAGTTCAACGGTGACACC
CCATAGTTTAGACAATGGCTCAAGTTGCCACTGTGG

G I K S V T E F N G D T

ATCACCAACACCATGACCCTGGGTGACATCGTTTAC
TAGTGGTTGTGGTACTGGGACCCACTGTAGCAAATG

I T N T M T L G D I V Y

AAACGTGTTTCTAAACGTATC
TTTGCACAAAGATTTGCATAG

K R V S K R I

2.2.1.4. Oligonucleotides used in Mutagenesis

End Primer (forward)

5' AAAAGAATTCCATATGAACTTCTCTGGTAAAT 3'

End Primer (reverse)

5' GTGCCAAGCTTCTATTAGATACG 3'

F3W Primer (Kunkel Method)

5' AAAAGAATTCCATATGAACTGGTCTGGTTAAATAC 3'

F18W Forward Primer (PCR Method)

5' GAAAACTTCGAACCGTGGATGAAAGCCATGGGT 3'

F18W Reverse Primer (PCR Method)

5' ACCCATGGCTTTCATCCACGGTTCGAAGTTTTC 3'

C69W Forward Primer (PCR Method)

5' CTGGGTGAAGAATGGGAACTCGAGACC 3'

C69W Reverse Primer (PCR Method)

5' GGTCTCGAGTTCCCATTCTTCACCCAG 3'

K20E Primer (Kunkel Method)

5' TTCGAACCGTTCATGGAAGCCATGGGTCTGCCG 3'

K31E Primer (Kunkel Method)

5' GAAGACCTGATCCAGGAAGGTAAAGATATCAAA 3'

K33E Primer (Kunkel Method)

5' CTGATCCAGAAAGGTGAAGATATCAAAGGTGTT 3'

K125E Primer (Kunkel Method)

5' TACAAACGTGTTTCTGAACGTATCTAATAG 3'

R126E Primer (Kunkel Method)

$^{5'}$ AAACGTGTTTCTAAAGAAATCTAATAG $^{3'}$

2.2.2. Agarose Gel Electrophoresis

Reagents: 50 x TAE (2 M Tris, 57.1 ml glacial acetic acid, 0.05 M EDTA in 1L, pH 7.2)
Agarose (Promega)
Ethidium bromide (10 mg/ml)
6 X Gel loading buffer (0.25% bromophenol blue, 30% glycerol)

Agarose gel horizontal electrophoresis was used to analyse DNA samples. The agarose was prepared using 1 X TAE buffer containing 0.6 μg/ml ethidium bromide and 0.8 % w/v agarose. Approximately 15 ml of gel was loaded onto a mini-gel plate (7.2 cm x 7.7 cm) and allowed to set with a comb placed onto the gel to form the wells. The gel was prepared for use by submerging the gel in an electrophoresis tank containing 1 X TAE buffer with 0.6 μg/ml ethidium bromide. Samples were prepared using between 1-5 μl DNA sample and 1 μl loading buffer, the entire prepared sample was loaded onto the gel. The gel was then run at a constant voltage of 120 V until the dye front reached between 1/2 and 3/4 of the way down the gel. A UV transilluminator was used visualize to DNA samples.

2.2.3. Preparation of Calcium Competent Cells

Overnight cultures were prepared in 10 ml LB (with 30 μg/ml chloramphenicol for CJ236 cells) and incubated at 37°C. The following day, 500 μl overnight culture was transferred to 10 ml fresh LB and incubated at 37°C until OD_{600}~0.6 (~1.5h). The

cells were then harvested at 3,000 g for 5 minutes at 4°C and resuspended in 5 ml ice cold 50 mM $CaCl_2$ and incubated on ice for 20 minutes. After a further centrifugation step, as before, the cells were resuspended in 500 µl ice cold 50 mM $CaCl_2$ and 300 µl of this was transferred to an ice cold microfuge tube ready for use. The cells either have to be used the same day or 15 % glycerol (v/v) can be added and the cells frozen in liquid nitrogen and stored at -80°C.

2.2.4. Estimation of DNA Concentration

The concentration of a sample of DNA can be estimated using the absorbance at 260nm. Using the A_{260} value the concentration can be calculated from the following equations:

Double-stranded DNA 1 OD_{260} unit ~ 50 µg/ml

Single-stranded DNA 1 OD_{260} unit ~ 33 µg/ml

2.2.5. Purification of Plasmid DNA

The cells from a 10 ml overnight culture were firstly harvested by centrifugation at 3,000 g for 10 minutes. The purification of the plasmid DNA from these cells was carried out using the QIAprep spin miniprep kit (Qiagen). The quality of the purified DNA from each miniprep was checked by running a sample on an agarose gel.

2.2.6. Restriction Digest of DNA

Restriction enzymes were used in accordance with the manufacturers instructions

and with the buffers supplied. Digestion reactions were carried out at 37°C for varying lengths of time according to the DNA being digested. Reactions were stopped by using QIAquick Nucleotide Removal kit (Qiagen).

2.2.7. Purification of M13 single-stranded DNA

5 μl of a CJ236 *E.coli* overnight culture was transferred to 10 ml LB containing 30 μg/ml chloramphenicol and incubated at 37°C for 6 hours. The culture was then inoculated with M13 FABP wild-type phage stock and incubated at 37°C overnight. The following day the purification of the single-stranded DNA was carried out using the QIAprep spin M13 kit (Qiagen).

2.2.8. Ligation of DNA

Reagents: 10x ligation buffer (30 mM Tris.HCl (pH 7.8), 10 mM $MgCl_2$, 10 mM DTT & 1 mM ATP)

T4 DNA ligase (3 u/μl)

The total ligation volume used was 10 μl and the gene:vector ratio was at least 3:1 for optimum ligation. 3 units of T4 DNA ligase were used in every 10 μl ligation reaction. The ligation reaction tubes were floated in 4 L of water at room temperature which was transferred to 4°C and allowed to cool slowly overnight.

2.2.9. DNA Sequencing

Sequencing of mutagenesis products was carried out by Oswel, Southampton, UK.

2.3. Purification of Recombinant Rat LFABP

A synthetic gene for rat liver FABP has been cloned into the pET11a vector using the Nde I and Hind III restriction sites and is expressed in BL21(DE3) *E.coli* cells. Two 10 ml volumes of Luria-Bertani (LB) broth containing 100 μg/ml ampicillin were inoculated with individual colonies of BL21(DE3)[pET11a FABP] and grown at 37°C overnight. These cultures were added to 2 x 1 litre flasks of LB containing 100 μg/ml ampicillin and grown until an OD_{600} of between 0.6-0.8 was reached. The cells were induced by the addition of a final concentration of 0.4 mM IPTG. The bacteria were harvested 5 hours later by centrifugation at 3,000 g for 20 minutes at 4°C.

The bacterial pellets were resuspended in 3 ml of cell lysis buffer (50 mM Tris.HCl pH 8.0, 1 mM EDTA, 100 mM NaCl) per gram of *E.coli*. 4 μl of 100 mM phenylmethylsulphonylfluoride per gram of *E.coli* and 80 μl of 10 mg/ml lysozyme per gram of *E.coli* were added to the cells and stirred at 4°C for 20 minutes. 4 mg of deoxycholate per gram of *E.coli* was added and the cells were incubated at 37°C for 30 minutes. Cells were disrupted using a probe sonicator for 5 cycles of 20 seconds on, 20 seconds off at 14 watts. Cell debris was then removed by centrifugation at 10,000 g for 25 minutes.

Purification of LFABP began with 30% saturation of the supernatent with ammonium

sulphate at 4°C for 1 hour followed by removal of the resultant precipitate by centrifugation at 10,000 g for 30 minutes. Further ammonium sulphate was added to the supernatent up to 60% saturation at 4°C for 1 hour followed by centrifugation at 10,000 g for 30 minutes. The majority of the LFABP remains in solution at 60% ammonium sulphate saturation. The supernatent was dialysed against 20 mM KH_2PO_4 buffer, pH 7.4, overnight to remove the ammonium sulphate from the protein sample. After this stage there have been three different methods used to purify the LFABP, as described below.

2.3.1. Napthoyiaminodecyl-agarose (NAG) Affinity Chromatography

Naphthoylaminodecyl-agarose was prepared by condensing 1-naphthoyl chloride with aminodecylagarose (Sigma) [68]. Such columns have a binding capacity for LFABP of about 1 mg protein per ml of bed volume. The LFABP-containing supernatent after ammonium sulphate fractionation and dialysis was applied to the column and unwanted proteins were eluted using 0.1 M KH_2PO_4 buffer, pH 7.4. The LFABP was eluted from the NAG column using 0.1 M KH_2PO_4 + 25% ethanol, pH 7.4, as the elution buffer. The eluted LFABP was detected in the elution buffer by analysing the DAUDA binding properties of a 100 μl sample of eluate. The eluate was added to 1 ml of a 1 μM solution of DAUDA in 10 mM Hepes buffer, pH 7.4 and the fluorescence emission of the sample was measured at 500 nm following excitation at 350 nm (Figure 2.3.1). Increases in the fluorescence emission of sample containing LFABP would be expected to be approximately 10-fold that of the fluorescence of DAUDA in 10 mM Hepes buffer. The eluted pure LFABP was then dialysed against 20 mM KH_2PO_4, pH 7.4, overnight to remove the ethanol.

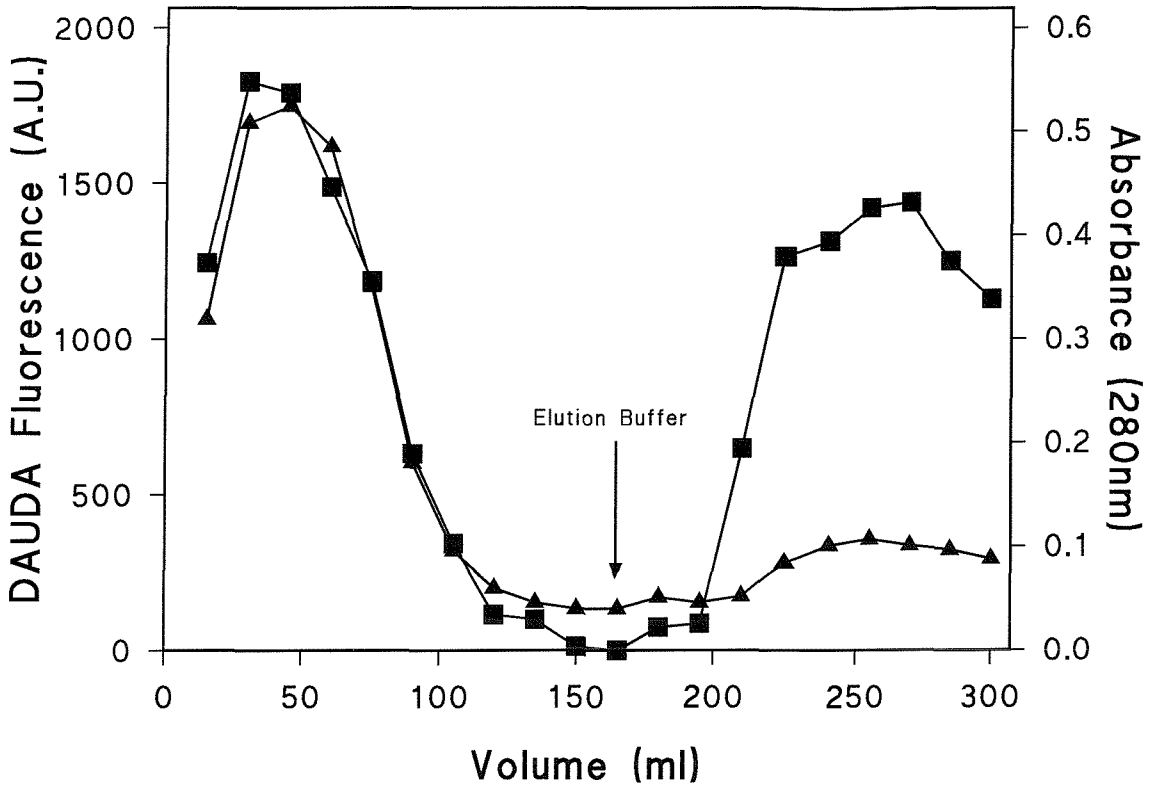

Figure 2.3.1. **Elution Profile of LFABP From NAG Column**

Fractions from the NAG column were assayed for DAUDA fluorescence (■), which was measured in Arbitrary Units (A.U.) at 500 nm following excitation at 350 nm, and also for absorbance at 280 nm (▲). LFABP was eluted in 0.1 M KH_2PO_4 + 25 % ethanol.

2.3.2. Dansylaminodecyl-agarose (DAG) Affinity Chromatography

Dansylaminodecyl-agarose affinity chromatography was the method originally developed for the purification of LFABP [69], however, there was some concern about the long term stability of this particular column. As a result, NAG was developed as an alternative. In fact both types of column lose binding capacity with time and are only effective for about 2-3 rounds of purification.

The DAG method utilised dansyl chloride to attach a dansyl group to the aminodecyl-agarose. The LFABP bound with high affinity to the dansylaminodecyl-agarose and all the other unwanted proteins were washed through with 0.1 M KH_2PO_4, pH 7.4, buffer. The LFABP was eluted from the column using 0.1 M KH_2PO_4 + 40% ethanol, pH 6.0, as the elution buffer. LFABP was detected in the elution buffer by using DAUDA binding. The pure LFABP was then dialysed against 20 mM KH_2PO_4, pH 7.4, overnight to remove the ethanol from the protein sample.

2.3.3. Dodecyl-agarose Purification

Aminodecyl-agarose that is required for the preparation of NAG and DAG is no longer available in the UK so alternative methods of purification using affinity chromatography were attempted. Octyl-agarose, decyl-agarose and dodecyl-agarose were all obtained from Sigma and investigated for LFABP binding properties. All of these aforementioned agarose compounds were found to be unsuitable for column packing as the packing density was too great to allow any flow through the column. As a result of this the different types of agarose were incubated

on ice in 50 ml centrifuge tubes with LFABP samples that had undergone 60 % ammonium sulphate fractionation and dialysis. The tubes were incubated on ice, shaking, for 10 minutes, the samples were centrifuged at 10,000g for 1 minute and the supernatent assayed for DAUDA binding as described above for the eluate from the NAG column. The LFABP was eluted from the agarose using 0.05 M KH_2PO_4 + 40 % ethanol. All the types of agarose that were tested bound LFABP to some extent, although the dodecyl-agarose was found to have a greater capacity for LFABP binding than either the octyl-agarose or the decyl-agarose. It was decided to use dodecyl-agarose as the purification matrix for LFABP.

The dodecyl-agarose binds LFABP wild-type in a ratio of about 1 mg LFABP/ml dodecyl-agarose. Approximately 20 mg LFABP was purified at a time. Firstly, 20 ml dodecyl-agarose was split between 2 X 50 ml centrifuge tubes and washed and equilibrated with 0.1 M KH_2PO_4, pH 7.4 buffer by centrifugation at 10,000 g, 4 C for 1 minute. The solution was poured off and the dodecyl-agarose resuspended in 0.1 M KH_2PO_4 followed by centrifugation. This was repeated several times to equilibrate the dodecyl-agarose with the buffer.

The impure LFABP sample (~20 mg) was loaded into the tubes instead of the phosphate buffer after the final wash step. The tubes were placed in ice on a shaker for 10 minutes to ensure complete binding of the LFABP to the dodecyl-agarose. The dodecyl-agarose was then washed again repeatedly with 0.1 M KH_2PO_4, pH 7.4 by centrifugation as before in order to remove any unbound proteins. The pure LFABP was eluted using 0.05 M KH_2PO_4, pH 7.4 buffer with between 20-40% ethanol which varies according to different mutations in the protein. Eluted LFABP

was dialysed against 20 mM KH_2PO_4, pH 7.4 buffer overnight to remove any ethanol.

2.3.4. Delipidation on Lipidex

The final stage of LFABP purification was to remove any bound fatty acids using a Lipidex (hydroxyalkoxypropyldextran) column. The principle of the method is that at 37 °C the fatty acids partition into the Lipidex beads rather than remain bound to the protein and so the protein flows freely through the column whilst the fatty acids remain bound within the beads. The Lipidex was hydrated in AnalaR water overnight and then equilibrated with 10 mM KH_2PO_4, pH 7.4 buffer at 37 °C prior to the loading of the LFABP. The LFABP sample was then washed through the Lipidex column with 10 mM KH_2PO_4, pH 7.4 buffer, all the fatty acids were retained on the Lipidex. The protein was concentrated on a YM3 membrane (molecular weight cut-off of 3000) in an Amicon concentrating cell.

2.3.5. SDS Polyacrylamide Gel Electrophoresis

SDS polyacrylamide gel electrophoresis (SDS-PAGE) was used to determine the molecular weight of the protein to ensure it is correct for LFABP and also to determine the purity of the protein. The method used is based on that of Laemmli (1970) [70].

2.3.5.1. Coomassie blue staining

Most SDS-PAGE staining was carried out using a coomassie blue stain (40 % methanol, 7 % acetic acid, 0.025% coomassie blue (w/v)). The destain solution used was 45 % methanol, 5 % acetic acid.

2.3.5.2. Silver staining

Where a very sensitive staining technique was required silver staining was used, this method can be used to visualize nanogram quantities of protein. This method was used when developing the dodecyl-agarose purification method the check that the LFABP samples were completely pure (Figure 2.3.5.2). The method involved using a Silver Stain Plus kit (Biorad) according to the manufacturers instructions.

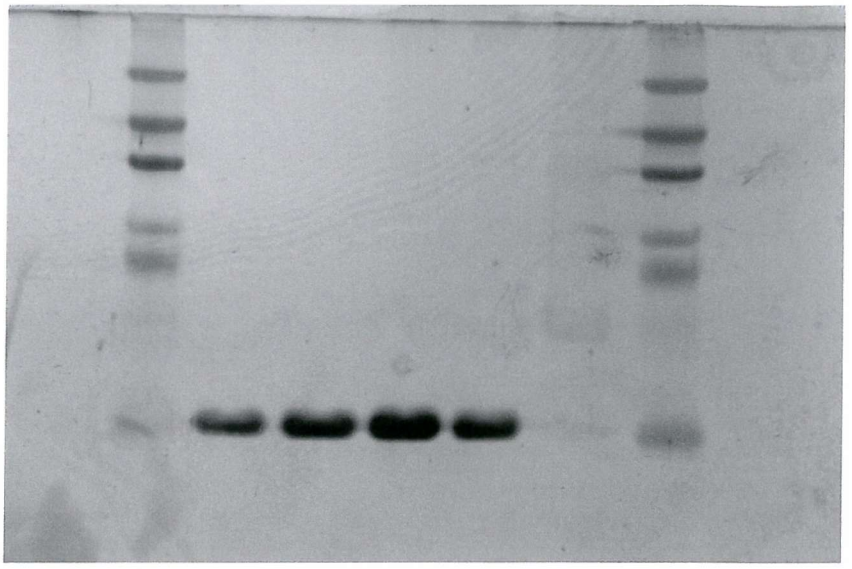

Lanes: 1 2 3 4 5 6 7

Figure 2.3.5.2. Silver Stained SDS-PAGE of LFABP Wild-Type Dodecyl Purification

Lanes 1 and 7 contain the low molecular weight markers showing, from the top of the gel, 66 kDa, 45 kDa, 36 kDa, 29 kDa, 24 kDa, 20 kDa and 14.2 kDa. Lanes 2-5 contain LFABP wild-type fractions from the dodecyl-agarose purification. Lane 6 contains a sample of the supernatent following the loading of the LFABP onto the dodecyl-agarose.

2.3.6. Determination of Protein Concentration

Protein concentration was determined based on a Bicinchoninic acid (BCA) method as described by Smith et al. (1985) [71]. The BCA system detects Cu^{1+} produced during the biuret reaction. The reagents were obtained from Sigma and the assay carried out according to the manufacturers instructions. The assays were performed in triplicate and the absorbance after 30 minutes was measured at 562 nm.

A further method used to determine the protein concentration of wild-type LFABP samples was using the absorbance at 280 nm. It has been found previously that a 1 mg/ml LFABP solution gives A_{280} = 0.45. Using this as a standard, the concentration of any pure LFABP solution can be worked out from the absorbance value at 280 nm providing that it is not a mutant with a changed aromatic amino acid or cysteine content [72].

2.4. Fluorescence Displacement Assay Preparation

2.4.1. Preparation of Small Unilamellar Vesicles (SUVs)

Phospholipids were obtained as either a lyophilised powder or dissolved in chloroform/methanol. The solubilized phospholipids were first dried down under a stream of nitrogen gas to remove any traces of solvent. Stock solutions of phospholipids were made up as either 10 mg/ml or 2 mg/ml dissolved in methanol. Phospholipids were added into the assay cuvette by methanol injection which produces the small unilamellar vesicle (SUVs). If the phospholipids required are not

soluble in methanol then SUVs have to be made by the probe sonication of multi-lamellar vesicles (MLVs). See below for MLV preparation.

2.4.2. Preparation of Multi-lamellar Vesicles (MLVs)

A known quantity of the methanol/chloroform stocks of phospholipids were dried down under a stream of nitrogen gas in a glass vial and a known volume of 10 mM KH_2PO_4, pH 7.4 buffer was added to the phospholipids. The suspension was left at room temperature for 10 minutes before vortexing for 10 minutes to produce the MLVs.

2.4.3. Preparation of mixed phospholipid vesicles

For the preparation of mixed phospholipid vesicles the required phospholipid methanol/chloroform stocks were dried down together in the required molar ratio under a stream of nitrogen gas. The mixed phospholipids were then either dissolved in methanol for preparing SUVs or suspended in buffer for preparing MLVs.

2.4.4. Rat Liver Microsome Preparation

Microsomes were prepared from the livers of female Wistar rats using a method developed from those of Hogeboom and also of Bustamante *et al* [73, 74]. Briefly, the livers were thoroughly homogenized in isotonic sucrose buffer and then subjected to differential centrifugation. The final microsomal pellet was suspended in 0.25 M sucrose, 10 mM Hepes, pH 7.5 buffer. The phospholipid content of the

microsomes was estimated using the method of Bartlett (phosphate assay) [75].

2.4.5. Fluorescence Displacement Assay

The fluorescence assay used is based on the binding of a fluorescent fatty acid analogue to LFABP (Figure 2.4.5). The fluorescent probe used was DAUDA which when bound to LFABP in the hydrophobic core and excited at 350 nm, showed greatly enhanced fluorescence compared to that of the probe in the aqueous phase. The increase in fluorescence seen is up to 18 times that of the fluorescence of the solution prior to the addition of LFABP. The spectral blue-shift of the fluorescence emission of DAUDA of about 50 nm is consistent with the probe binding in the hydrophobic cavity of the LFABP. Other ligands for LFABP that bind in the central cavity are able to displace DAUDA from the protein into the aqueous environment, monitored as a loss of fluorescence. This DAUDA displacement provides a convenient assay for assessing the binding of other ligands to the FABP by monitoring loss of fluorescence as the competitive ligand is titrated into a highly fluorescent LFABP/DAUDA complex. The majority of assays were carried out in 10 mM Hepes, pH 7.5 buffer containing 1 μM DAUDA with the further addition of 8 μg LFABP. Measurements were carried out on an Hitachi F-2000 fluorescence spectrophotometer, excitation wavelength 350 nm and emission wavelength 500 nm. All data shown are representative of assays repeated in triplicate and are subject to errors of <10%. Error bars are not always shown for clarity. Analysis of ligand binding by measuring DAUDA displacement was performed using the method of Kane and Bernlohr [76] according to the equation:

$$K_i = [I_{50}]/(1 + [L]/Kd)$$

Where *Ki* = apparent inhibitor concentration, [L] = free concentration of fluorescence fatty acid analogue (DAUDA) and *Kd* = apparent dissociation constant of LFABP for DAUDA. This method requires that 50 % displacement of DAUDA by the ligand is achieved and was not applicable to lower affinity ligands that had limited monomeric solubility, such as lysophospholipids.

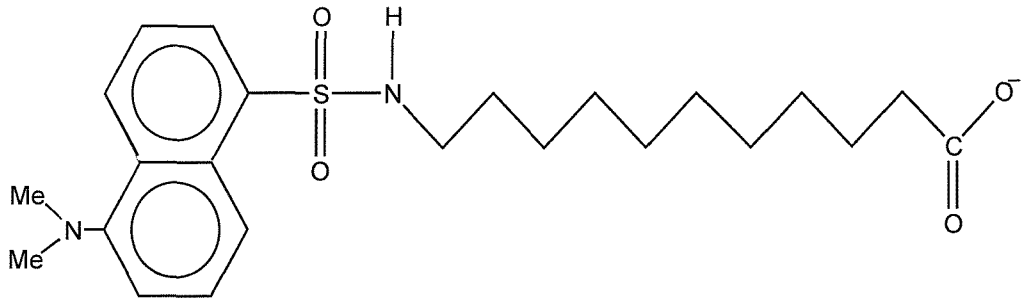

Figure 2.4.5. (11-(5-dimethylaminonapthalenesulphonylamino)undecanoic acid

2.4.6. Assay of LFABP Binding to Phospholipid Vesicles Monitored by Loss of DAUDA Fluorescence

Assays involving the addition of phospholipid vesicles via methanol injection into the LFABP/DAUDA complex were corrected for changes in fluorescence due to the DAUDA partitioning into the vesicles. Blank titrations were carried out of phospholipid into 1 μM DAUDA in 10 mM Hepes, pH 7.5 buffer.

2.5. Tryptophan Fluorescence Assays

2.5.1. Tryptophan Fluorescence

All the fluorescence studies carried out on tryptophan mutants were using an F-4500 fluorescence spectrophotometer set at an excitation wavelength of 280 nm with the emission data measured at between 300-400 nm. Assays using the tryptophan mutants were carried out in 10 mM Hepes, pH 7.5 buffer with 1 μM LFABP. Phospholipids were titrated into the assay cuvette by methanol injection. Blanks titrations of methanol into LFABP in 10 mM Hepes and of phospholipid into 10 mM Hepes, pH 7.4 buffer in order to correct for any direct effect of methanol on LFABP and any effect of phospholipids on the background fluorescence of the sample.

2.5.2. Fluorescence Resonance Energy Transfer (FRET) using DHPE

SUVs containing DHPE were titrated into the assay cuvette by methanol injection as a 5 mol% mixture with DOPG. As described above, the conditions for the assay were 10 mM Hepes, pH 7.5 buffer containing 1 μM LFABP. The tryptophan residue was excited at 280 nm and the emission spectrum measured between 300-550 nm.

2.5.3. Fluorescence Quenching Using Succinimide

Succinimide was titrated as an aqueous solution into 1 μM LFABP in 10 mM Hepes buffer up to a concentration of 0.5 M, both in the presence and absence of 20 μg DOPG SUVs. The F4500 fluorescence spectrophotometer was set at an excitation

wavelength of 280 nm and an emission scan was performed between 300-400 nm. Quenching curves were analysed by the modified Stern-Volmer method [77].

Chapter Three:

Binding of Recombinant Rat Liver FABP to Small Anionic Phospholipid Vesicles

3.1. Introduction

In Chapter 1 the structure and functions of FABPs were discussed both in relation to ligand binding and possible mechanisms for ligand transfer to membranes. In terms of the release of fatty acids to membranes, previous work carried out on FABP has shown LFABP to behave differently to other forms of the protein, for example, heart FABP (HFABP), adipocyte FABP (AFABP) and intestinal FABP (IFABP). Work published by Storch et al [26-28] provides evidence for a collisional mechanism for the transfer of fatty acids from FABP to model phospholipid membranes. It has been proposed that these collisional interactions between FABP and membranes occur with several forms of the protein but not LFABP, for which it was suggested that fatty acids released from the protein are delivered to membranes by an aqueous diffusion mechanism. This mechanism of aqueous diffusion was proposed following observations that the rate of transfer of anthroyloxy-labelled fatty acids to model membranes from LFABP was substantially affected by aqueous phase variables and also by properties of the membrane itself [78]. The work of Storch *et al* has been discussed in more detail in Chapter 1 of this work.

Preliminary studies in our laboratory had demonstrated that under conditions of low ionic strength, the fluorescence of the LFABP/DAUDA complex decreased significantly in the presence of small anionic phospholipid vesicles. This phenomenon is investigated further in order to define the molecular basis of the binding of LFABP to the anionic phospholipid interface.

3.2. Anionic Phospholipid Vesicles Cause the loss of LFABP-enhanced DAUDA Fluorescence

The fluorescence displacement assay was used to study the binding of LFABP to phospholipid vesicles, as described in the Materials and Methods section of this work. Briefly, this assay involves the binding of DAUDA, a fluorescent fatty acid analogue, to LFABP, which results in a large fluorescence enhancement of the probe compared to the fluorescence of the probe in an aqueous environment. The addition of SUVs of anionic phospholipid (DOPG), formed through injection of a methanol solution into 50 mM Hepes buffer, to the LFABP/DAUDA complex was found to cause a significant loss of protein-enhanced DAUDA fluorescence. The addition of excess DOPG SUVs achieved fluorescence values comparable to those of DAUDA in 50 mM Hepes buffer in the absence of LFABP, which is consistent with the release of the DAUDA from LFABP into the aqueous phase. This is shown in Figure 3.2.1. That the DAUDA was indeed released and not simply bound to LFABP in a non-fluorescent complex due to conformational changes was supported by further addition of LFABP. This addition of excess LFABP resulted in an increase in fluorescence consistent with the protein binding to DAUDA in solution (data not shown). Therefore, it can be concluded that the addition of DOPG vesicles into the LFABP/DAUDA complex results in the release of the DAUDA from the LFABP.

The effects of SUVs prepared from neutral phospholipid, such as PC, were also investigated in order to establish whether the phenomenon of loss of LFABP/DAUDA fluorescence could be attributed to phospholipid vesicles in general or whether there is a specific requirement for anionic phospholipid vesicles. DOPC is a zwitterionic

phospholipid, which is neutral at pH 7.5 and is, therefore, considered to be a neutral phospholipid for the purpose of this study. The experiment was performed as for the DOPG titration, with DOPC titrated by methanol injection into a solution of the LFABP/DAUDA complex in 50 mM Hepes buffer. The results show that there was no detectable loss of protein enhanced DAUDA fluorescence upon addition of DOPC SUVs to the LFABP/DAUDA complex (Figure 3.2.2). Data was corrected for the partitioning of DAUDA into the DOPC SUVs as this is significant and was observed as an enhancement of the DAUDA fluorescence by approximately 10-20 %. The effect of DOPE SUVs was also investigated under the same conditions as for DOPC SUVs as DOPE is also a zwitterionic phospholipid that is essentially neutral at pH 7.5 (Figure 3.2.2). As shown by the data in Figure 3.2.2., there was no significant loss of LFABP/DAUDA fluorescence in the presence of DOPE SUVs. It can, therefore, be concluded that the phenomenon of loss of LFABP/DAUDA fluorescence in the presence of phospholipid vesicles has a requirement for anionic vesicles and is not observed with zwitterionic vesicles.

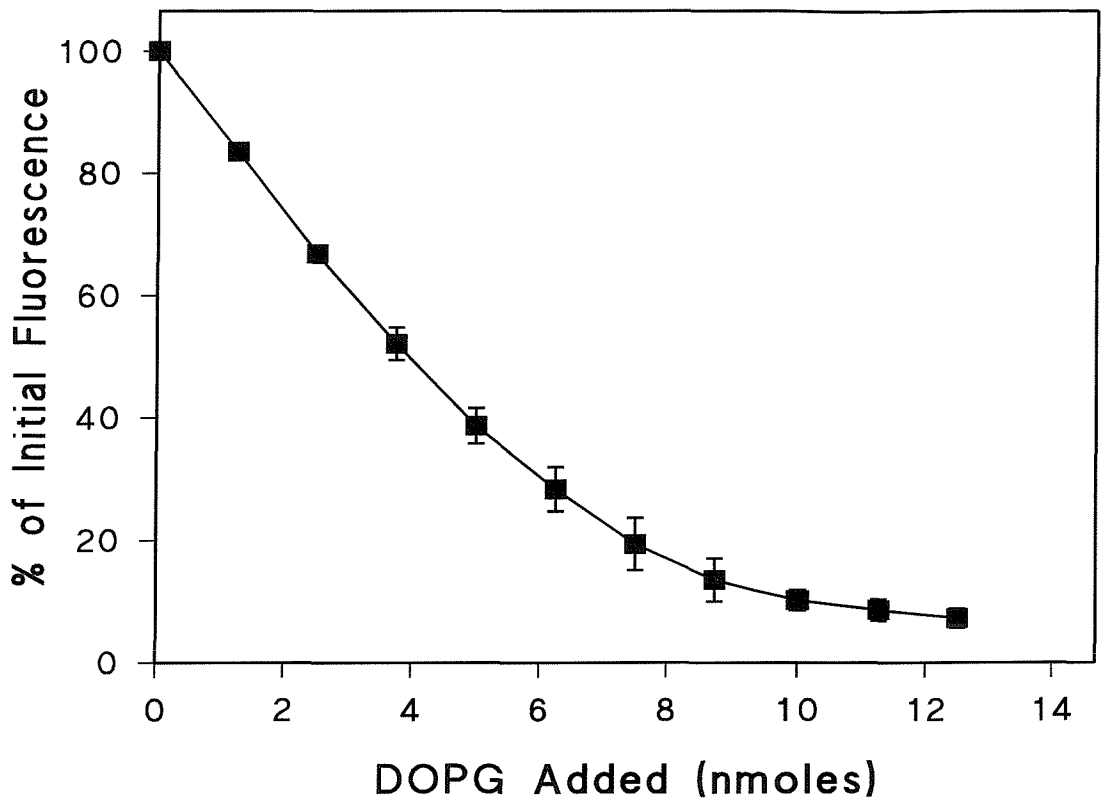

Figure 3.2.1. **Effect of 100% DOPG SUVs on LFABP/DAUDA Fluorescence**

DOPG was titrated by methanol injection into 50 mM Hepes, pH 7.5, buffer in the presence of 1 μM DAUDA and 5 μg (0.4 nmoles) LFABP. The fluorescence of the LFABP/DAUDA complex was measured at 500 nm following excitation of the dansyl group of DAUDA at 350 nm. All data points are the mean values of three separate titrations and are not corrected for the partitioning of DAUDA into the phospholipid vesicles.

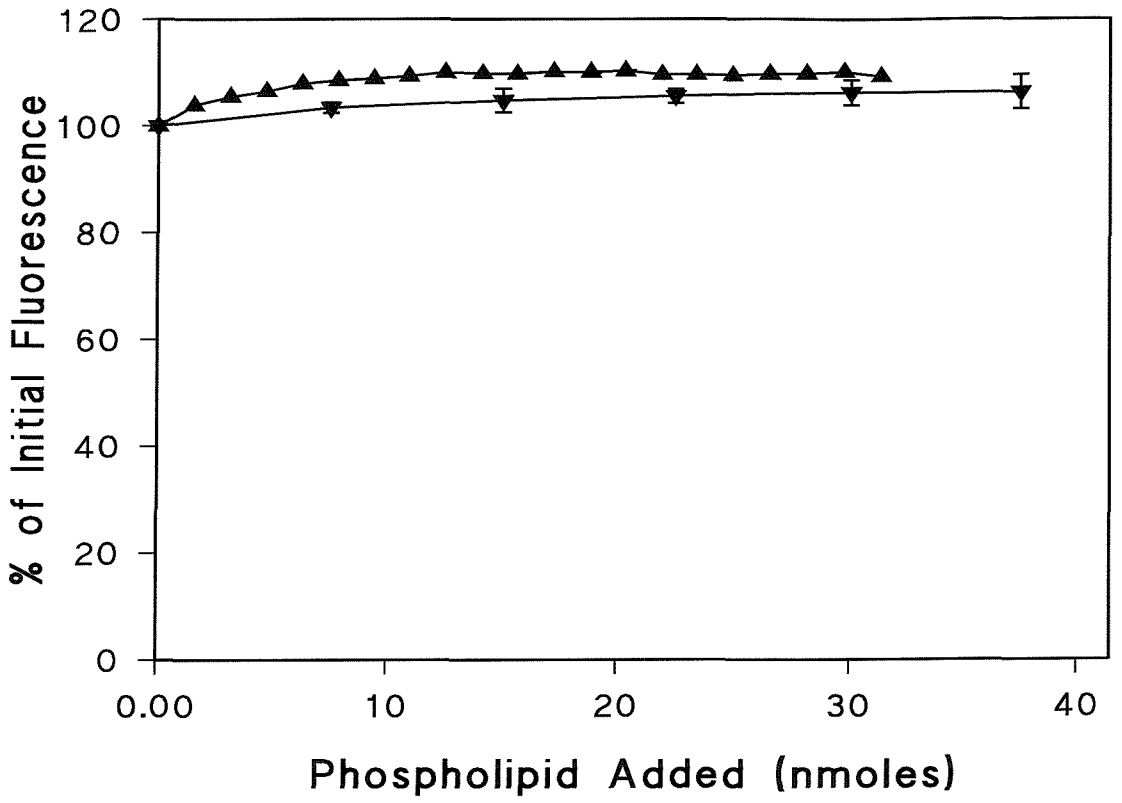

Figure 3.2.2. **The Effect of 100% DOPC and 100% DOPE SUVs on the Fluorescence of the LFABP/DAUDA complex**

DOPC (▼) and DOPE (▲) were titrated by methanol injection into 50 mM Hepes buffer containing 5 μg (0.4 nmoles) LFABP and 1 μM DAUDA. The fluorescence of the LFABP/DAUDA complex was measured at 500 nm following excitation at 350 nm. Values are corrected for the partitioning of DAUDA into the phospholipid vesicles and are the mean values of three separate titrations.

The same phenomenon of loss of LFABP-enhanced fluorescence should be observed when the order of addition is reversed, i.e. the LFABP/DAUDA complex is titrated into buffer containing DOPG SUVs. This is indeed the case as shown in Figure 3.2.3. The titration of LFABP/DAUDA into 10 mM Hepes containing DOPG SUVs showed an initial lack of response and this lack of fluorescence increase was consistent with the inhibition of DAUDA binding to LFABP until the LFABP is present in stoichiometric excess to the DOPG vesicles. Titrations of the LFABP/DAUDA complex into 10 mM Hepes alone and into 10 mM Hepes containing DOPC SUVs were also carried out and showed a linear increase in fluorescence upon addition of the LFABP/DAUDA complex (Figure 3.2.3). The titration of LFABP/DAUDA into the assay containing DOPC was greater than that seen when titrating into buffer alone. This increase could be due either to free DAUDA partitioning into the DOPC vesicles or because the LFABP/DAUDA complex is able to bind to the DOPC interface and this binding enhances the LFABP/DAUDA fluorescence (Figure 3.2.3.)

The end point stoichiometry for both the titration of DOPG SUVs into LFABP/DAUDA and for LFABP/DAUDA titration into DOPG SUVs the stoichiometry was calculated to be 12.5 nmoles (10 μg) DOPG : 0.4 nmoles LFABP, thereby giving a ratio of approximately 30. Evidence that this data is consistent with the LFABP coating the phospholipid surface comes from similar studies with $sPLA_2$. This 14 kDa protein has been shown to coat the surface of anionic phospholipid vesicles as a result of high affinity binding until a stoichiometry of about 30 nmoles of phospholipid per mole of enzyme [79]. Similarly, studies conducted on cytochrome C [50] have concluded that this protein has a tendency to aggregate on the surface of lipid

vesicles, in particular this has been observed when the vesicles are composed of anionic phospholipid.

Because the phenomenon of loss of fluorescence required charged (anionic) vesicles and low ionic strength, this suggests that the binding of the LFABP to the phospholipid interface is, at least in part, due to electrostatic forces. The nature of these electrostatic interactions was investigated.

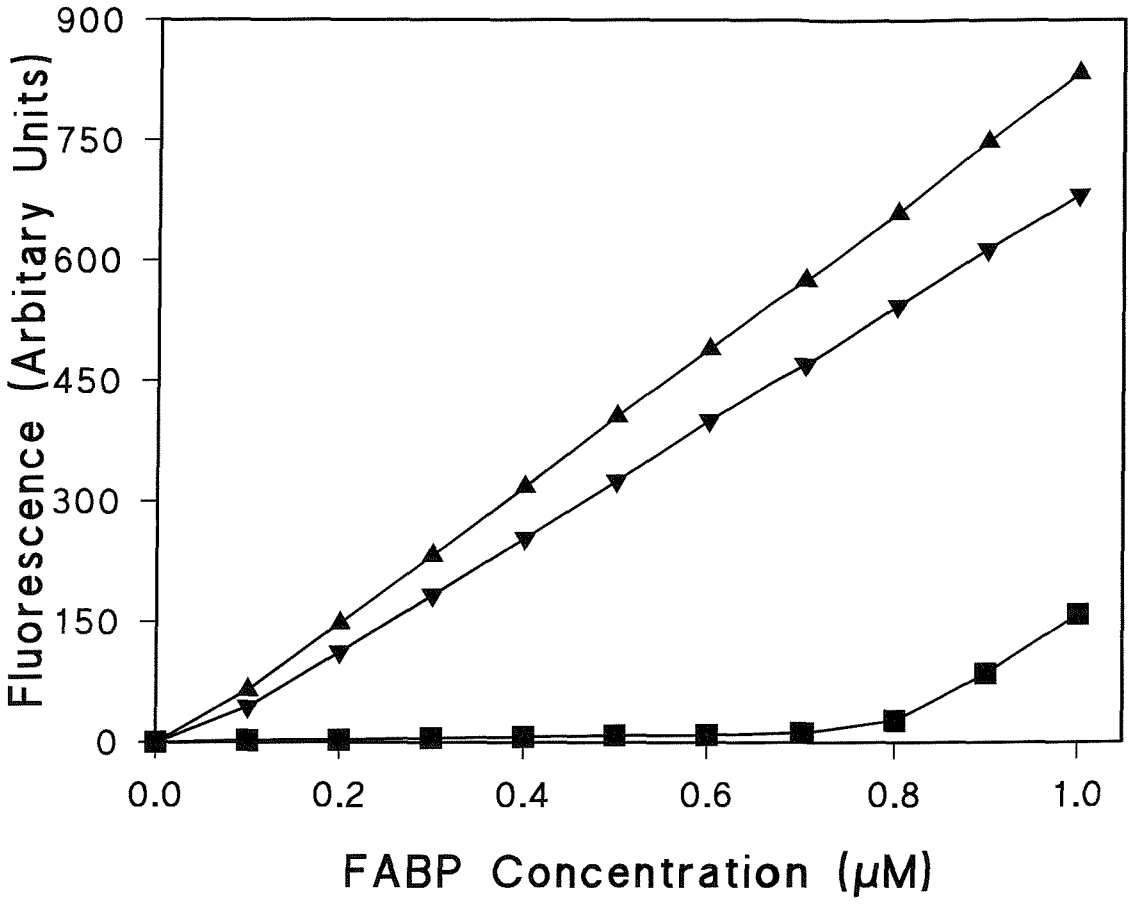

Figure 3.2.3. **Effect of the Titration of the fluorescence LFABP/DAUDA complex into DOPG vesicles**

The fluorescence increase achieved upon the addition of LFABP/DAUDA in a 0.6:1.0 molar ratio into 10 μg (12.5 nmoles) of DOPG SUVs (■), and controls of DOPC (▲) or 10 mM Hepes buffer alone (▼), was monitored. Fluorescence emission was measured at 500 nm following excitation at 350 nm. All data points shown are the mean values of three separate titrations and are corrected for the effect of DAUDA titration alone into the assay systems.

3.3. Phospholipid Charge Density is Important in the Loss of LFABP/DAUDA Fluorescence

The effect of charge density (mol% anionic phospholipid) on loss of fluorescence was investigated. This was particularly relevant because 100 mol% anionic interfaces are not believed to be present in cell membranes. Indeed most internal cell membranes only contain about 10-20 mol% of anionic phospholipid, mostly as PS.

Phospholipid mixtures were prepared with molar ratios of between 100 mol% DOPG and 100 mol% DOPC as methanol stock solutions. A known amount of total phospholipid (8 μg; ~10 nmoles) was added to the LFABP/DAUDA complex in 10 mM Hepes buffer, as shown in Figure 3.3.1. The results indicated a requirement for a minimum charge density of 20 mol% DOPG and an overall sigmoidal relationship between increasing mol% DOPG and % fluorescence of the LFABP/DAUDA complex while no loss of DAUDA fluorescence could be observed with 10 mol% DOPG. This sigmoidal relationship shown between mol% anionic phospholipid and loss of DAUDA fluorescence is a trend characteristic of proteins binding specifically to a phospholipid interface containing anionic phospholipid. There would appear to be a threshold of minimum charge density, typically 10-20 mol% anionic phospholipid, required for the binding of such proteins to anionic phospholipid vesicles which is a result of multiple electrostatic interactions [80, 81].

These investigations were extended to use cardiolipin in place of DOPG as the anionic phospholipid. Titrations of phospholipid vesicles of varying ratios of

DOPG:DOPC and cardiolipin:DOPC were performed into LFABP/DAUDA in 10 mM Hepes buffer (Figure 3.3.2). Cardiolipin-containing vesicles were found to produce a more sensitive system compared with DOPG-containing vesicles. These vesicles were shown to cause a loss of LFABP/DAUDA fluorescence at 10 mol% anionic phospholipid, compared with the 20 mol% required for loss of fluorescence of the complex using DOPG vesicles. This apparent lower charge density required for the displacement of DAUDA from LFABP by cardiolipin can be attributed, at least in part, to the fact that cardiolipin molecules are dianionic and carry twice the charge density per mole as that of DOPG molecules.

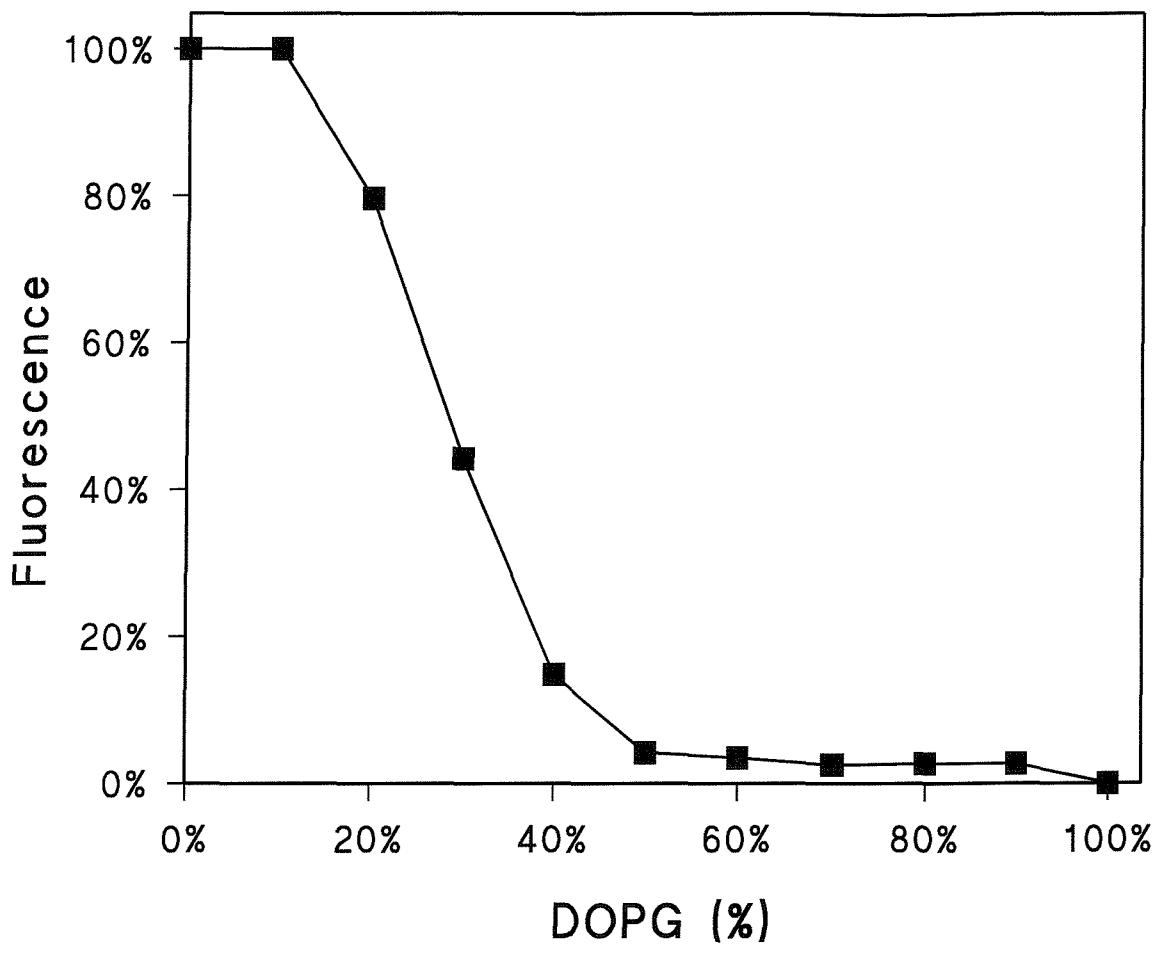

Figure 3.3.1. **Effect of Phospholipid Charge Density on the loss of LFABP/DAUDA Fluorescence**

8 μg (10 nmoles) of total phospholipid of between 0-100% DOPG with DOPC was added into 5 μg (0.4 nmoles) LFABP with 1 μM DAUDA in 10 mM Hepes, pH 7.5 buffer. Fluorescence emission was measured at 500 nm following excitation at 350 nm. Each data point is the mean value of three separate phospholipid additions and is corrected for the effect of phospholipid on DAUDA fluorescence in the absence of LFABP.

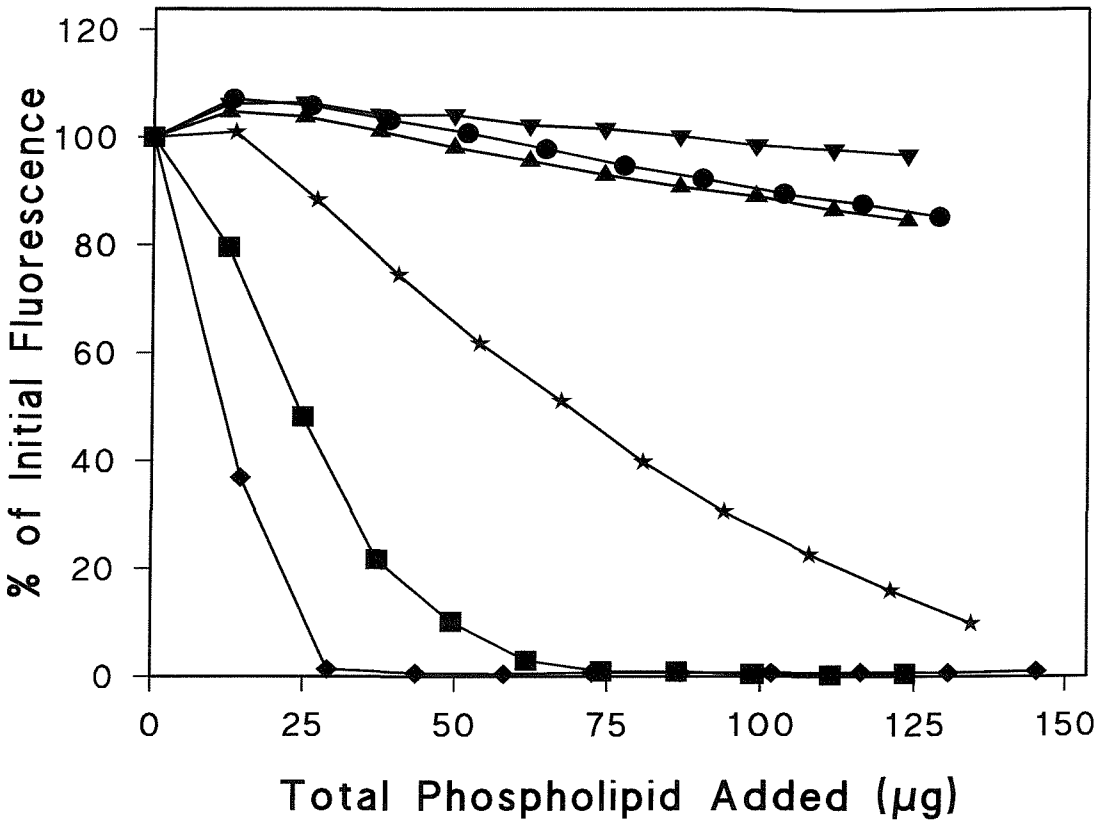

Figure 3.3.2. **A Comparison of the Effects of DOPG and of Cardiolipin SUVs on loss of LFABP/DAUDA Fluorescence**

Varying molar ratios of anionic phospholipid:DOPC were titrated into 8 μg (0.5 nmoles) LFABP in 10 mM Hepes, pH 7.5, buffer containing 1 μM DAUDA. The molar ratios used were: 20 mol% DOPG in DOPC (■), 10 mol% DOPG in DOPC (▲), 5 mol% DOPG in DOPC (▼), 20 mol% Cardiolipin in DOPC (◆), 10 mol% Cardiolipin in DOPC (★) and 5 mol% Cardiolipin in DOPC (●). Fluorescence emission was measured at 500 nm following excitation at 350 nm. All data points are the mean values of three separate titrations and are corrected for titrations in the absence of LFABP.

3.4. The Binding of LFABP to Phospholipid with Different Anionic Headgroups

The binding of LFABP to anionic phospholipids was investigated further by looking at the specificity of binding within this group of phospholipids. 20 mol% mixtures of anionic phospholipid with DOPC were titrated into the LFABP/DAUDA complex in 10 mM Hepes buffer. Mixed vesicles of anionic phospholipid with DOPC were used in order to provide a more physiological model than using 100% anionic phospholipid vesicles. A 20 mol% concentration of anionic phospholipid in DOPC was used to compare the effectiveness of different anionic phospholipids on loss of LFABP/DAUDA fluorescence as it was determined that 20 mol% anionic phospholipid was the minimum amount required to cause the displacement of DAUDA from LFABP using DOPG (Figure 3.3.1)

The phospholipids used to investigate the specificity of LFABP were cardiolipin, DOPG, DOPS and PI mixed with DOPC. Results show cardiolipin to be the most effective anionic phospholipid for displacing DAUDA from LFABP. As mentioned previously, this can be explained by the structure of cardiolipin being similar to that of two molecules of DOPG and therefore it carries twice the charge density of DOPG per molecule. DOPG, DOPS and PI showed similar affinities for LFABP in that there were comparable decreases in DAUDA fluorescence seen upon addition of SUV preparations of these phospholipids (Figure 3.4.1).

The affinity of LFABP for DOPA was also investigated in the same manner as described above. The results are not included in Figure 3.4.1. as the data for this

particular phospholipid varied considerably between assays. It was decided that this was possibly due to the presence of trace amounts of calcium in the assay system which, at the low concentrations of ionic strength used, may cause the DOPA to aggregate. DOPA is known to be particularly sensitive to calcium ions and this would explain the inconsistency of results obtained for this particular phospholipid. Therefore, the titrations were repeated in the presence of 1 mM EGTA in order to chelate any trace calcium ions. Results showed that in the presence of EGTA, LFABP had similar affinities for both DOPG and DOPA (Figure 3.4.2). Overall it was concluded that the apparent head group specificity that LFABP seems to exhibit is more a preference for higher charge density molecules rather than any preference for specific phospholipid headgroups while a minimum charge density is required to demonstrate binding. These characteristics of non-specific electrostatic interactions are very different to those seen when proteins bind to specific phospholipid, e.g. PH domains binding to PIP_2 [3].

It was decided to use 20 mol% DOPG with DOPC SUVs for further work as DOPG behaves similarly to DOPS, the most abundant anionic phospholipid in mammalian cell membranes, in that it is a bilayer forming phospholipid that readily mixes with DOPC.

The effect of using MLVs of anionic phospholipid instead of SUVs was investigated in order to assess the importance of vesicle structure for the loss of LFABP/DAUDA fluorescence. MLVs were prepared as discussed in Section 2.4.2. of this work. There was shown to be no significant loss of fluorescence when MLVs of DOPG were titrated into the LFABP/DAUDA complex in Hepes buffer (data not shown).

This demonstrates the importance of membrane curvature for the interaction of phospholpid vesicles with LFABP. This requirement is also seen for other proteins that bind to phospholipid vesicles, such as sterol carrier protein-2 (SCP2) [82] and *Thermomyces lanuginose* triglyceride lipase [56].

Evidence so far would suggest that electrostatic interactions form at least part of the driving force behind the binding of anionic phospholipid vesicles to LFABP because these interactions are dependant on charge density. These interactions required further investigation to more fully ascertain the nature of the binding of LFABP to phospholipid vesicles.

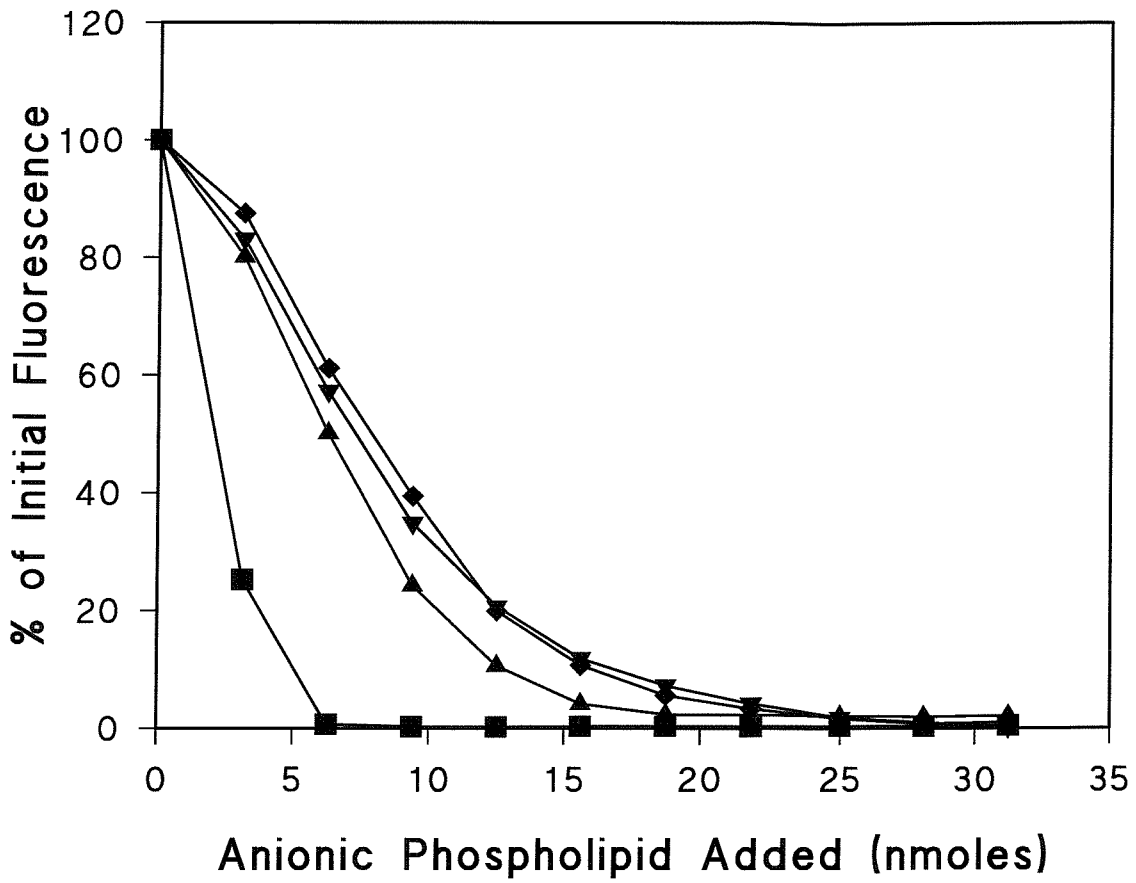

Figure 3.4.1. **Effect of phospholipid head group specificity on the loss of LFABP/DAUDA Fluorescence**

Anionic phospholipids were titrated into 5μg (0.4 nmoles) LFABP in 10 mM Hepes & 1 μM DAUDA as 20 mol% vesicles of cardiolipin (■), DOPG (▲), DOPS (▼) and PI (◆) with DOPC. All data points are the mean values of a total of six separate titrations, 3 from each of two separate phospholipid preparations. Values are corrected for the effect of phospholipid vesicles on DAUDA in 10 mM Hepes buffer.

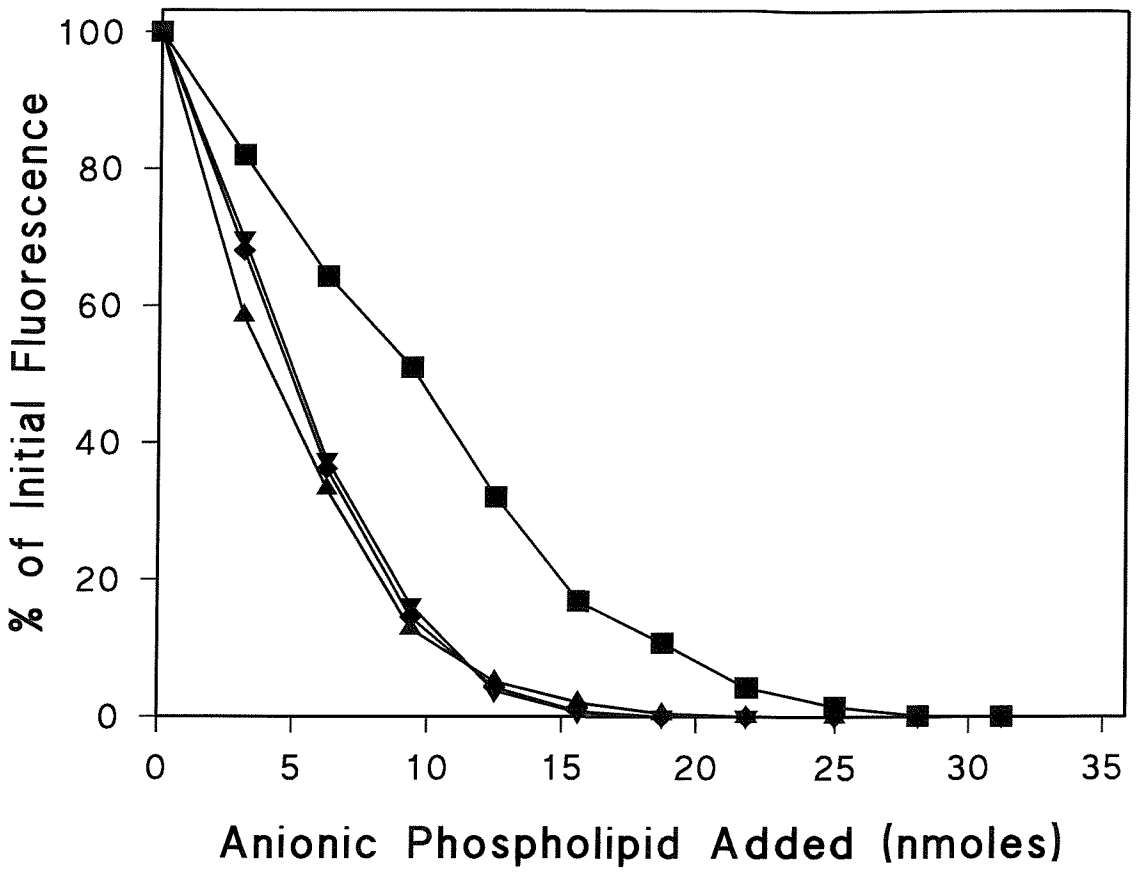

Figure 3.4.2. **The effect of EGTA on the loss of fluorescence of the LFABP/DAUDA complex by 20 mol% DOPA with DOPC and 20 mol% DOPG with DOPC**

20 mol% mixtures of DOPA with DOPC and DOPG with DOPC were titrated into the LFABP/DAUDA complex in the presence and absence of 1 mM EGTA. Data points are the mean values of 3 separate titrations and are corrected for the effect of phospholipid on DAUDA in buffer. DOPA with EGTA (▲), DOPA without EGTA (■), DOPG with EGTA (◆) and DOPG without EGTA (▼).

3.5. The Effect of the Ionic Strength of the Assay on the loss of Protein Enhanced DAUDA Fluorescence by Anionic Vesicles

As has already been demonstrated, it would appear that electrostatic interactions are important in the loss of fluorescence of the LFABP/DAUDA complex by phospholipid. This conclusion was based on the requirement for anionic phospholipids to displace DAUDA from LFABP and that fluorescence is lost from the DAUDA/LFABP complex most readily when cardiolipin is the anionic phospholipid species used, suggesting charge density is important.

In order to provide further evidence for the important role of electrostatic interactions, assays were performed under conditions of increasing ionic strength as shown in Figure 3.5.1. Varying concentrations of NaCl were added to the assay cocktail (50 mM Hepes + 1 μM DAUDA) with final concentrations of NaCl being 20 mM, 50 mM, 100 mM or 200 mM. In addition an assay was performed in 10 mM Hepes. It was found that increasing the ionic strength of the buffer affected the ability of the phospholipid to displace DAUDA from LFABP, while inhibition was almost complete at 200 mM NaCl. The experiment was repeated in the presence of $CaCl_2$ in place of NaCl and inhibition of DAUDA displacement from LFABP by DOPG was found to be complete at a concentration of 5 mM $CaCl_2$ (Figure 3.5.2). These results show that electrostatic forces are indeed important in the initial interaction between anionic phospholipids and LFABP.

The overall importance of electrostatic interactions was further defined in an attempt to recover the LFABP from the bound phospholipid vesicles. The basis of this

approach was that 200 mM NaCl (Figure 3.5.1.) and 5 mM $CaCl_2$ (Figure 3.5.2.) almost completely prevented the binding of the LFABP to the anionic vesicles. The recovery of the protein was determined by the enhancement of DAUDA fluorescence, compared with the fluorescence in the aqueous phase, caused by DAUDA re-binding to LFABP upon release from the phospholipid surface. The method used to recover the protein involved the addition of 200 mM NaCl to the assay immediately following a titration of 20 mol% DOPG with DOPC SUVs into the LFABP/DAUDA complex in Hepes buffer. This produced limited recovery of the LFABP/DAUDA fluorescence (Figure 3.5.3.). The effect of the addition of 5 mM $CaCl_2$, in place of 200 mM NaCl, was also investigated, as Ca^{2+} has previously been shown to be a more effective cation for inhibiting DOPG interaction with LFABP than Na^+. It was found that using $CaCl_2$ produced no increase in the recovery of the protein compared to the recovery achieved using NaCl (Figure 3.5.3.). Approximately 60% of the initial LFABP/DAUDA fluorescence was recovered upon addition of 200 mM NaCl and approximately 60% was also recovered by the addition of 5 mM $CaCl_2$.

The data discussed so far on the recovery of LFABP/DAUDA fluorescence by the addition of salt into the assay system following a titration of phospholipid vesicles has only involved the use of 20 mol% DOPG in DOPC SUVs. It was, therefore, decided to extend the study to include fluorescence recovery following titration of 100% DOPG vesicles into the LFABP/DAUDA complex (Figure 3.5.4). The extent of recovery of fluorescence was found to be significantly less when 100% DOPG vesicles were used, compared with 20 mol% DOPG with DOPC vesicles. When 200 mM NaCl was added to LFABP/DAUDA immediately following a titration of 100%

DOPG vesicles, there was approximately 10-15% recovery of the initial fluorescence values, compared to 60 % recovery in the presence of 20 mol% DOPG vesicles. The recovery of LFABP/DAUDA fluorescence using 5 mM $CaCl_2$ following 100 % DOPG titration produced a three-fold greater increase in the initial fluorescence than did 200 mM NaCl. The greater recovery of LFABP/DAUDA fluorescence produced by $CaCl_2$ compared to NaCl must reflect the nature of the interaction between the divalent calcium ion and the DOPG interface. The reduction of recovery of the LFABP/DAUDA fluorescence when 100 % DOPG vesicles were used compared to 20 mol% DOPG vesicles is not surprising as the higher charge density of the 100 % DOPG vesicles may be producing stronger interactions with LFABP.

The inability to obtain complete release of LFABP from the interface as monitored by recovery of DAUDA fluorescence was a surprising observation and was most apparent with 100 mol% DOPG vesicles. The results suggested a subsequent membrane penetration event probably involving hydrophobic interactions.

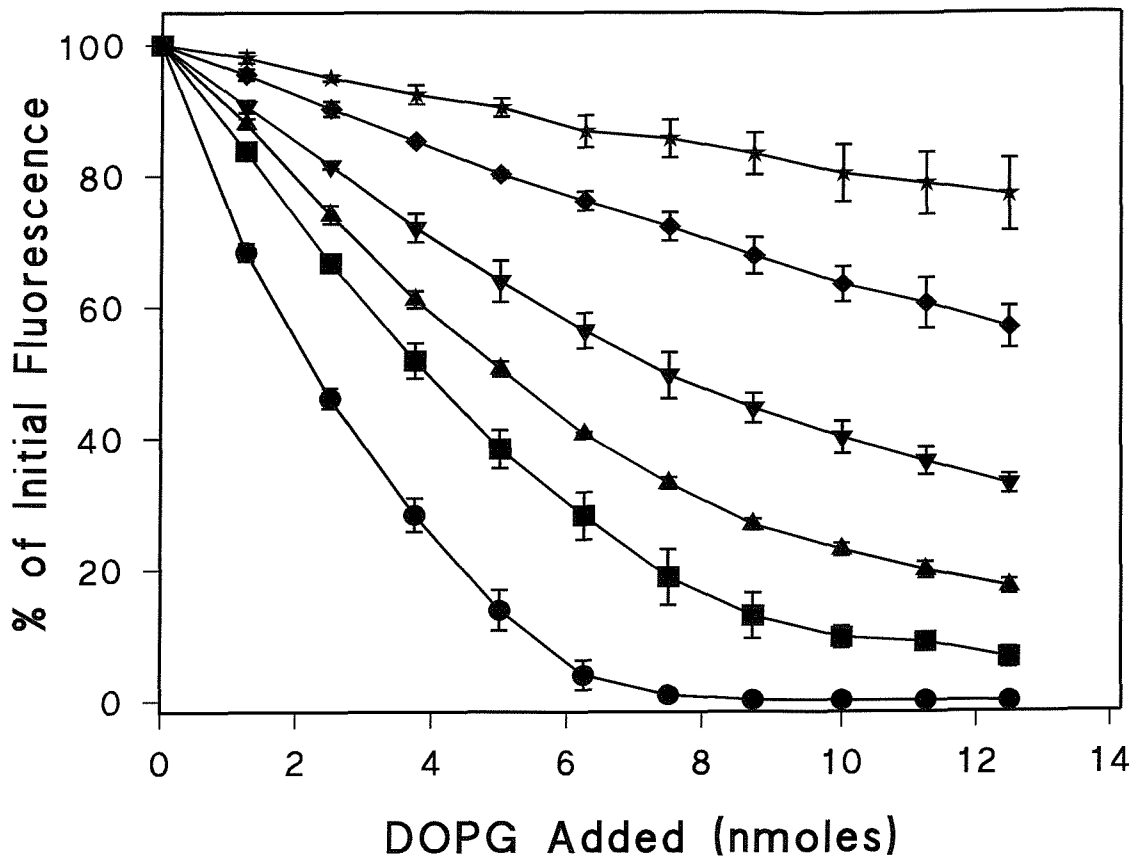

Figure 3.5.1. **Effect of Varying Ionic Strength on the Loss of LFABP/DAUDA Fluorescence Upon Addition of 100% DOPG SUVs**

100 % DOPG SUVs were titrated by methanol injection into 5 μg (0.4 nmoles) LFABP, 1 μM DAUDA under the following conditions, 10 mM Hepes (●), 50 mM Hepes (■), the remaining titrations used 50 mM Hepes & 20 mM NaCl (▲), 50 mM NaCl (▼), 100 mM NaCl (◆) and 200 mM NaCl (★). Fluorescence emission was measured at 500 nm following excitation at 350 nm. All data points are the mean values of three separate titrations.

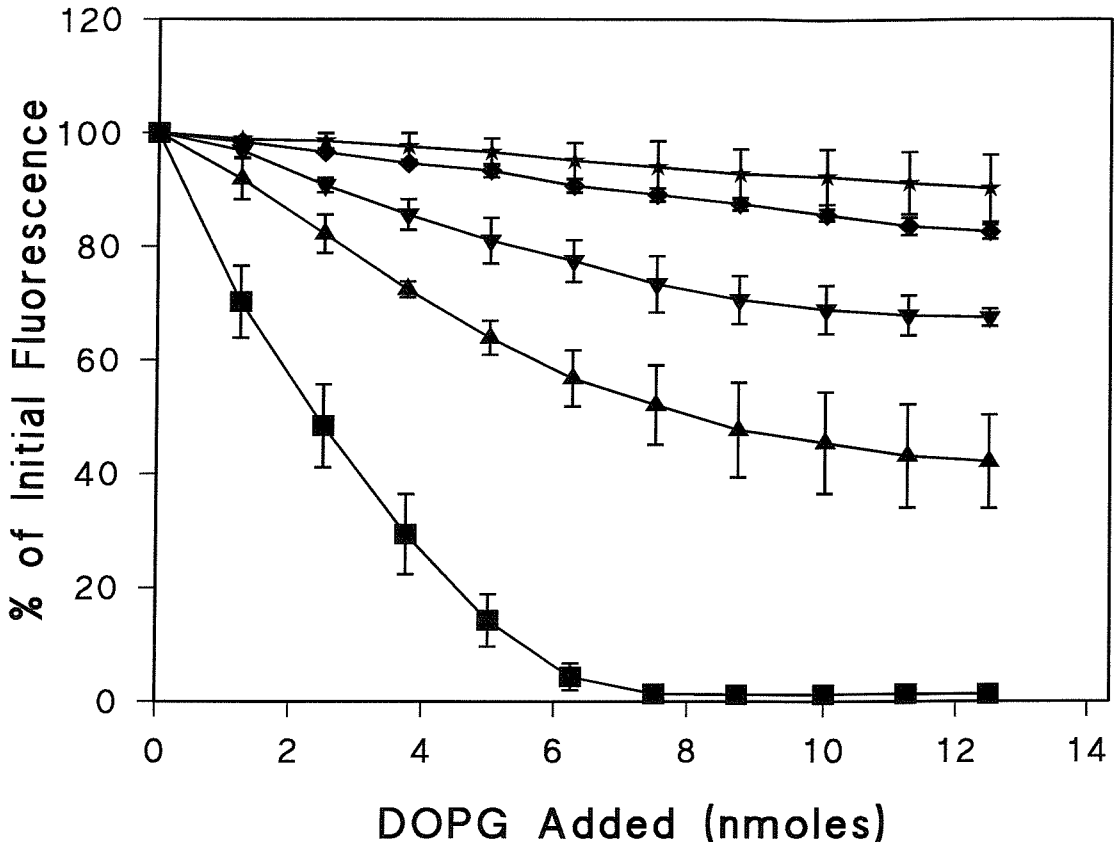

Figure 3.5.2. **Effect of Varying $CaCl_2$ Concentration on the Loss of LFABP/DAUDA Fluorescence Upon Addition of 100% DOPG SUVs**

100 % DOPG SUVs were titrated by methanol injection into 5 μg (0.4 nmoles) LFABP, 1 μM DAUDA under the following ionic conditions: 10 mM Hepes and 0 mM $CaCl_2$ (■), 0.5 mM $CaCl_2$ (▲), 1 mM $CaCl_2$ (▼), 2 mM $CaCl_2$ (◆) and 5mM $CaCl_2$ (★). Fluorescence emission was measured at 500 nm following excitation at 350 nm. All data points are the mean values of three separate titrations and are corrected for the effect of DOPG titration into DAUDA in buffer.

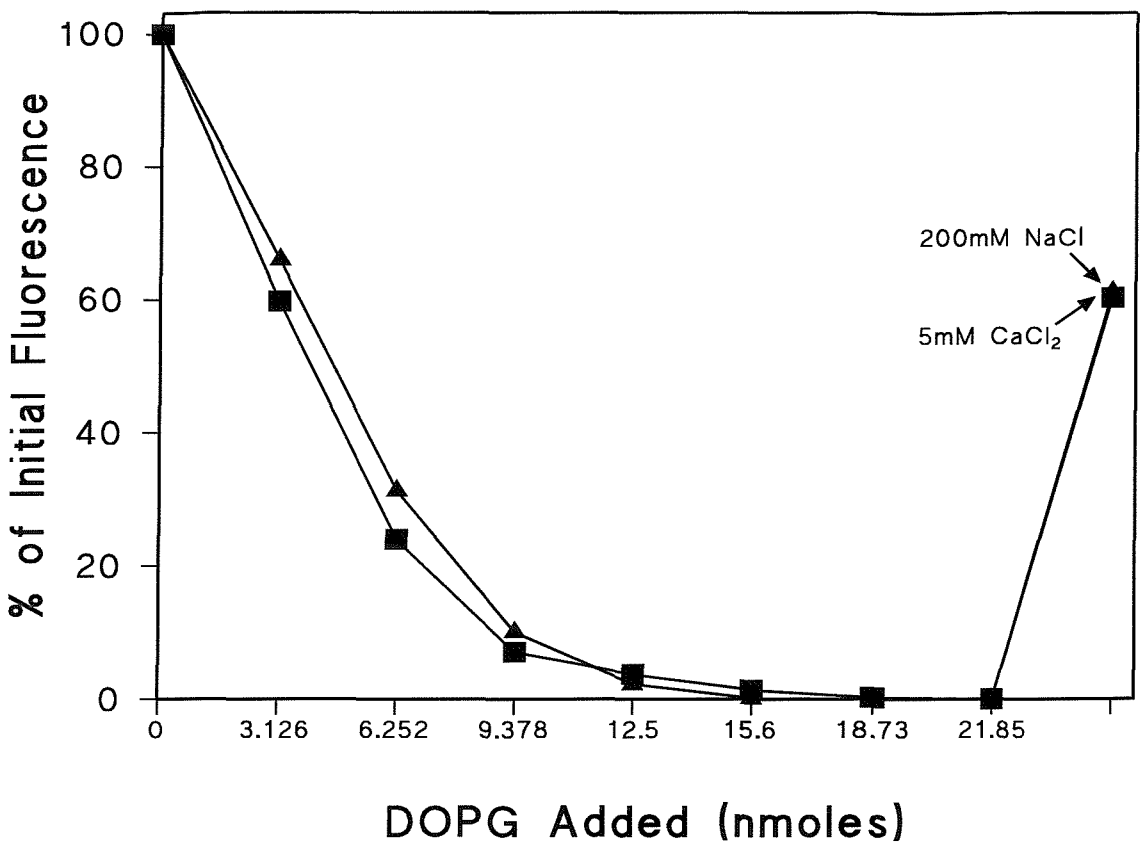

Figure 3.5.3. **The Effect of the Addition of Either 200 mM NaCl or 5 mM $CaCl_2$ to LFABP following a Titration of 20 mol% DOPG with DOPC SUVs in the presence of DAUDA**

The titrations of 20 mol% DOPG with DOPC SUVs into the LFABP/DAUDA complex by methanol injection were carried out in the presence of 10 mM Hepes, pH 7.5, buffer containing 5 μg (0.4 nmoles) LFABP and 1 μM DAUDA. Following each titration of phospholipid vesicles, either 200 mM NaCl (■) or 5 mM $CaCl_2$ (▲) was added into the assay cuvette. Fluorescence emission was measured at 500 nm following excitation at 350 nm. All data points shown are the mean values of three separate titrations and are corrected for dilution factors and also for the effect of the NaCl or $CaCl_2$ on the fluorescence of the LFABP/DAUDA complex.

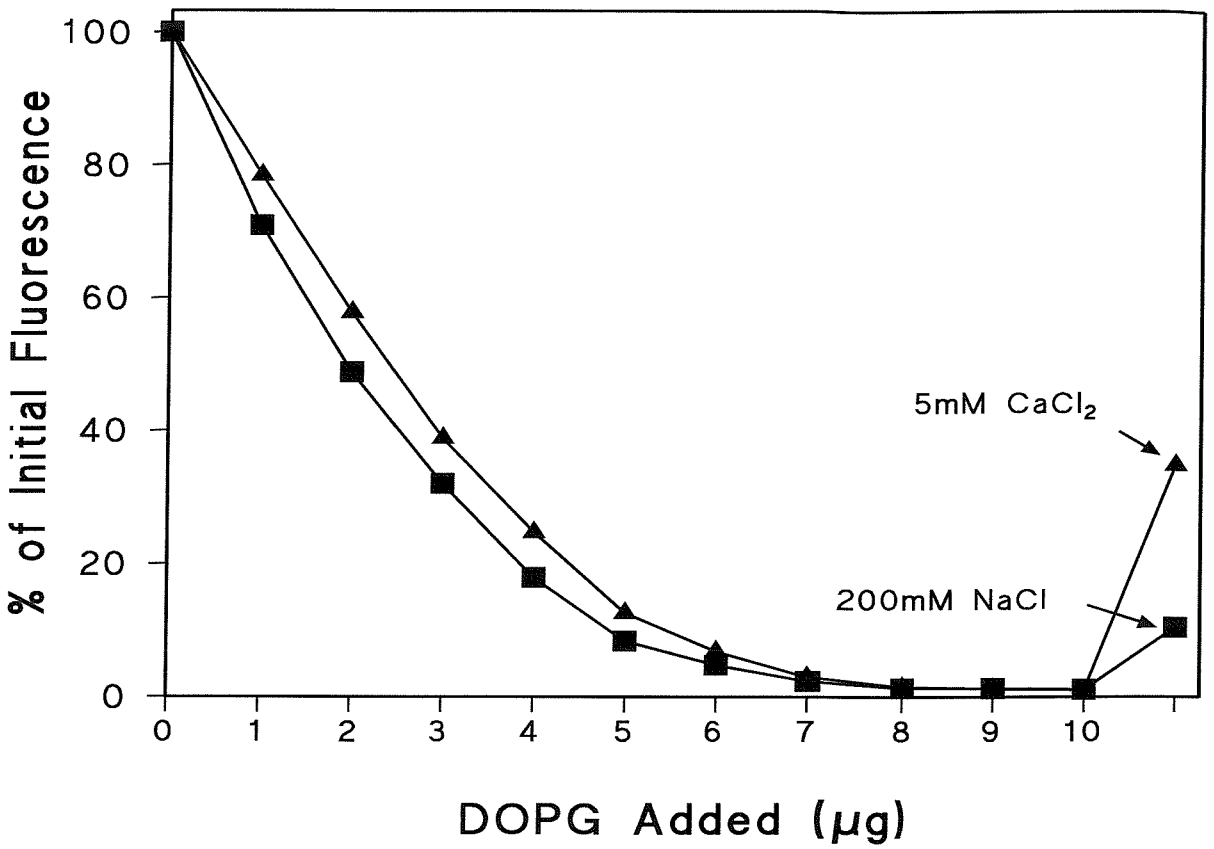

Figure 3.5.4. **The Effect of the Addition of Either 200 mM NaCl or 5 mM $CaCl_2$ to LFABP following a Titration of 100% DOPG SUVs in the presence of DAUDA**

The titrations of 100% DOPG SUVs (1 μg = 1.25 nmoles) into LFABP/DAUDA complex by methanol injection were carried out in the presence of 10 mM Hepes, pH 7.5, buffer. Following each titration of phospholipid vesicles, either 200 mM NaCl (■) or 5 mM $CaCl_2$ (▲) was added into the assay cuvette. All data points shown are the mean values of three separate titrations and are corrected for dilution factors and also for the effect of the NaCl or $CaCl_2$ on the fluorescence of the LFABP/DAUDA complex.

3.6. The Nature of the Interaction Between LFABP and the Phospholipid Interface

Work carried out in this laboratory using indirect fluorescence evidence from dansyl DHPE vesicles and direct evidence from gel filtration has shown that LFABP binds to the anionic phospholipid interface [83]. In the previous section of this thesis (3.5) it has been shown that binding of LFABP to anionic phospholipid vesicles, monitored by loss of DAUDA fluorescence, involves initial electrostatic interactions and is prevented by the presence of high salt concentrations in the assay medium. However, the fact that the addition of high salt subsequent to the binding process caused only partial release of the LFABP indicated that there may be further interactions and changes in LFABP conformation. One explanation is that the LFABP becomes unfolded and denatured at the anionic phospholipid interface. Alternatively there may be a membrane insertion event involving hydrophobic interactions.

As it was important to show that the loss of LFABP/DAUDA fluorescence was not just simply due to irreversible denaturation of the protein, experiments were carried out with the initial aim of disrupting the vesicle structure by modifying hydrophobic interactions in an attempt to release the LFABP and to recover LFABP/DAUDA fluorescence.

The first method employed to modify hydrophobic interactions was the addition of ethanol to the system. LFABP has previously been shown, in work carried out by Schroeder *et al*, to have little sensitivity to ethanol as far as its fatty acid binding

properties are concerned [84]. Although the fatty acid binding properties of LFABP are unaffected by lower concentrations of ethanol, a correction still had to be made for the effect of ethanol on the LFABP/DAUDA fluorescence. Ethanol was shown to have a modest effect on the recovery of LFABP/DAUDA fluorescence from 100 % DOPG vesicles, the maximal recovery achieved was approximately 23 % after the addition of ethanol to a concentration of 10 % (v/v). This suggests that interactions between LFABP and anionic phospholipid do, to some extent, involve interactions of a hydrophobic nature. From these results it may be concluded that a combination of both electrostatic and hydrophobic interactions are involved between LFABP and the anionic phospholipid interface, as partial recovery of fluorescence can be achieved by the addition of either high salt concentrations or ethanol. Therefore, a combination of high salt concentration and ethanol was tried in an attempt to disrupt both the electrostatic and the hydrophobic interactions. The procedure involved the addition of 200 mM NaCl or 5 mM $CaCl_2$ to the LFABP/DOPG complex prior to the titration of ethanol in order to achieve a greater recovery of LFABP/DAUDA fluorescence. This produced an enhanced recovery of fluorescence compared with either salt or ethanol alone as shown by a return to approximately 40 % of the fluorescence of the LFABP/DAUDA complex seen prior to addition of 100 % DOPG vesicles.

These experiments were repeated using 20 mol% DOPG with DOPC vesicles in place of 100 % DOPG vesicles. Both the addition of 200 mM NaCl and the addition of 5 mM $CaCl_2$ to LFABP following a titration of 20 mol% DOPG with DOPC vesicles have shown a higher recovery of the initial LFABP/DAUDA fluorescence than when the vesicles used were composed of 100 % DOPG as discussed previously. In the

present experiments combinations of 200 mM NaCl, 5 mM $CaCl_2$ and ethanol were added to LFABP immediately following a titration of 20 mol% DOPG with DOPC vesicles in an attempt to improve the maximum fluorescence recovery. The maximal fluorescence recovery achieved was approximately 60 % and no further recovery of fluorescence was achieved from that provided by salt alone.

In summary, the binding of LFABP to DOPG vesicles can be partially reversed by conditions of high ionic strength or by addition of ethanol which should weaken hydrophobic interactions. The percentage reversal varied with the nature of the vesicle with the greatest recovery being achieved in experiments involving 20 mol% DOPG where either high ionic strength or ethanol could achieve the maximum recovery of about 60 %.

Owing to the importance of demonstrating that LFABP was still in its native form and not irreversibly denatured by the presence of phospholipid vesicles, it was necessary to use harsher methods than had so far been employed in order to disrupt the LFABP/DOPG interaction. The method of choice was to use the non-ionic detergent Triton X-100 in order to disrupt the structure of the anionic phospholipid interface. Triton X-100 was added as a 0.1 % stock solution in water (v/v) into an assay following a titration of 20 mol% DOPG vesicles. The effect of Triton X-100 on the LFABP/DAUDA complex was assessed and, although minimal, was allowed for in any data shown (Figure 3.6.1). Addition of 0.01% Triton X-100 to LFABP bound to DOPG vesicles resulted in >85% recovery of DAUDA fluorescence (Figure 3.6.1). When 200 mM NaCl was added to the cuvette after the Triton X-100, there was little improvement in the recovery of LFABP/DAUDA fluorescence. Similarly, the addition

of 200 mM NaCl prior to the addition of Triton X-100 showed no enhancement of the recovery of LFABP/DAUDA fluorescence, there appeared to be less overall recovery when the reagents were added in this sequence.

The increase in fluorescence that was observed in these experiments appeared to be showing that LFABP was being released from the phospholipid vesicles and re-binding DAUDA. To confirm that this was the case, oleic acid was titrated into the LFABP/DAUDA complex immediately following maximal recovery of DAUDA fluorescence by 0.01% Triton X-100 (Figure 3.6.2). The displacement of DAUDA from LFABP by oleic acid demonstrates that the protein has maintained the ability to bind DAUDA with high affinity and that such binding was competitive with long chain fatty acids.

Overall it would appear that the binding of LFABP to DOPG vesicles involves both electrostatic and non-polar interactions and are consistent with a membrane insertion event that may be linked to a major conformational change within the protein. By the use of a non-ionic detergent, Triton X-100, it was possible to recover over 80 % of the DAUDA binding potential of the LFABP. This is an important result as it establishes that the phenomenon being observed is not simply due to irreversible denaturation of the LFABP at an anionic surface.

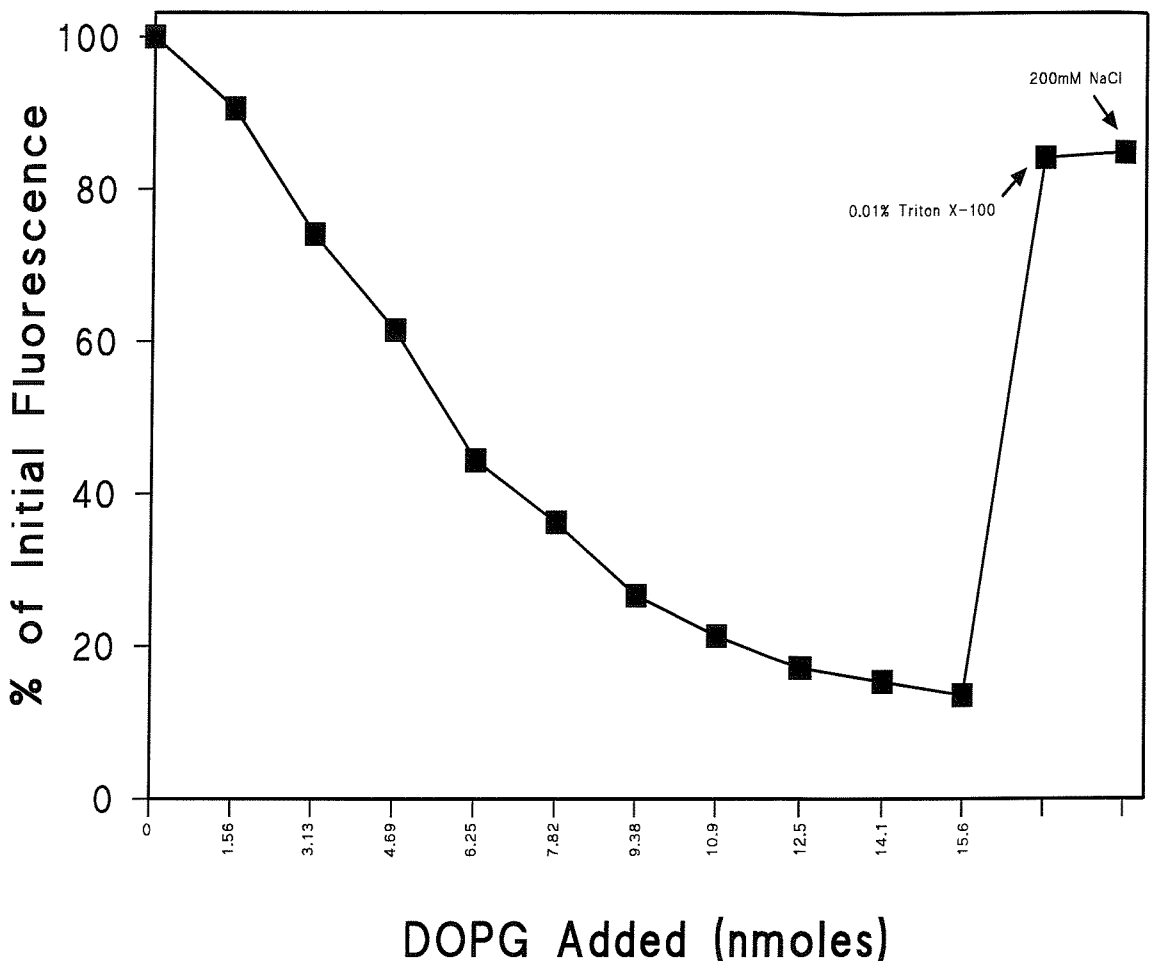

Figure 3.6.1. **The Recovery of LFABP/DAUDA Fluorescence by Triton X-100 and NaCl**

20 mol% DOPG with DOPC was titrated into LFABP/DAUDA by methanol injection, as described previously, until near-maximal loss of fluorescence was achieved. A final concentration of 0.01% Triton X-100 (v/v) was added to the cuvette, followed by a final concentration of 200 mM NaCl. Data points are corrected for the effect of Triton X-100 on LFABP/DAUDA fluorescence but not for the effect of phospholipid vesicles on DAUDA fluorescence. Data points shown are the average values of three separate titrations

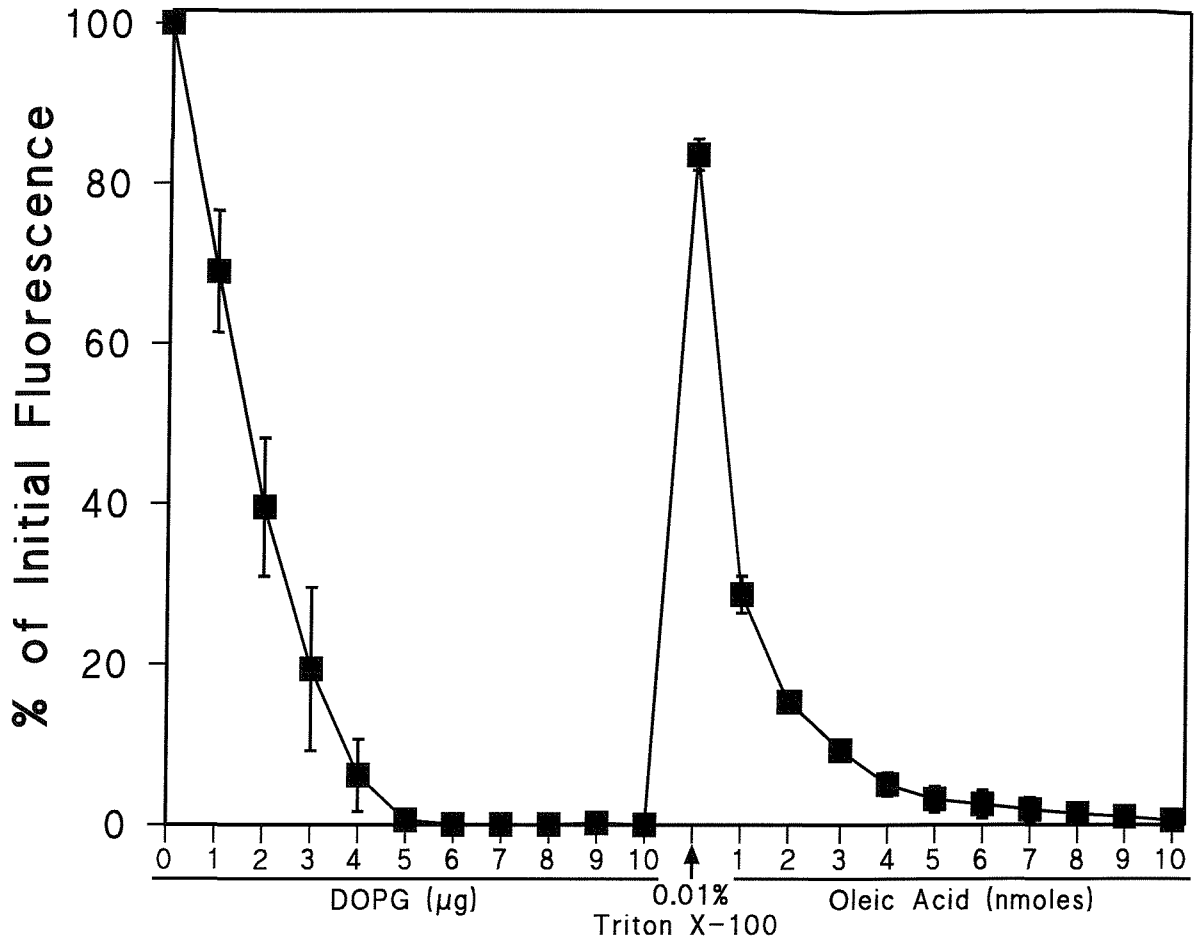

Figure 3.6.2. **Recovery of LFABP from 100% DOPG Vesicles using Triton X-100 and then Displacement of Re-bound DAUDA from LFABP by Oleic Acid**

Up to 10 μg (12.5 nmoles) 100% DOPG vesicles were titrated into LFABP/DAUDA to achieve complete loss of fluorescence, then 0.01% final concentration of Triton X-100 (v/v) was added to recover LFABP/DAUDA fluorescence. Then oleic acid (1 mM in methanol) was titrated into the cuvette to displace the DAUDA from the LFABP. Each data point is the mean value of three separate titrations and is corrected for the effects of DAUDA partitioning into DOPG vesicles and for the effect of Triton X-100 on LFABP/DAUDA fluorescence.

3.7. The Binding of Rat LFABP to Rat Liver Microsomes

So far all the data discussed regarding LFABP interactions with phospholipids has been produced using synthetic vesicles to mimic a physiological membrane. Therefore, it was important to extend the studies to the use of cell membranes and rat liver microsomes were used as an obvious physiological choice when studying rat LFABP.

Rat liver microsomes were titrated into 5 μg (0.4 nmoles) LFABP in 10 mM Hepes buffer containing 1 μM DAUDA. Initial data showed that the addition of microsomes to the LFABP/DAUDA complex produced approximately 55 % loss of fluorescence from the complex (Figure 3.7.1). However, it is known that biological membrane preparations can contain significant levels of free fatty acids resulting from lipolysis during preparation and that these fatty acids would result in loss of DAUDA fluorescence because of simple ligand displacement. Therefore, the microsome titration was carried out in the presence of 200 mM NaCl, conditions that do not affect ligand binding but prevent binding to anionic phopsholipid vesicles. The results (Figure 3.7.1) show only a 15 % reduction in the loss of fluorescence indicating that the major effect of microsomes on the loss of LFABP/DAUDA fluorescence is probably due to the presence of long chain fatty acids.

In a different approach to demonstrate LFABP binding to microsomes, samples of LFABP were incubated with the microsomes and then centrifuged at 70,000 g for 30 minutes at 4 °C to pellet the microsomal fraction. A control experiment was carried out at the same time which contained LFABP in 10 mM Hepes buffer in the absence

of microsomes. Following centrifugation the supernatent was removed and assayed for DAUDA binding, this being a functional assay for the amount of LFABP in the supernatent. It was found that the LFABP/microsome sample showed 50 % less fluorescence upon addition of DAUDA than the control sample of LFABP alone. From the data shown it would seem that there is some interaction occurring between LFABP and the microsomal membrane. Saturation occurred with the addition of 5 μl of microsomes which corresponds to ~100 nmoles of microsomal phospholipid. Thus the ratio of phospholipid:LFABP is 250:1 and is considerably greater than the 35:1 ratio seen with 100 % DOPG. This may reflect the low percentage of anionic phospholipids in mammalian membranes.

Further work is needed to clarify the ability of LFABP to bind to microsomal membranes. In the absence of an available antibody to LFABP, these binding studies would require labelled protein and the preparation of radiolabelled LFABP by reductive methylation has been employed previously in this laboratory [85].

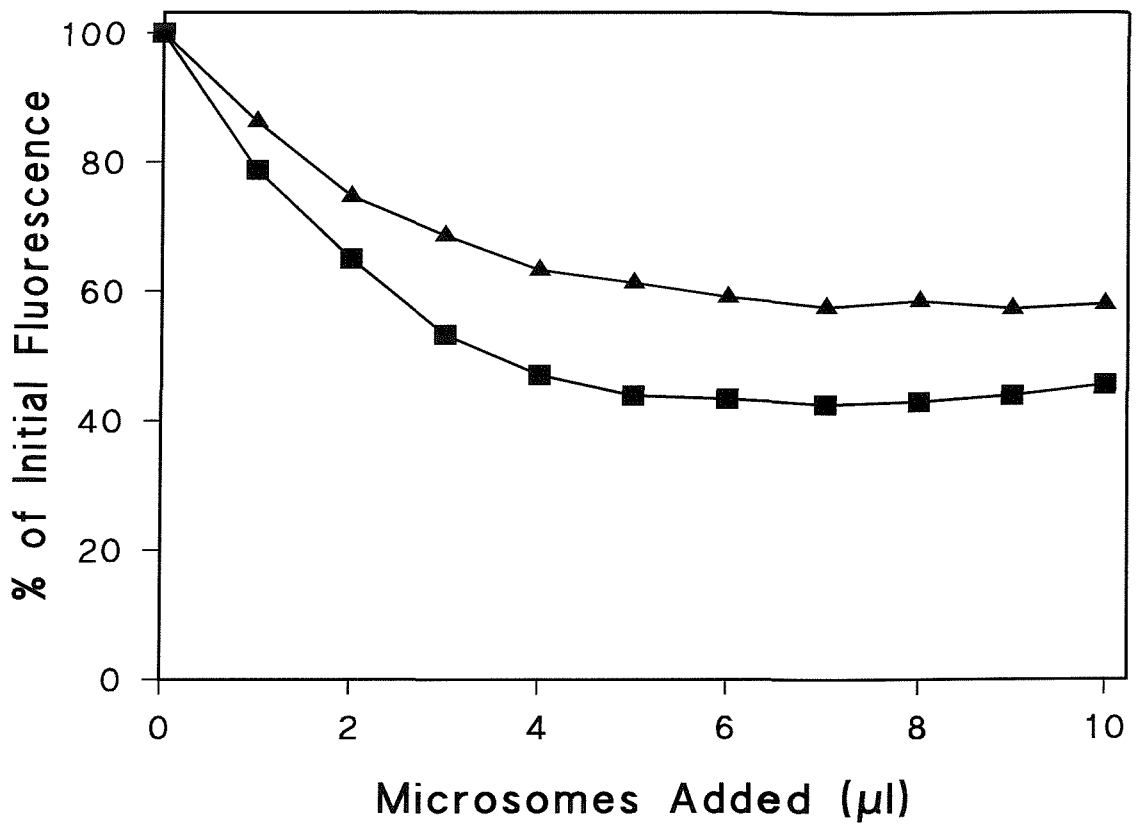

Figure 3.7.1. **Effect of Titration of Microsomes into LFABP/DAUDA Complex**

Preparation of rat liver microsomes (~20 nmoles phospholipid/μl) were titrated into 5 μg (0.4 nmoles) LFABP in 10 mM Hepes, pH 7.5, containing 1 μM DAUDA in the absence (■) and presence (▲) of 200 mM NaCl. Titrations were carried out at 37°C and fluorescence emission was measured at 500 nm following excitiation at 350 nm. All data points shown are the mean values of three separate titrations and are corrected for the titration of microsomes in the absence of LFABP.

3.8. Discussion

The work described in this Chapter highlights the ability of LFABP to bind to small anionic vesicles as monitored by the release of DAUDA from a highly fluorescent LFABP/DAUDA complex. The initial interactions have all the characteristics of a non-specific electrostatic interaction, being sensitive to ionic strength and charge density and not demonstrating headgroup specificity. However, it is difficult to reconcile electrostatic interactions with the major conformational change that must result in the relatively rigid internal cavity of this β-barrel protein. The inability of the LFABP to be effectively released from the anionic phospholipid vesicle except under conditions that affect vesicle integrity suggest that a membrane insertion event must also have occurred. Such an event would be consistent with a larger conformational change that could also result in ligand release. The inability to demonstrate ligand release with larger MLVs which have a much less curved interface and less packing distortions of the outer monolayer are consistent with a membrane penetration phenomenon.

The overall characteristics of the phenomenon are not unique and the binding of cytochrome c to phospholipid vesicles is a well-studied model system. In the case of cytochrome c, it has been proposed that an initial electrostatic interaction is followed by a membrane insertion event [86]. More recently, studies of the binding of the lid region of the lipase from *Thermomyces langinosa* to phospholipid vesicles [56] highlight the importance of using anionic SUVs but not LUVs to allow lid penetration and enzyme activation. Binding to phospholipid vesicles also requires the use of low ionic strength buffer and is not seen at all with PC vesicles.

The stringent assay requirements that are needed to demonstrate this membrane binding phenomenon of LFABP to explain to a large degree the apparent discrepancy with the work from the laboratory of Storch. In these studies it is argued that ligand transfer between LFABP and membranes is not proceeded by a collisional mechanism whereas this is the case with other FABPs. Work from the Storch laboratory is performed under conditions of higher ionic strength and normally lower anionic charge density. In fact Judy Storch has recently reported that she can see evidence of a collisional mechanism for LFABP when highly anionic vesicles are used (personal communication to D. C. Wilton).

Preliminary studies using rat liver microsomes have highlighted possible interactions between LFABP and the membrane interface. Further work is necessary to be able to draw any firm conclusions from this study.

The nature of the interaction of the LFABP with the interface and the conformational changes that must occur to allow ligand release are investigated in subsequent chapters of this thesis using site-directed mutagenesis.

Chapter Four:

Importance of Lysine Residues in the α-Helical Region of LFABP for Interactions with Anionic Phospholipid Vesicles

4.1. Introduction

In the previous chapter it has been shown that LFABP binds to anionic phospholipid vesicles with a conformational change that results in ligand (DAUDA) release. This binding is consistent with initial non-specific electrostatic interactions, as the binding is sensitive to the ionic strength of the medium and the anionic charge density of the phospholipid interface. However, the inability of a high salt concentration to release all the previously bound LFABP indicates that a possible membrane insertion event occurs after the initial electrostatic interaction and now maximum protein release is only possible after addition of detergent to disrupt the vesicle structure.

LFABP is by no means unique in its behaviour in the presence of anionic phospholipid vesicles. There are numerous examples in the literature of proteins that bind non-specifically to anionic membranes including a wide range of antibacterial proteins and peptides that show bacterial-selectivity because of their ability to bind to the surface of the anionic bacterial membrane [87]. In contrast, the external monolayer of the eukaryotic cell membrane is zwitterionic. Much work has been done with cytochrome c in model systems where the binding to membrane vesicles is highly dependent on the presence of anionic phospholipids and the ionic strength of the medium. In the case of cytochrome c a membrane insertion event has also been identified after initial electrostatic interactions [86]. Overall, the consensus is that interaction with membrane surfaces induces a partial unfolding of the protein, however, the nature of the interactions that induce such unfolding is not clear. Indeed, interactions may vary with the protein under study. Examples of

conformational change induced by binding to anionic phospholipids have been discussed in Chapter One.

An example of a protein that is more relevant to the FABP family is sterol carrier protein-2 (SCP2), a 13kDa protein that is involved in the intracellular transport of lipids, in particular cholesterol. This protein shows a large conformational change upon interacting with small unilamellar vesicles [82] resulting in an alteration of the secondary structure of the protein [88]. It is the N-terminal region of the protein that preferentially binds to high curvature vesicles rich in anionic phospholipid and cholesterol. [82, 88]. Such interactions are believed to facilitate inter-membrane sterol transfer activity [89].

The most relevant literature that relates to ligand transfer linked to membrane-protein interaction is that from the Storch laboratory. As discussed in Chapter 1, an assay was used in which the rate of transfer of a fluorescent fatty acid to phospholipid vesicles was monitored as a result of quenching by the acceptor vesicle. Storch *et al* provided evidence for a collisional mechanism for such transfer for all FABPs studied with the notable exception of LFABP. Moreover such transfer was greatly facilitated by the presence of anionic phospholipids. Work from the Storch and Cistola laboratories highlighted the importance of the α-helical region of FABPs in membrane interactions. In addition, as a result of mutagenesis studies, specific lysine residues in α-helix I have been identified as being involved in electrostatic interactions with the anionic phospholipid interface.

Liver FABP has three lysine residues in the α-helical region of this protein, K20 on α-helix I and K31 and K33 both on α-helix II. In order to investigate the effect of each of these residues on the interaction of liver FABP with anionic vesicles, each lysine in turn was mutated to a glutamate using site directed mutagenesis. It was decided to carry out charge-reversal mutagenesis, rather than simply removing the positive charge by conversion to a residue such as glutamine, in order to maximise the effectiveness of the mutagenesis. Such a strategy has already been employed in the case of the human group IIA secreted phospholipase A2 to identify cationic residues that might be responsible for the binding of this enzyme to the phospholipid interface and to heparin [89] where up to 5 cationic residues have been mutated with minimal loss of enzyme function.

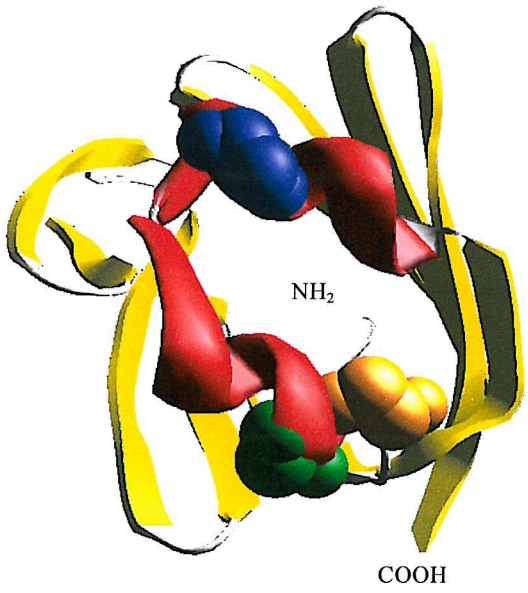

Figure 4.1.1. **The Structure of LFABP as Viewed From the α-Helical Region Looking Through the Proposed Portal Region to the N-Terminus**

Lysine 20 is shown in blue, Lysine 31 is shown in green and Lysine 33 is shown in orange

4.2. Expression and Purification of the Mutants: K20E, K31E and K33E LFABP

The mutants K20E, K31E and K33E were produced using the Kunkel method of site-directed mutagenesis [65, 66] then expressed and purified using the same method as for wild-type LFABP as described in Chapter 2 of this work. The yield of the mutant proteins was comparable to that of the wild-type protein, producing ~ 15-20 mg per litre of bacterial culture. Sample purity was checked on SDS-PAGE with coomassie blue staining (Figure 4.2).

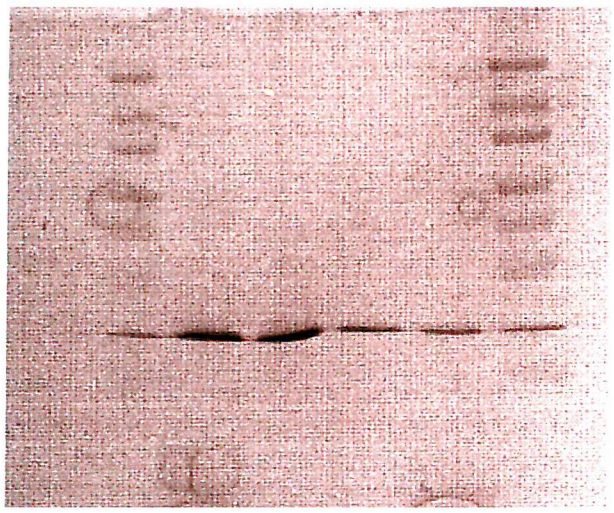

1 2 3 4 5 6

Figure 4.2. SDS-PAGE of Wild-type LFABP, K20E, K31E and K33E

Lanes 1 and 6 contain low molecular weight markers showing, from the top of the gel, 66 kDa, 45 kDa, 36 kDa, 29 kDa, 24 kDa, 20 kDa and 14.2 kDa. Lane 2 contains a sample of wild-type LFABP, lane 3 K20E, lane 4 K31E and lane 5 K33E.

4.3. Ligand Binding Properties of the K20E, K31E and K33E Mutants of LFABP

In order to characterise the functional properties of the mutants K20E, K31E and K33E the ligand binding properties of the proteins were first determined. Ligand binding was evaluated both in terms of DAUDA binding and the ability of other ligands to displace DAUDA from the proteins. The fluorescent fatty acid analogue DAUDA is an effective probe for the study of ligand binding due to its high affinity together with a large increase in fluorescence intensity and spectral shift on binding to wild-type LFABP [85].

4.3.1. DAUDA Binding to Wild-type, K20E, K31E and K33E LFABP

DAUDA binding properties were assessed by the titration of the fluorescent fatty acid analogue in methanol into a solution of the protein and measuring the fluorescence enhancement of the probe. The corrected binding curves from this experiment as shown in Figure 4.3.1.

As can be seen from the data, the binding curves for wild-type, K20E and K31E LFABP are almost super-imposable. Analysis of the binding curves showed all four proteins to have similar affinities for DAUDA (Table 4.3.1.). In all cases the λ max was at 500 nm, however, a reduction in maximum fluorescence intensity was observed with the K33E mutant together with a small increase in affinity. There is no obvious explanation for the lower fluorescence intensity of DAUDA when bound to the K33E mutant. Although a trivial explanation would be that this mutant was not

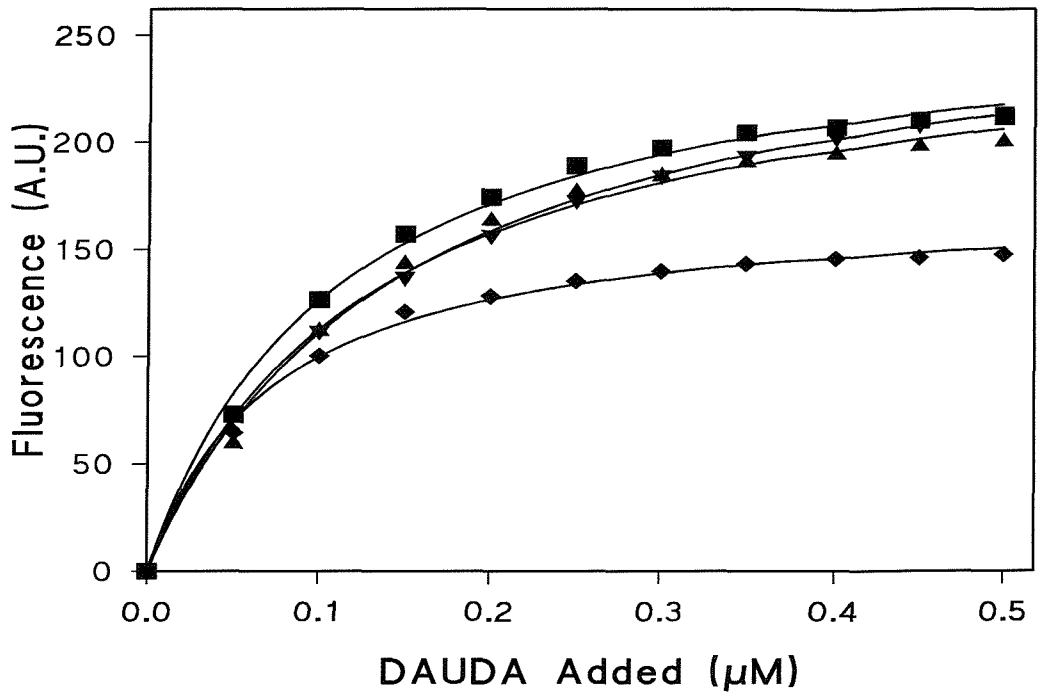

Figure 4.3.1. **The DAUDA Binding Properties of LFABP Mutants K20E, K31E and K33E Compared to DAUDA Binding to Wild-type LFABP**

DAUDA was titrated as a methanol solution into 5 μg (0.4 nmoles) of either wild-type (■), K20E (▲), K31E (▼) or K33E (◆) LFABP in 10 mM Hepes, pH 7.5, buffer. Fluorescence data is displayed as Arbitrary Units (A.U.). All data points shown are the mean values of three separate titrations and are corrected for the titration of DAUDA into buffer alone.

fully functional, i.e. partially denatured, later work (see Table 4.5.1. and Figure 4.5.2) argues against this.

Table 4.3.1. **The Binding Affinities and Maxima of the Mutants K20E, K31E and K33E for DAUDA with Comparison to Wild-type LFABP**

Data generated from graph in figure 4.3.1. using Fig.P. software.

	FABP WT	FABP K20E	FABP K31E	FABP K33E
Kd (μM)	0.11 +/- 0.01	0.13 +/- 0.01	0.15 +/- 0.004	0.07 +/- 0.01
Bmax (Arbitrary Units)	266 +/- 6	260 +/- 9	277 +/- 2	173 +/- 3

4.3.2. Oleic Acid Binding to Wild-type, K20E, K31E and K33E LFABP

Fluorescence displacement studies were performed on the wild-type and the charge reversal mutants in order to investigate the binding properties of physiological ligands. These assays were carried out as previously described in Chapter 2 of this work, a method derived from work published by Wilkinson and Wilton (1986) and Wilton (1990) [85, 90]. Oleic acid was chosen as a physiologically relevant fatty acid

that was known to have a high affinity for the wild-type LFABP. Oleic acid, as a methanol solution, was titrated into LFABP/DAUDA and loss of fluorescence was measured as oleic acid molecules completely displaced the DAUDA molecules from LFABP. Displacement curves are shown in Figure 4.3.2. and are corrected for oleic acid titration into 1 μM DAUDA in Hepes buffer.

As is shown in Figure 4.3.2. there is no major difference between the displacement curves of DAUDA by oleic acid for wild-type LFABP and the charge reversal mutants. The DAUDA displacement curves by oleic acid were analysed by the method of Kane and Bernlohr [76] in order to determine Ki_{app} values. The mutations had no major effect on oleic acid binding, the Ki_{app} values being 0.03, 0.04, 0.08 and 0.03 μM respectively for the wild-type, K20E, K31E and K33E proteins. However, a small decrease in affinity of the K31E for oleic acid is seen.

K31 has been implicated in the binding of the carboxyl group at the second fatty acid binding site [8, 13] while the mutation, K31E, has minimal effect on DAUDA binding. These observations would support the proposal that DAUDA occupies primarily the first fatty acid binding site with the carboxyl of the DAUDA buried in the protein and interacting with a hydrogen-bonding network involving R122. Conversion of R122 to lysine or glutamine reduces DAUDA binding 2-4 fold [91, 92] consistent with this particular residue making a contribution to DAUDA binding. Unfortunately, complete charge reversal of R122 was not performed. The fact that K31 is involved in the binding of the second fatty acid within the LFABP cavity may provide an explanation for the lower apparent affinity of the K31E mutant for oleic acid.

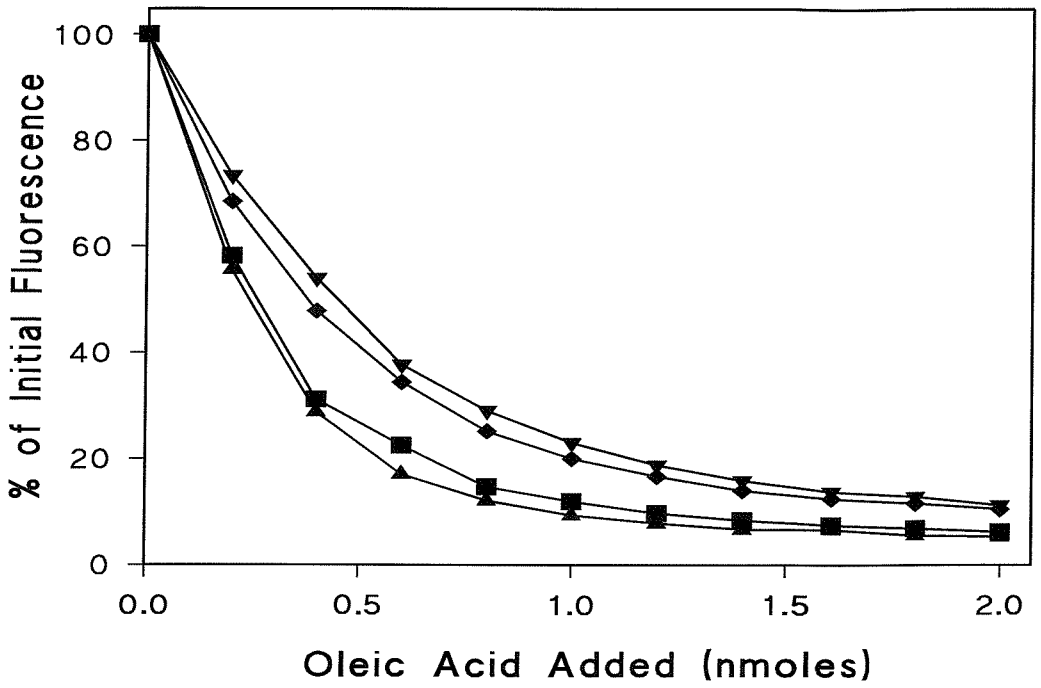

Figure 4.3.2. **Investigation of the Effects of the Mutations, K20E, K31E and K33E on the Ability of LFABP to Bind Oleic Acid with Comparison to Wild-type LFABP**

Oleic Acid was titrated as a methanol solution into 10 mM Hepes containing 1 μM DAUDA and 5 μg (0.4 nmoles) of either wild-type (■), K20E (▲), K31E (▼) or K33E (◆) LFABP. The loss of fluorescence of the LFABP/DAUDA complex was measured at 500 nm following excitation at 350 nm. All data points shown are the mean values of three separate titrations and are corrected for the effect of oleic acid on DAUDA fluorescence in 10 mM Hepes.

4.3.3. The Binding of Oleoyl CoA to Wild-type, K20E, K31E and K33E LFABP

Fatty acyl CoA has long been recognised as a potential physiological ligand for LFABP although binding affinities for this class of ligand have been lower than the corresponding fatty acid [19, 21, 92]. Oleoyl CoA has previously been modelled into the crystal structure of LFABP [8]. This model clearly showed that one molecule of LFABP could bind one molecule of oleoyl CoA in the binding cavity of the protein with the bulky CoA moiety extending via the portal region of the protein into the medium. The pyrophosphate of the ADP moiety would appear to interact within the portal region itself [8]. The modelling of oleoyl CoA into the crystal structure for LFABP agreed with previous data published that suggested the binding ratio of oleoyl CoA to LFABP was 1:1 [91, 92].

Oleoyl CoA in methanol was titrated into the LFABP/DAUDA complex in 10 mM Hepes, up to, approximately, a 10-fold molar excess over LFABP/DAUDA (Figure 4.3.3.1). Under these assay conditions the Ki_{app} values, measured by DAUDA displacement, are 0.24, 0.49, 0.6 and 0.35 μM respectively for wild-type, K20E, K31E and K33E LFABP. Thus in all cases the affinity for oleoyl CoA is about 8-12 fold less than for oleic acid (Table 4.3.3.) and hence no major differential effect of mutations on oleoyl CoA binding is observed. However, a small decrease in affinity of the K31E mutant for oleoyl CoA is noted.

Table 4.3.3. **Table of Apparent Ki Values of Wild-type LFABP, K20E, K31E and K33E for Oleic Acid and Oleoyl CoA**

Apparent Ki values were calculated from DAUDA displacements curves using the method of Kane and Bernlohr [76].

	FABP WT	FABP K20E	FABP K31E	FABP K33E
Ki Oleic Acid (μM)	0.03	0.04	0.08	0.03
Ki Oleoyl CoA (μM)	0.24	0.49	0.6	0.35
Ki O.CoA / Ki O.A.	8	12.3	7.5	11.7

The model produced by Thompson *et al* of oleoyl CoA positioned within the crystal structure of LFABP [8] reveals that residue K31 and possibly K33 are in close proximity to the site of interaction of the pyrophosphate group of the ADP moiety within the portal region of LFABP. Therefore, one might expect to observe a significant difference between wild-type, K31E and K33E LFABP in terms of oleoyl CoA binding properties. In fact, a small reduction in affinity is seen for the K31E mutant but no significant effect is seen with the K33E mutant.

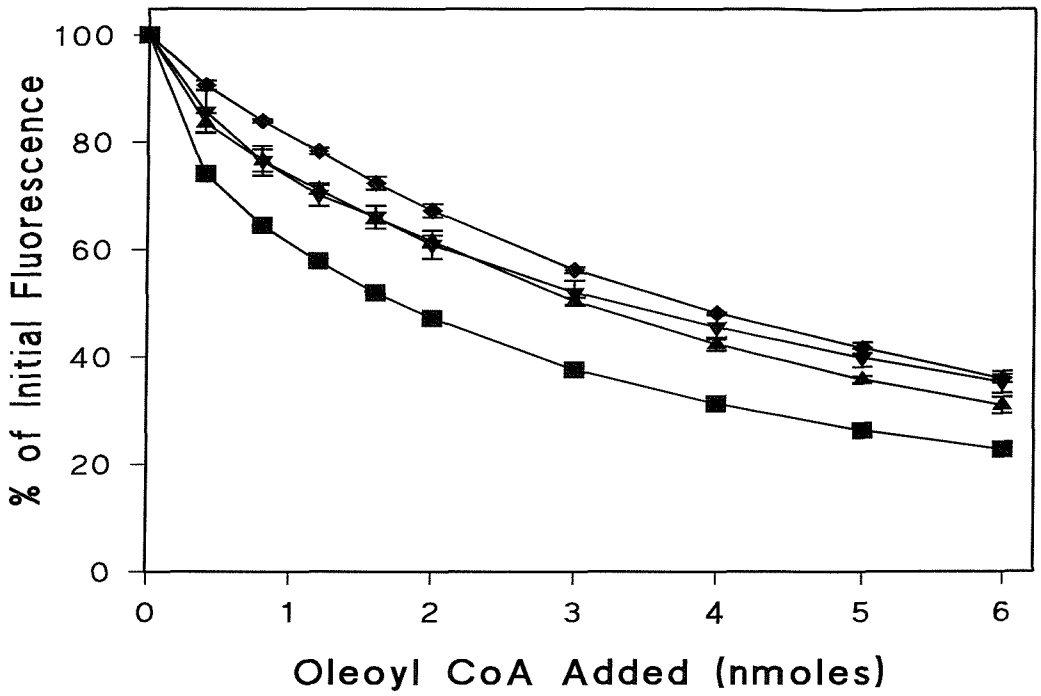

Figure 4.3.3.1. Comparison of the Oleoyl CoA Binding Properties of Wild-type LFABP and the Mutants of LFABP; K20E, K31E and K33E

Oleoyl CoA was titrated as a methanol solution into 10 mM Hepes, pH 7.5 buffer containing 1 μM DAUDA and 5 μg (0.4 nmoles) of either wild-type (■), K20E (▲), K31E (▼) or K33E (◆) LFABP. Loss of fluorescence was measured at an emission wavelength of 500 nm following excitation at 350 nm. All data points shown are the mean values of three separate titrations and are corrected for the effect of oleoyi CoA on DAUDA in 10 mM Hepes buffer.

This lack of major effect of these portal mutants on the binding of oleoyl CoA can be explained by examination of the model of oleoyl CoA within the crystal structure of LFABP. In this model the entire non-polar oleoyl-pantathene moiety is buried in the cavity while the ADP is surface exposed [8]. Such a model would suggest that non-polar interactions would play a dominant role in ligand binding and specific electrostatic interactions make a minor contribution.

Hydrophobic binding would be facilitated by the presence of high ionic strength buffer. Therefore, the effect of 100 mM NaCl upon the loss of fluorescence of the LFABP/DAUDA complex following titration of oleoyl CoA was investigated. At 100 mM NaCl the binding of oleoyl CoA to wild-type, K20E, K31E and K33E was greatly enhanced as measured as loss of LFABP/DAUDA fluorescence (Figure 4.3.3.2). The calculated [76] Ki_{app} values for oleoyl CoA in the presence of 100 mM NaCl were 0.07, 0.1, 0.16 and 0.1 μM respectively for wild-type, K20E, K31E and K33E LFABP. These values presented show little differences between the four proteins in terms of affinity for oleoyl CoA but are significantly lower than those seen for the displacement studies in the absence of 100 mM NaCl consistent with enhanced hydrophobic binding.

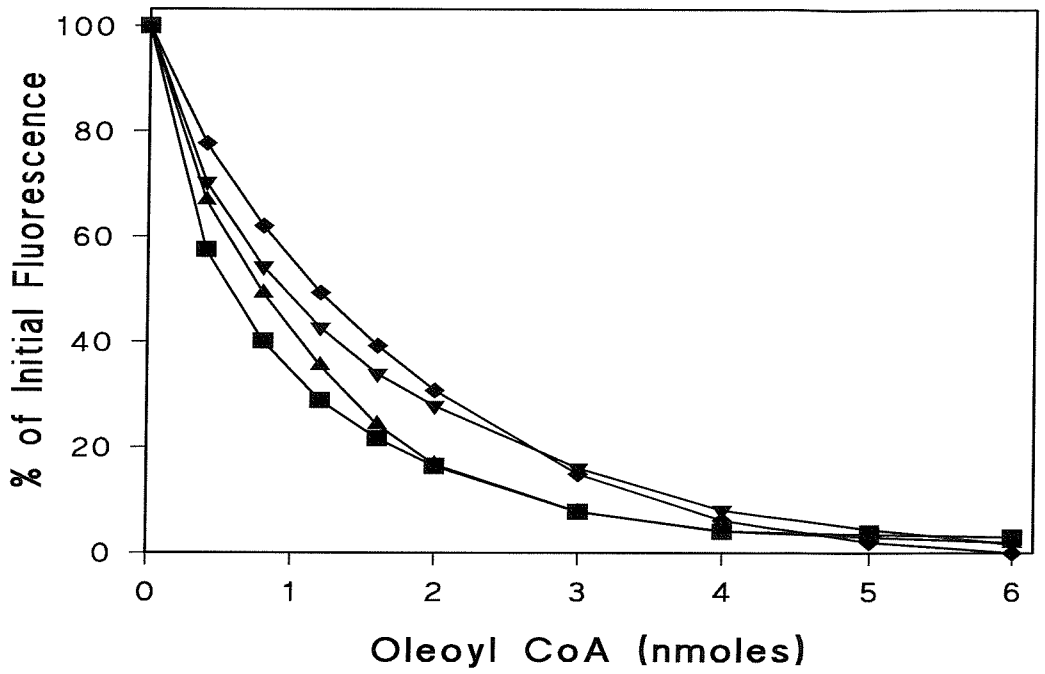

Figure 4.3.3.2. Comparison of the Oleoyl CoA Binding Properties of Wild-type, K20E, K31E and K33E LFABP in the Presence of 100 mM NaCl

Oleoyl CoA was titrated as a methanol solution into 10 mM Hepes, pH 7.5 buffer containing 100 mM NaCl, 1 μM DAUDA and 5 μg (0.4 nmoles) of either wild-type (■), K20E (▲), K31E (▼) or K33E (◆) LFABP. Loss of fluorescence was measured at an emission wavelength of 500 nm following excitation at 350 nm. All data points shown are the mean values of three separate titrations and are corrected for the effect of oleoyl CoA on DAUDA in 10 mM Hepes buffer.

4.3.4. The Binding of Lysophospholipids to Wild-type LFABP, K20E, K31E and K33E

Lysophospholipids have previously been identified as potential ligands for LFABP, however, affinities are low compared to the corresponding fatty acid/fatty acyl CoA and the physiological relevance of such interactions has yet to be established. Oleoyl lysoPA has previously been shown to be the most effective lysophospholipid at displacing DAUDA from LFABP [20, 93]. Moreover, Vancura and Haldar [90] have suggested that LFABP plays a major role in mitochondrial and microsomal metabolism by regulating both the synthesis and utilisation of lysoPA.

When the oleoyl lysoPA binding properties were assessed there appeared to be a clear distinction between the properties of wild-type and K20E compared to K31E and K33E. The binding affinity of LFABP K31E and LFABP K33E was considerably lower than that seen for LFABP WT and LFABP K20E. Approximately 20 % loss of LFABP/DAUDA fluorescence could be achieved in the presence of 10-fold molar excess of oleoyl-lysoPA for wild-type LFABP and for LFABP K20E, whereas only between 5-10 % could be seen for the LFABP K31E and LFABP K33E.

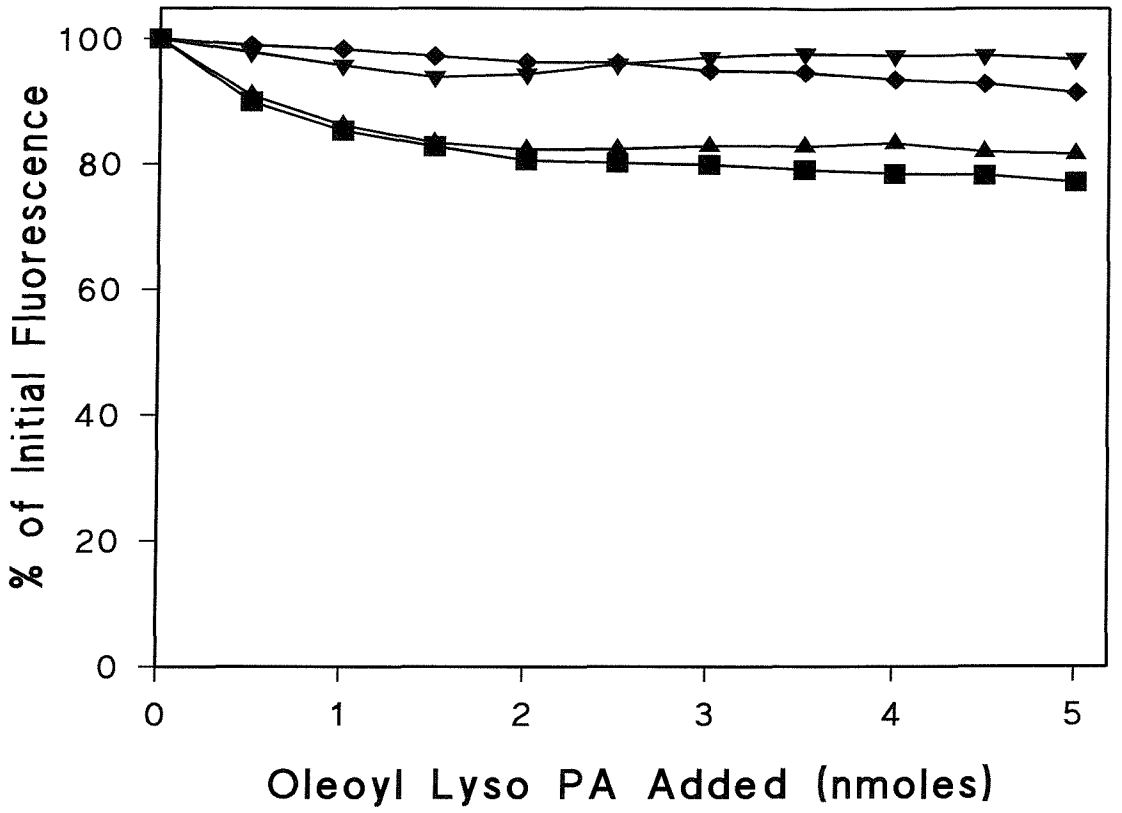

Figure 4.3.4. **Effect of K20E, K31E and K33E Mutations of LFABP on the Oleoyl Lysophosphatidic Acid Binding Properties Compared with Wild-type LFABP**

Oleoyl lysoPA was titrated as an aqueous solution into 10 mM Hepes, pH 7.5 buffer containing 1 μM DAUDA and 5 μg (0.4 nmoles) of either wild-type (■), K20E (▲), K31E (▼) or K33E (◆) LFABP. Changes in the fluorescence of the LFABP/DAUDA complex were measured at an emission wavelength of 500 nm following excitation at 350 nm. All data points shown are the mean values of three separate titrations and are corrected for titration of lysophospholipid into DAUDA in 10 mM Hepes.

As can been seen from the data, the affinity of oleoyl-lysoPA for wild-type LFABP is low, as shown by the poor ability of these ligands to displace DAUDA. Owing to the low affinity of LFABP and the poor monomer solubility of these ligands it was not possible to achieve the 50 % displacement required to quantify binding.

Unlike oleoyl CoA, lysophospholipids have not, as of yet, been modelled into the crystal structure of wild-type LFABP, although the structure of ileal lipid binding protein complexed with glycocholate has recently been solved [94]. This structure showed the glycine moiety of glycocholate extending through the portal region of ileal lipid binding protein into the surrounding medium. From these findings it would be anticipated that lysophospholipids bind to LFABP with the fatty acyl chain buried in the binding cavity and the bulky headgroup extending through the portal region into the surrounding medium.

4.4. A Comparison of the Structural Stability of the Wild-type LFABP with K20E, K31E and K33E

From the data already presented, it is clear that the ligand binding properties of the K20E, K31E and K33E mutants of LFABP do not deviate to a major degree from those for wild-type LFABP. From this it can be concluded that the mutation of these particular residues has little effect on the overall structure of the protein. However, such mutations could significantly affect the stability of LFABP. The standard method for investigating the structural integrity or stability of a protein is by carrying out unfolding studies using either urea or guanidine hydrochloride. This method relies on the presence of tryptophan residues within the protein to enable monitoring

of unfolding by changes in the fluorescence spectra of tryptophan residues. Unfortunately, wild-type LFABP does not contain tryptophan residues so this method cannot be applied to this particular protein. As the ligand binding site is within the cavity of the β-barrel structure of LFABP, the binding capacity for DAUDA and the resulting increase in fluorescence could be used as a measure of gross structural stability to denaturant and also to heat.

4.4.1. Effect of Urea on the Structural Stability of Wild-type LFABP, K20E, K31E and K33E

Incubating the wild-type, K20E, K31E and K33E proteins with varying concentrations of urea and then assessing the effect on the ability of the protein to bind DAUDA was used to investigate the stability of LFABP to chemical denaturants. Equal concentrations (0.4 μM) of protein were incubated in varying concentrations of urea for one hour at 25°C and then assayed for DAUDA binding. The effect of urea on the DAUDA binding as measured by fluorescence intensity is shown in Figure 4.4.1.1. The concentration of urea that was required to reduce the fluorescence of an assay containing 1 μM DAUDA by 50 % was determined and found to be 3.5 M for the wild-type, K31E and K33E LFABP proteins

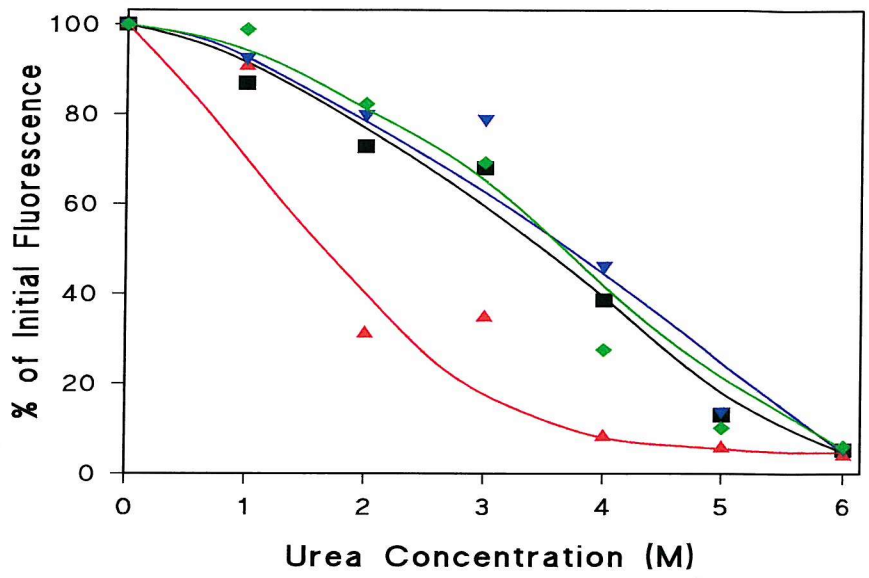

Figure 4.4.1.1. The Effect of Urea on the Ability of Wild-type, K20E, K31E and K33E LFABP to Bind DAUDA

Equal concentrations (0.4 nmoles) of Wild-type (black ■), K20E (red ▲), K31E (blue ▼) and K33E (green ◆) were incubated in varying concentrations of urea for one hour at 25°C. The samples were then subjected to a DAUDA titration and the maximum increase in DAUDA fluorescence was measured. All data points are the mean values of three separate titration and are corrected for the titration of DAUDA into urea buffer.

whereas a value of 1.5 M urea was observed for the K20E mutant.

Thus it would appear that the K20E mutation was significantly more sensitive to urea and, therefore, structurally less stable than the other proteins, as determined by DAUDA binding. This result would suggest that K20 may be involved in stabilising electrostatic interactions with adjacent surface anionic residues. The most obvious residue is E16 within the α-helix I region of the protein. Both E16 and K(R)20 are conserved within all LFABP sequences from different species [8] suggesting an important structural/functional role.

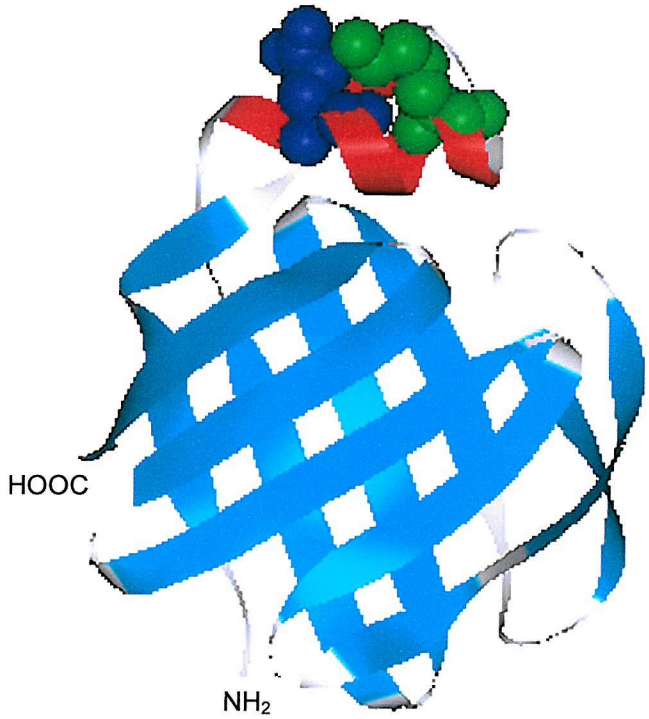

Figure 4.4.1.2. LFABP Structure Highlighting Residues E16 and K20

Residue E16 is shown in dark blue, residue K20 is shown in green.

4.4.2. Effect of Temperature on the Structural Stability of Wild-type LFABP, K20E, K31E and K33E

In order to determine the thermostability of wild-type LFABP and the K20E, K31E and K33E mutants, the effect of exposure to high temperature on the DAUDA binding potential of the proteins was determined. Wild-type LFABP is in fact very stable to heat and previous preliminary experiments had determined that pre-incubation at 70°C prior to an assay of DAUDA binding at room temperature provided a convenient rate of denaturation. The four proteins were therefore incubated at approximately the same concentration of 0.3 mg/ml (~20 μM) in buffer at 70°C and aliquots of 50 μl were removed at regular intervals over a period of 5 hours and assayed for DAUDA binding. In each assay the fluorescence enhancement was measured at room temperature in the presence of 1μM DAUDA. The time course of loss of DAUDA binding capacity, calculated as a % of the fluorescence at zero time, is shown in Figure 4.4.2.1.

From this data the time taken for the DAUDA binding capacity of each protein to be reduced by 50 % could be determined, these values were 10, 7, 150 and 10 minutes for the wild-type, K20E, K31E and K33E mutations respectively. Moreover, when assessed over a longer time course, it is clear that the K20E mutation is significantly less stable than the wild-type protein. In marked contrast the K31E mutant is considerably more stable to heat denaturation but this was not consistent with the urea data (Figure 4.4.1). In order to confirm the unexpected stability of the K31E mutation, protein samples were incubated at 70°C for a fixed time, 15 minutes, then the DAUDA binding properties of all the proteins was measured.

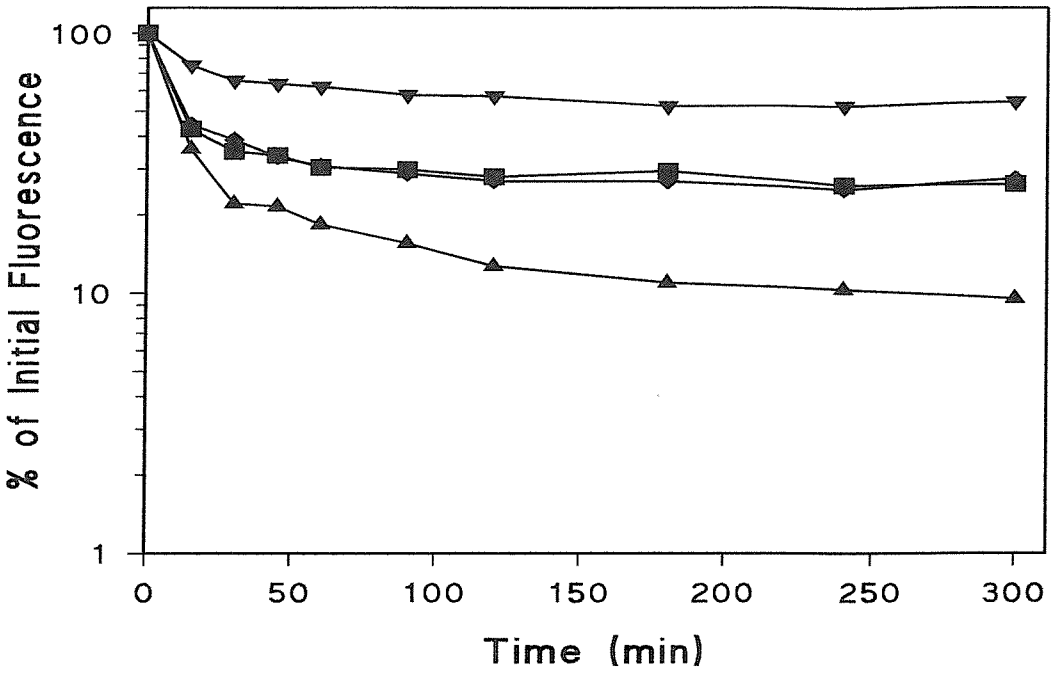

Figure 4.4.2.1. Thermostability of the Mutants of LFABP; K20E, K31E and K33E in Comparison to Wild-type LFABP

The protein samples were incubated at 70°C and samples of each protein were taken at regular time intervals and assayed for DAUDA Binding. A single addition of DAUDA to a final concentration of 1 μM was made to each 5 μg (0.4 nmoles) sample of either wild-type (■), K20E (▲), K31E (▼) or K33E (◆) LFABP and the fluorescence emission at 500 nm recorded following excitation of the sample at 350 nm. All data points are the averages of three separate titrations.

The results (Figure 4.4.2.2. and Table 4.4.2.) clearly demonstrate that the K31E mutant is more stable at elevated temperatures with minimal loss of binding activity shown after 15 minutes. Although there was no significant change in the K_d values for DAUDA with all the proteins after heat treatment, the DAUDA binding capacity of the K31E was still 98 % of the value before heat treatment (Table 4.3.1.) whereas the WT, K20E and K33E proteins showed 57, 45 and 68 % retention of binding capacity respectively.

Table 4.4.2. **The Binding Affinities and Maxima of the Mutants K20E, K31E and K33E LFABP for DAUDA with Comparison to Wild-type Following Heat Treatment at 70°C for 15 Minutes**

	FABP WT	FABP K20E	FABP K31E	FABP K33E
Kd (μM)	0.13 +/- 0.01	0.09 +/- 0.003	0.15 +/- 0.02	0.06 +/- 0.001
Bmax (Arbitrary Units)	143 +/- 2	118 +/- 1	271 +/- 2	117 +/- 1

The reason for the increased stability of the K31E under heat-denaturing conditions is not known. It is known that K31 is a residue that, along with L28, defines the cavity opening in rat LFABP and also contributes significantly to the positive potential on the surface of LFABP [8]. However, the urea denaturation studies would suggest that the effect seen during thermostability studies is not due to intrinsic

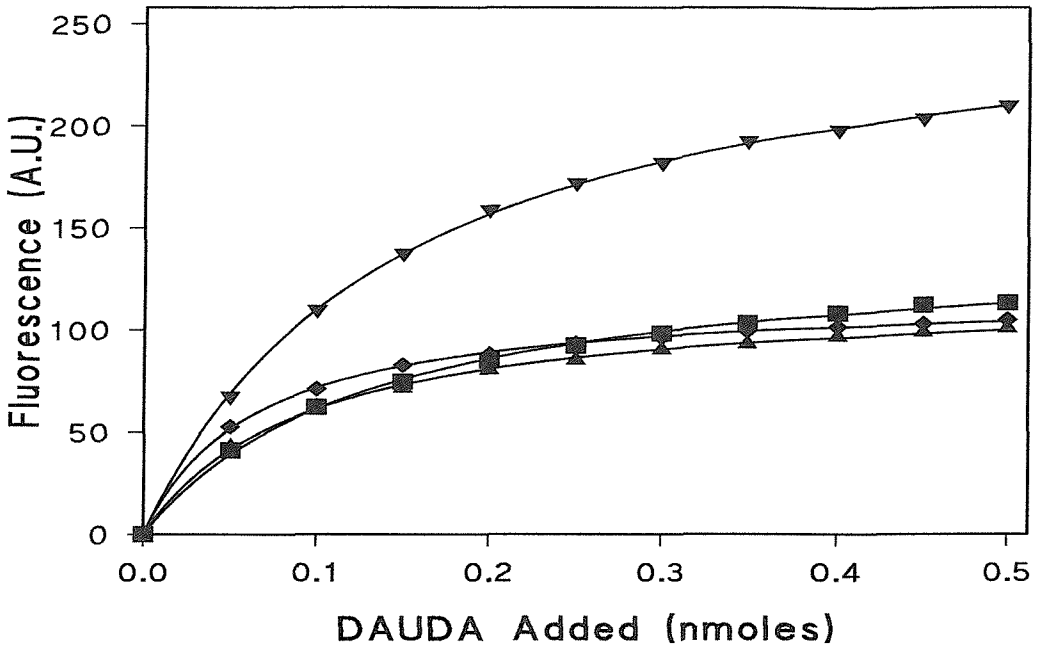

Figure 4.4.2.2. DAUDA Binding Properties of Wild-type, K20E, K31E and K33E LFABP following a 15 minute incubation at 70°C

20 μM samples of wild-type (■), K20E (▲), K31E (▼) and K33E (◆) were incubated at 70°C for 15 minutes. A 50 μl sample was then taken and assayed for DAUDA binding. All data points are the mean values of three separate titrations and are corrected for DAUDA titration into buffer.

stability of the K31E mutant protein. It may be that a change in the surface electrostatic potential of the protein alters the functional stability by, for example, reducing the tendency of the protein to aggregate. Such a property would be useful in future structural studies such as NMR measurement and crystallography.

4.5. Phospholipid vesicle binding properties of the mutants K20E, K31E and K33E measured indirectly by DAUDA release

We have previously demonstrated the importance of electrostatic interactions in the stoichiometric binding of LFABP to small unilamellar vesicles containing anionic phospholipid, (Chapter 3). These electrostatic interactions were highlighted by the importance of low ionic strength conditions and of anionic phospholipid charge density for binding to occur [83]. In order to identify individual cationic residues on LFABP that might participate in binding to anionic phospholipids, the mutants K20E, K31E and K33E were studied in the first instance for reasons already discussed in section 4.1. of this work. Binding studies were conducted by monitoring the displacement of DAUDA from LFABP, which could be seen as a loss of fluorescence of the LFABP/DAUDA complex, when the protein binds to anionic phospholipid vesicles.

4.5.1. The Binding of Wild-type, K20E, K31E and K33E LFABP to 100 % DOPG Vesicles

The binding of wild-type LFABP and the three mutants, K20E, K31E and K33E to DOPG vesicles (Figure 4.5.1.) highlighted the K31E mutant as having a reduced

binding affinity for these vesicles. This was assessed as the amount of DOPG that needed to be added to reduce DAUDA fluorescence by 50 % (Table 4.5.1.) The K20E and K33E mutants showed a very similar affinity for DOPG to that shown by wild-type FABP and bind DOPG with a comparable stoichiometry. This stoichiometric ratio of approximately 30 molecules DOPG per molecule of protein is characteristic of a protein of this size coating the surface of the phospholipid vesicle as has been discussed in Chapter 3. The K31E mutant, however, shows a significantly lower affinity for DOPG vesicles than either the wild-type protein or K20E or K33E.

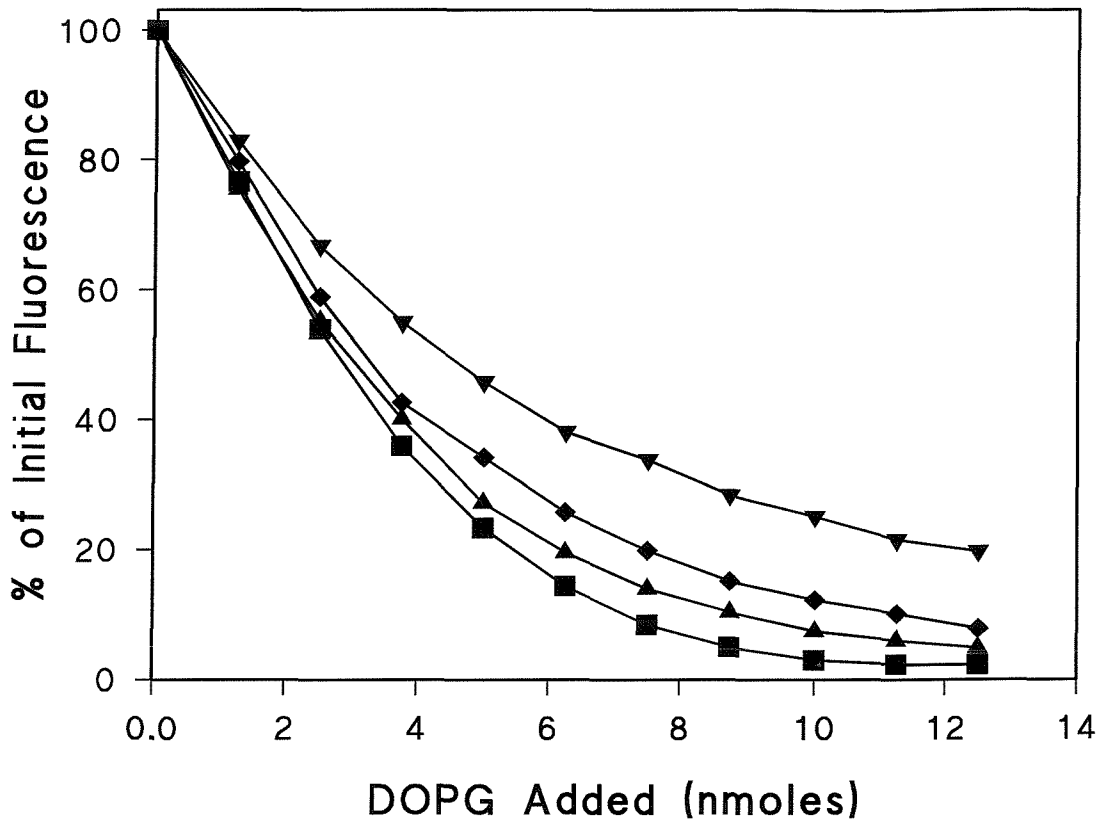

Figure 4.5.1. **Effect of 100 % DOPG vesicles on the fluorescence of either wild-type, K20E, K31E or K33E LFABP complexed with DAUDA**

100 % DOPG SUVs were titrated by methanol injection into 10 mM Hepes, pH 7.5, buffer in the presence of 1 μM DAUDA and 5 μg (nmoles) of either wild-type (■), K20E (▲), K31E (▼) or K33E (◆) LFABP. All data points are the mean values of three separate titrations and are corrected for the partitioning of DAUDA into the phospholipid vesicles.

Table 4.5.1. Amount of DOPG required in 100 % SUVs to Produce 50 % Loss of LFABP/DAUDA Fluorescence

100 % DOPG SUVs were titrated by methanol injection into 5 μg (0.4 μM) of either wild-type, K20E, K31E or K33E LFABP in 10 mM Hepes containing 1 μM DAUDA. The data shown are the mean values calculated from three separate DOPG titrations.

	Amount of DOPG Required for 50 % Loss of Fluorescence (nmoles)
LFABP Wild-Type	2.8
LFABP K20E	3.0
LFABP K31E	4.6
LFABP K33E	3.2

4.5.2. The Binding of Wild-type, K20E, K31E and K33E LFABP to 20 mol% DOPG with DOPC Vesicles

The fact that the titration curves for DOPG vesicles were almost stoichiometric in nature (Figure 3.2.3) highlighted the high affinity of the protein for the phospholipid interface. In an attempt to discriminate even further the differences between wild-type, K20E, K31E and K33E proteins, the titration of phospholipid vesicles into LFABP/DAUDA was repeated using SUVs consisting of 20 mol% DOPG in DOPC. This investigation revealed a clear distinction between the properties of vesicle binding of K31E and those of K20E and K33E LFABP as shown in Figure 4.5.2. The amount of DOPG in 20 mol% vesicles with DOPC required to produce a 50 % loss of LFABP/DAUDA fluorescence was calculated for each of the wild-type, K20E, K31E and K33E LFABP (Table 4.5.2). The data clearly shows the K31E mutant to have a significantly lower affinity for 20 mol% DOPG vesicles than any of the other three proteins investigated. Approximately 2-fold more these vesicles were required to produce 50 % loss of K31E LFABP/DAUDA fluorescence than either wild-type, K20E or K33E LFABP.

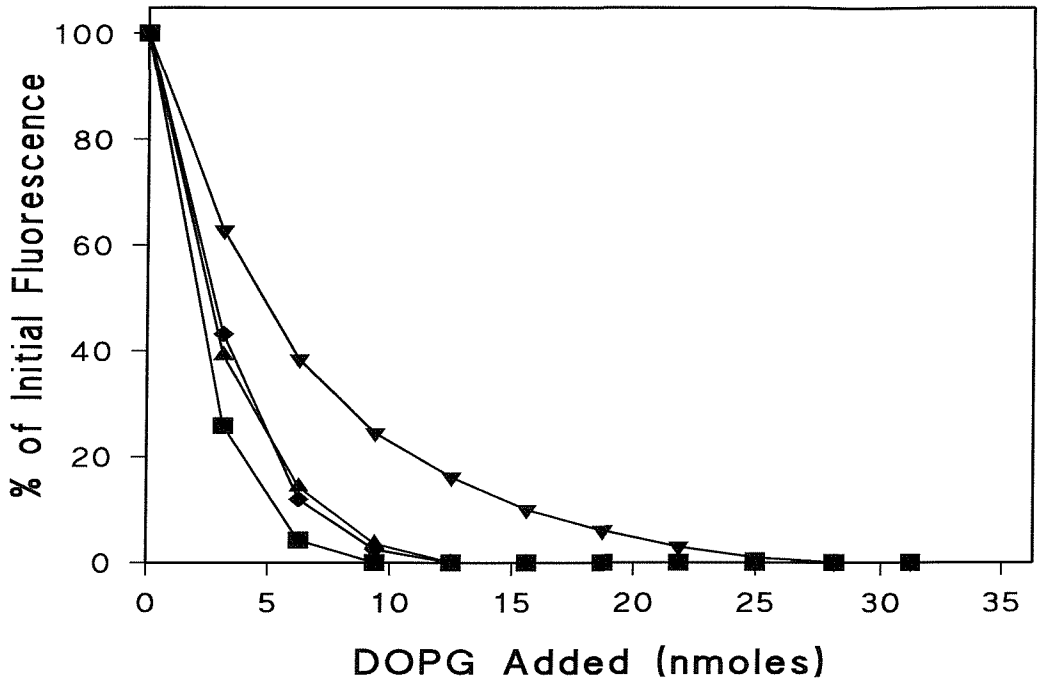

Figure 4.5.2 **Effect of 20 mol% DOPG with 80 mol% DOPC vesicles on the fluorescence of either wild-type, K20E, K31E or K33E LFABP compiexed with DAUDA**

20 mol% DOPG with DOPC SUVs were titrated by methanol injection into 10 mM Hepes, pH 7.5, buffer in the presence of 1 μM DAUDA and 5 μg (0.4 nmoles) of either wild-type (■), K20E (▲), K31E (▼) or K33E (◆) LFABP. All data points are the mean values of three separate titrations and are corrected for the partitioning of DAUDA into the phospholipid vesicles.

Table 4.5.2. Amount of DOPG in 20 mol% SUVs with DOPC Required to Produce a 50 % Loss of LFABP/DAUDA Fluorescence: A Comparison of Wild-type, K20E, K31E and K33E LFABP

Data shown was taken from figure 4.5.2. and are the mean values of three separate titrations.

	Amount of DOPG Required in 20 % SUVs with DOPC for 50 % Loss of Fluorescence (nmoles)
LFABP Wild-type	2.1
LFABP K20E	2.9
LFABP K31E	5.0
LFABP K33E	3.1

4.5.3. The Effect of NaCl on the Binding of Wild-type, K20E, K31E and K33E LFABP to 20 mol% DOPG Vesicles

In Chapter 3 it was demonstrated that the binding of LFABP to DOPG vesicles was very sensitive to ionic strength (Figure 3.5.1). The effect of salt concentration on the binding of DOPG vesicles to wild-type, K20E, K31E and K33E LFABP was investigated. The ability of 20 mol% DOPG vesicles to displace DAUDA from wild-type, K20E, K31E and K33E LFABP in the presence of 200 mM NaCl was measured as shown in Figure 4.5.3. Up to 20 % loss of LFABP/DAUDA fluorescence could be achieved for wild-type, K20E and K33E LFABP whereas no significant loss of LFABP/DAUDA fluorescence was observed for the LFABP K31E mutant in the presence of 200 mM NaCl (Figure 4.5.3).

As has already been determined, the initial interactions between LFABP and anionic phospholipid vesicles are characteristic of electrostatic interactions [83]. Combining this knowledge with that of Herr *et al* [28] and Smith and Storch [95] it would be reasonable to expect that charge reversal mutations within the α-helical region of LFABP may result in weaker protein/phospholipid interactions. The data shown suggests that K31 is a key residue in the electrostatic interactions between LFABP and anionic phospholipid and that reversal of the charge of this residue reduces the capacity of the protein for electrostatic interactions.

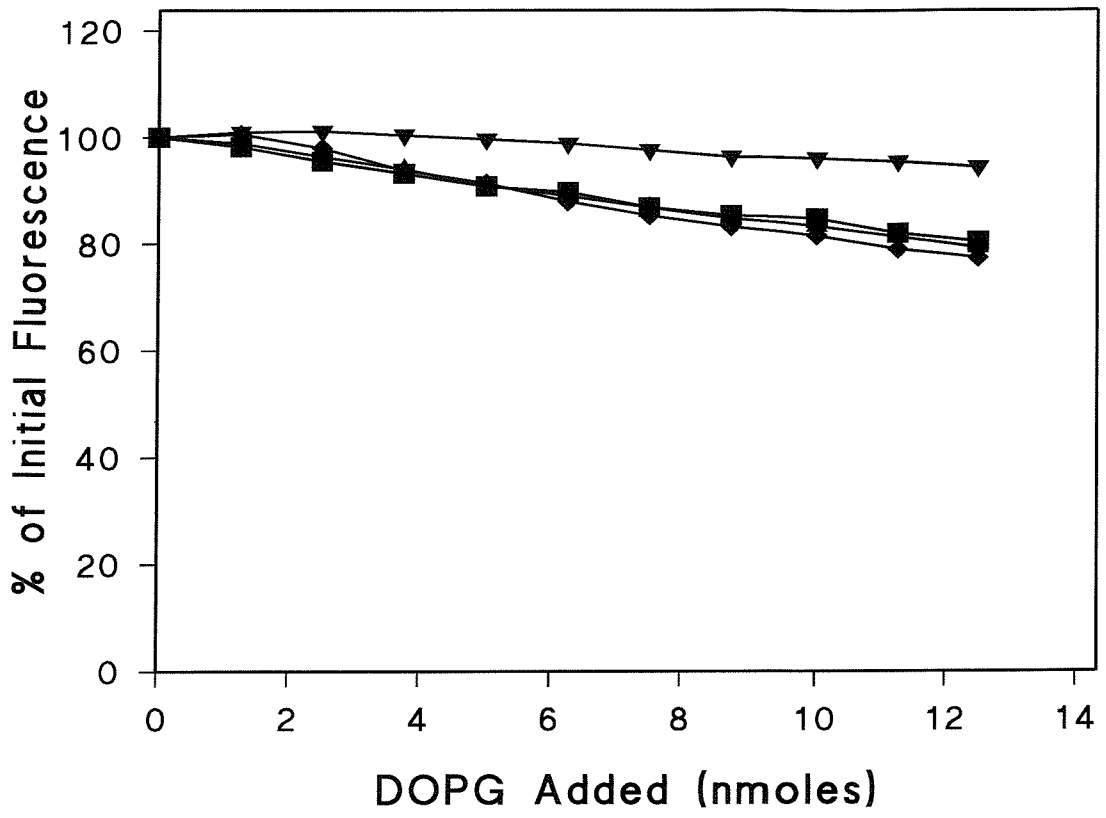

Figure 4.5.3. **Effect of 200 mM NaCl on the loss of LFABP/DAUDA Fluorescence by 20 mol% DOPG with DOPC SUVs**

20 mol% DOPG with DOPC SUVs were titrated into 10 mM Hepes, pH 7.5, 200 mM NaCl, 1 μM DAUDA and 5 μg (0.4 nmoles) of either wild-type (■), K20E (▲), K31E (▼) or K33E (◆) LFABP by methanol injection. All data points are the mean values of three separate titrations and are corrected for DAUDA partitioning into the phospholipid vesicles.

4.5.4. The Binding of Wild-type, K20E, K31E and K33E LFABP to DOPC Vesicles

As has previously been demonstrated in Chapter 3, the addition of zwitterionic DOPC vesicles to the wild-type LFABP/DAUDA complex results in no significant loss of fluorescence of the complex, suggesting that there is no interaction between wild-type LFABP and DOPC. The results of the study of the effect of NaCl on DOPG binding to LFABP K31E suggested that it may be possible to demonstrate differences in interaction with DOPC vesicles between wild-type, K20E, K31E and K33E LFABP. Upon titration of DOPC vesicles into the LFABP/DAUDA complex, this was indeed found to be the case. The wild-type, K20E and K33E LFABPs were found to behave in a similar manner in the presence of DOPC vesicles with no significant loss of LFABP/DAUDA fluorescence. LFABP K31E, however, was shown to demonstrate an increase in fluorescence of approximately 10 % in the presence of DOPC vesicles as shown in Figure 4.5.4. That this small increase in fluorescence is significant is supported by later work with other charge reversal mutants (Chapter 5).

The increase in fluorescence intensity seen for the K31E/DAUDA complex would suggest that there is some interaction of the complex with the DOPC vesicles. It is possible that the presence of this particular mutation allows some interaction with DOPC that produces a small conformational change in the protein that results in an increased affinity of LFABP for DAUDA. Alternatively, an increase in the fluorescence intensity of the bound DAUDA, could be achieved by an increase in the hydrophobicity of the binding cavity as a result of conformational changes. It was not possible to detect any change in the emission maximum of the bound DAUDA

under these conditions. Although DAUDA partitions into DOPC vesicles with enhanced fluorescence, such an increase is corrected for by blank titrations in the absence of protein and confirmed by the absence of increase seen with the other proteins. It should be noted that the K31E mutant has a slightly lower affinity for DAUDA than the wild-type protein so a reversal of this loss of binding affinity could produce the small increase in fluorescence under the conditions of the assay.

The cumulative results clearly demonstrate that of the three cationic lysine residues in the α-helical region, only the residue K31 makes a significant contribution to the binding of LFABP to anionic vesicles resulting in release of DAUDA. It is K31 in α-helix II that also makes a significant contribution to the surface positive potential of the protein [8]. The apparent ability of the K31E mutant to interact with DOPC vesicles but without loss of ligand further highlights the dramatic effect the binding to an anionic interface, resulting in complete loss of ligand, must have on the protein structure.

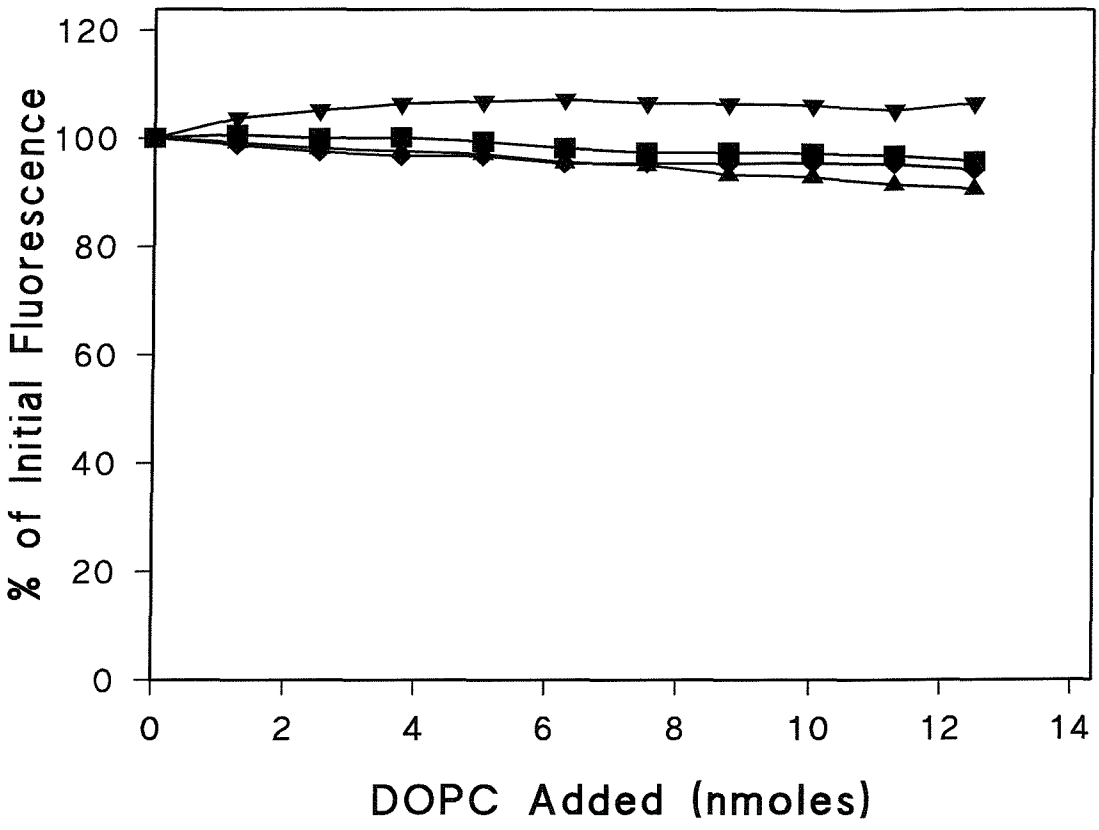

Figure 4.5.4. **Effect of DOPC SUVs on the Fluorescence of the LFABP/DAUDA Complex: A Comparison of Wild-type LFABP with the Mutants, K20E, K31E and K33E**

100 % DOPC SUVs were titrated into 10 mM Hepes, 1 μM DAUDA and 5 μg (0.4 nmoles) of either wild-type (■), K20E (▲), K31E (▼) or K33E (◆) LFABP by methanol injection. Fluorescence emission was measured at 500 nm following excitation at 350 nm. All points shown are the mean values of three separate titrations and are corrected for the partitioning of DAUDA into DOPC vesicles.

4.5.5. The Binding of Wild-type, K20E, K31E and K33E LFABP to Fluorescent Phospholipid Vesicles

The ability of proteins to bind to phospholipid vesicles has been previously studied by utilising anionic vesicles containing a small mol% of the fluorescent phospholipid dansyl DHPE. The attachment of the polarity sensitive dansyl fluorophore to the head group of the PE means that this fluorophore is located at the vesicle interface. The binding of proteins to such an interface will change the environment and normally result in enhanced fluorescence due to interfacial dehydration [96]. This technique has been used successfully to study the binding of $sPLA_2$ [96-98] and wild-type LFABP to anionic vesicles [83].

In this investigation, LFABP was titrated into DOPG vesicles with 5 mol% dansyl DHPE and fluorescence emission was measured at 500 nm following excitation of the sample at 335 nm. It would appear from the results that although all the proteins produced similar binding curves the LFABP K31E mutant binds to the phospholipid vesicles with a higher affinity than the wild-type, K20E and K33E LFABP (Figure 4.5.5.1). This apparent higher affinity is shown by the steeper increase in fluorescence when K31E LFABP was titrated into the 5 mol% dansyl DHPE vesicle than when either wild-type, K20E or K33E LFABP were titrated into the vesicles. The emission maxima for all the proteins were shown to be at the same wavelength (Figure 4.5.5.2). The saturable increase in fluorescence seen for all of the protein samples tested is indicative of interfacial binding by a peripheral membrane binding protein. This was a surprising result as it had been assumed that the K31E would bind less well to such vesicles, based on DAUDA release studies. The use of 20

mol% DOPG in DOPC vesicles would have provided a more discriminating assay to monitor DAUDA release (Figure 4.5.2.). However, it was not possible to perform binding assays with 20 mol% DOPG with 5 mol% dansyl DHPE as the fluorescence yield was already enhanced compared with the dansyl DHPE in 100 % DOPG and no further enhancement could be detected by the addition of LFABP.

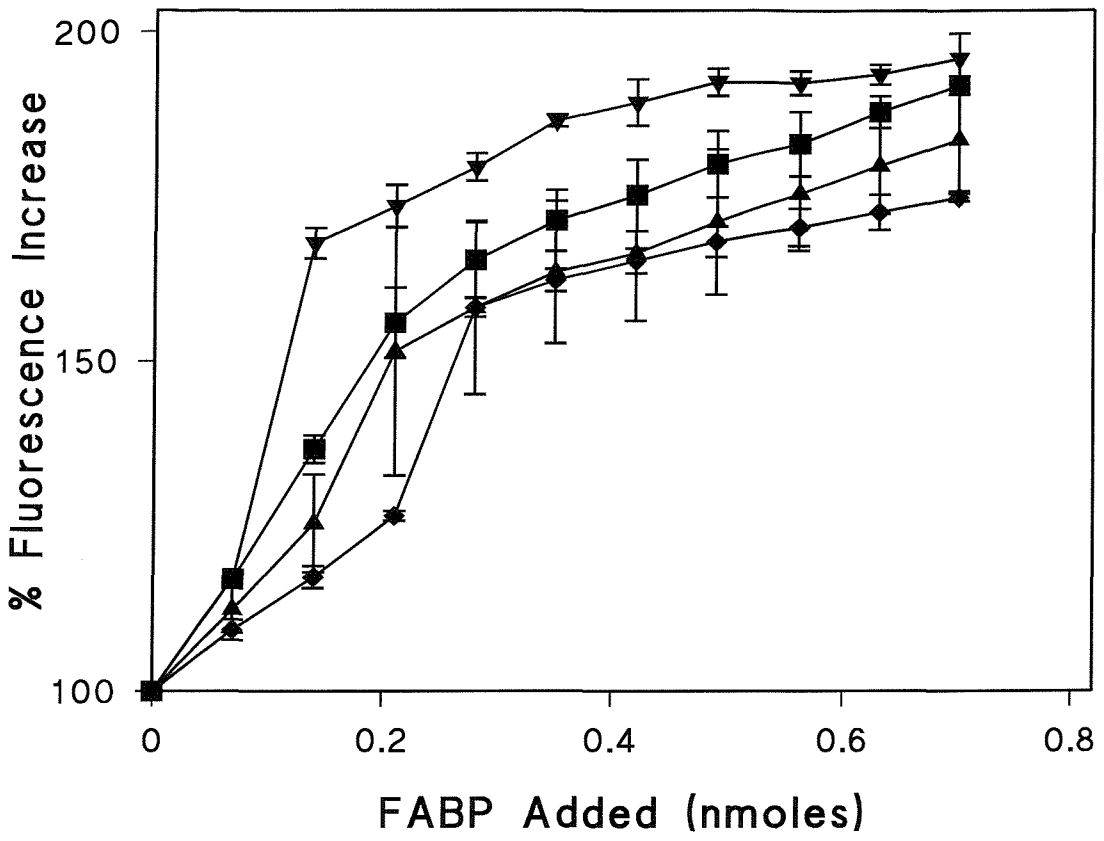

Figure 4.5.5.1. Effect of Titration of LFABP into 5 μg (~6 nmoles) DOPG with 5 mol% Dansyl DHPE SUVs

Wild-type (■), K20E (▲), K31E (▼) and K33E (◆) LFABP were titrated into 50 mM Hepes, pH 7.5 buffer containing 5 μg (6.25 nmoles) DOPG with 5 mol% dansyl DHPE SUVs. The increase in fluorescence emission was measured at 500 nm following excitation of the sample at 335nm. All data points are the mean values of three separate titrations.

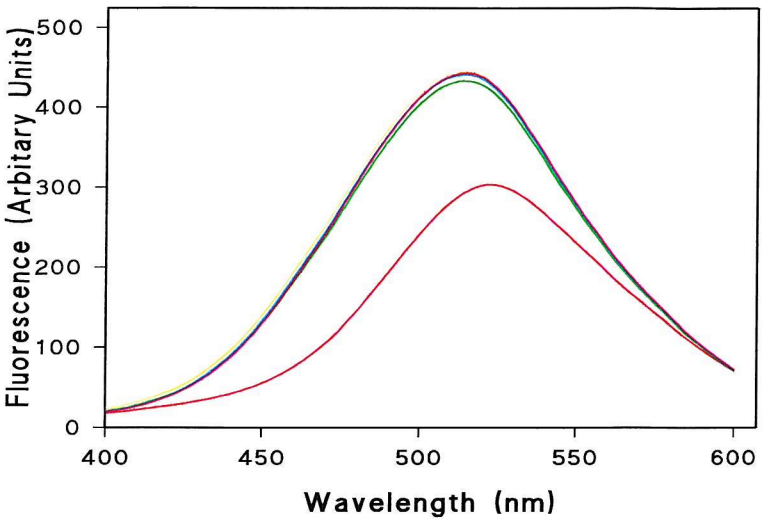

Figure 4.5.5.2. Emission Spectrum of Wild-type, K20E, K31E and K33E LFABP +/- DHPE Vesicles

The emission spectrum of 10 μg (0.7 nmoles) of either wild-type (yellow), K20E (green), K31E (blue) or K33E (pink) LFABP bound to 5 mol% DHPE with DOPG SUVs following excitation at 335nm. The emission spectrum of 5 μg DOPG with 5 mol% DHPE in 10 mM Hepes buffer is shown in red.

The titrations were repeated using 10 mM Hepes rather than the 50 mM Hepes used previously (Figure 4.5.5.3) as these are the normal conditions for the vesicle binding assays that monitor loss of DAUDA fluorescence. Under these conditions of low ionic strength all titrations were distinctly sigmoidal and showed a clear "lag" with no significant increase in fluorescence being seen until about 50 % of the protein required for maximum fluorescence enhancement was added. This is a remarkable result and a possible explanation is that under these conditions electrostatic interactions between cationic groups on the protein surface and the anionic interface dominate events and that the zwitterionic probe prefers to reside outside the protein phospholipid contact interface. Eventually after enough protein is added, the dansyl DHPE is forced into such a desolvated environment as the protein completely covers the phospholipid surface.

These results using dansyl DHPE demonstrate the ability of LFABP to bind to anionic vesicles. However, the results also highlight the potential dangers of using a fluorescent probe with a different net charge to that of the bulk phospholipid.

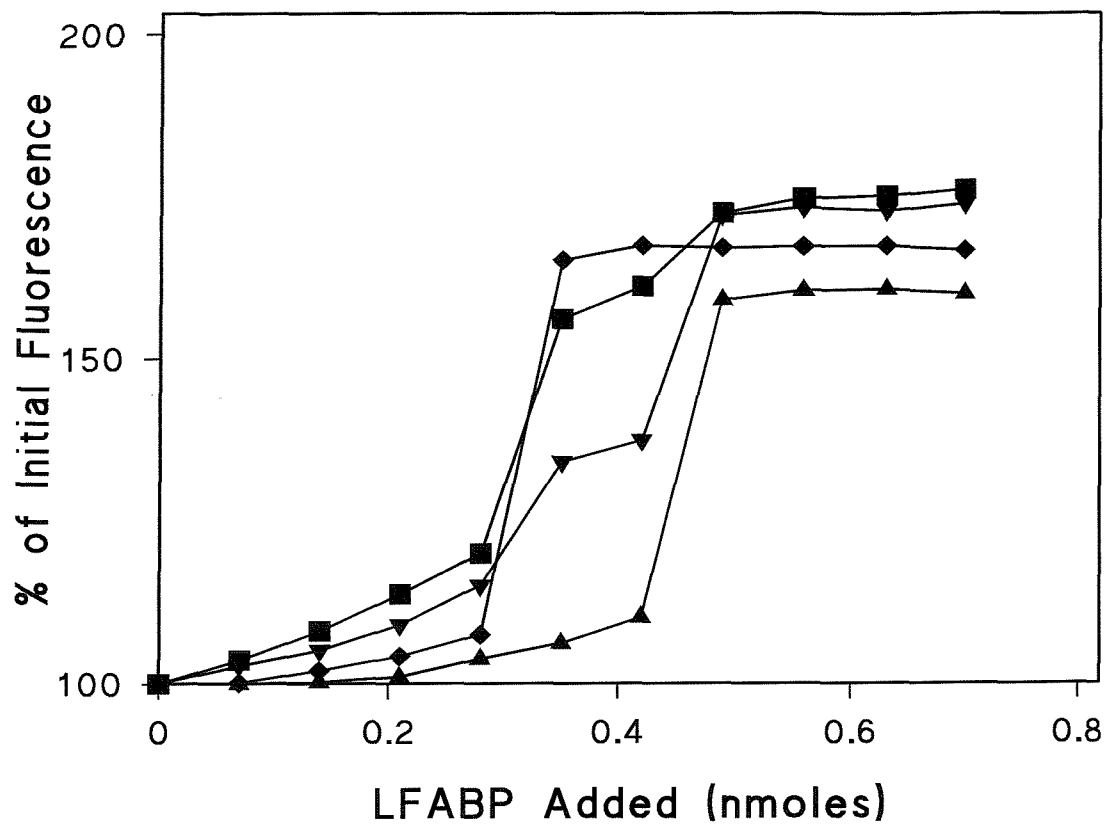

Figure 4.5.5.3. Effect of Titrating LFABP into 5 μg (~6 nmoles) DOPG with 5 mol% Dansyl DHPE SUVs in 10 mM Hepes Buffer

Wild-type (■), K20E (▲), K31E (▼) and K33E (◆) LFABP were titrated into 10 mM Hepes, pH 7.5, buffer containing 5 μg (6.25 nmoles) DOPG with 5 mol% dansyl DHPE SUVs. The increase in fluorescence emission was measured at 500 nm following excitation at 335 nm. All data points are the mean values of three separate titrations.

4.6. Discussion

The significance of the binding of LFABP to anionic phospholipid interfaces in terms of fatty acid targeting to sites of further metabolism within the cell has been discussed previously in Chapter 3. In the case of the LFABP, the mutagenesis studies described in this chapter suggest that α-helix II is most directly involved in membrane interactions, in particular residue K31. In contrast, in the case of other mammalian FABPs that have been studied it is the amphipathic nature of the α-helix I that suggests this helix as the major site of interaction with the membrane [6]. In the case of HFABP, mutagenesis of K22 (a residue present in α-helix I and equivalent to K20 in LFABP) to glutamate (K22E) caused a 3-fold decrease in rates of collisional transfer, a similar change also being seen by the neutral mutation K22L [30].

In summary, charge reversal mutations in the α-helical region of LFABP highlight differential effects on ligand binding to anionic phospholipid vesicles. The mutant K31E makes a significant contribution to the binding of the protein to anionic vesicles whereas the other two cationic residues are without significant effect.

The ligand binding properties of the charge reversal mutants support the proposal that ligands such as lysophospholipids bind with their bulky charged head groups located in the portal region of the protein where cationic groups on α-helix II can make an electrostatic contribution to ligand binding. In contrast, mutation within the α-helical region had no effect on DAUDA binding.

Studies on a cytosolic fatty acid binding protein homologue of the human blood fluke *Schistosoma japonicum* (Sj-FABPc) have identified α-helix II as being necessary for ligand binding [99]. In these studies on Sj-FABPc a deletion mutant was created that lacked α-helix II, it was found that this deletion mutant was no longer able to bind DAUDA. It remains to be determined if the DAUDA binds to Sj-FABPc with a different orientation requiring the direct involvement of α-helix II or that this mutation results in a more profound change to the overall protein structure.

Chapter Five:

Studies on Tryptophan Mutants of LFABP and the Possible Role of the C-terminus in Binding to Anionic Vesicles

5.1. Introduction

As has already been discussed in Chapters 3 and 4, LFABP binds to anionic phospholipid vesicles with high affinity. Disruption of the interactions involved in the binding of anionic phospholipids to LFABP proved difficult and was achieved most effectively by the use of non-ionic detergent in the assay system [83]. This result, together with the fact that DAUDA release was observed on binding to these anionic vesicles, means that significant conformational changes have occurred to the LFABP as a result of this interfacial interaction.

Changes in protein conformation can be studied by observing changes in the fluorescence of tryptophan residues contained within the protein. These changes can be observed either as changes in the intensity of the tryptophan fluorescence and/or as a change in the wavelength at which the fluorescence emission is maximal. Studying the tryptophan fluorescence of a protein can give information on any change in the environment surrounding these particular residues. A blue shift in the emission maxima is consistent with the tryptophan residue moving from a more aqueous environment to a more hydrophobic environment, for example, a residue embedding into a membrane.

LFABP in its wild-type form does not contain tryptophan and so in order for conformational studies to be undertaken as described, tryptophan residues had to be inserted into the protein using site-directed mutagenesis. The mutation of residues of LFABP to tryptophan had previously been carried out by Alfred Thumser in this laboratory who produced the F3W, F18W and C69W single mutants of LFABP [100].

These particular residues were chosen for mutation because of their location in the protein, they have been used previously to study the binding and structural characteristics of rat LFABP using fluorescent fatty acid analogues [100].

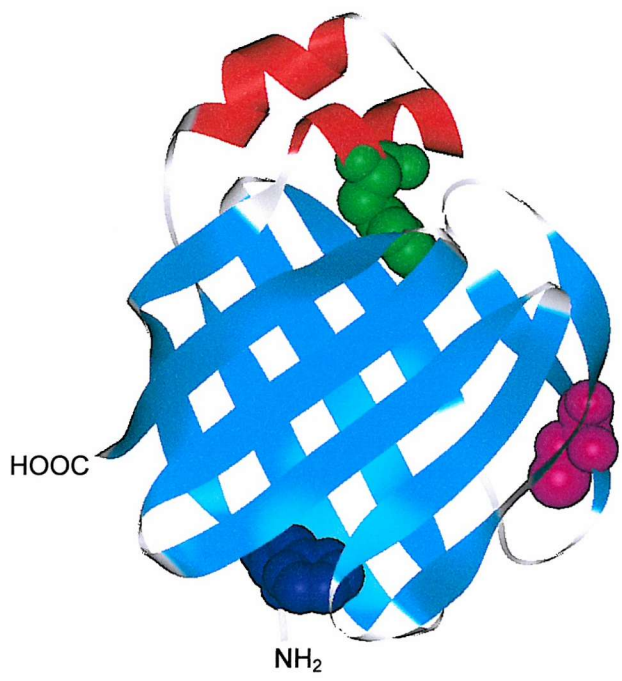

Figure 5.1.1. Structure of LFABP Highlighting Residues F3, F18 and C69

Residue F3 is shown in dark blue, residue F18 is shown in green and C69 is shown in magenta.

The structure of LFABP highlighting the positions of the mutated residues is shown in figure 5.1.1. The phenylalanine at position 3 is located at the base of the β-barrel structure at the opposite end of the protein to the α-helical region. The

phenylalanine at position 18 is located within the α-helical region on helix I that forms the top of the proposed portal region of the protein and the cysteine at position 69 forms a part of β-strand 5 of the β-barrel structure. C69 is thought to be a residue that exhibits some conformational flexibility, as it has not been possible to assign a fixed orientation for this residue using X-ray crystallographic studies [13]. Although these mutants had been made previously the expression system was no longer functional and, as a result, the mutagenesis had to be repeated. The F3W mutation was made using the Kunkel method and the F18W and C69W mutations were produced using a PCR method for site-directed mutagenesis, as described in the Material and Methods section of this work.

The mutated gene was cloned into the pET11a expression system and transformed into BL21(DE3) *E.coli* cells for expression. Characterisation of these mutants has previously shown them to behave similarly to the wild-type protein in terms of the binding of fluorescent fatty acid analogues [100]. The tryptophan fluorescence of the F3W and C69W proteins was found to be unaffected by the binding of fatty acids whereas there was noted to be a slight increase in the tryptophan fluorescence upon the binding of fatty acids to the F18W protein [100] suggesting that the position of the residue had changed slightly resulting in a less quenching environment.

The results obtained with the tryptophan mutants indicated conformational changes at the N-terminal region of LFABP when the protein is bound to DOPG vesicles. In order to investigate further the possible residues on LFABP involved in electrostatic interactions with anionic phospholipids, attention was focussed on the C-terminal of

the protein where residues K125 and R126 lie in close proximity to the N-terminus of the protein.

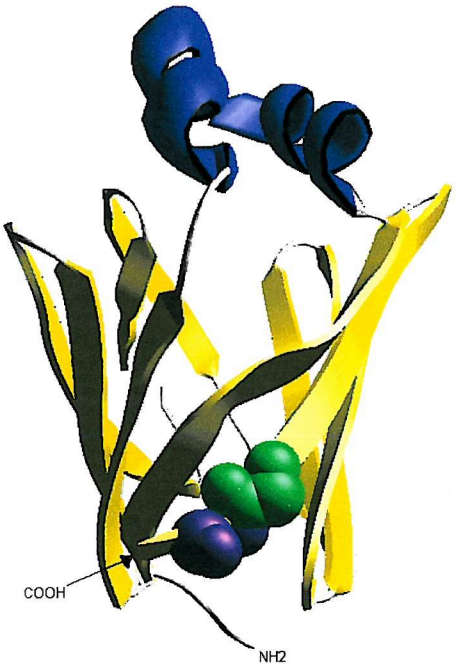

Figure 5.1.2. **The Structure of LFABP as Viewed Looking Between β-Strands 1 and 2**

Lysine 125 is shown in green and Arginine 126 is shown in purple

5.2. DAUDA Binding to LFABP Tryptophan Mutants

The ability of the tryptophan mutants of LFABP to bind DAUDA has been investigated previously by Alfred Thumser at the time the mutants were first produced [100]. The K_d values of the proteins for DAUDA were shown in these studies to be 0.3, 0.46 and 0.36 μM for F3W, F18W and C69W LFABP respectively [100] compared with a Kd for wild-type LFABP of 0.58 μM. Thus there were no adverse effects of tryptophan mutagenesis on DAUDA binding.

5.3. Conformational Changes on the Binding of Phospholipids to Tryptophan Mutants of LFABP

The ability of the tryptophan mutants of LFABP to bind DOPG vesicles was investigated. DOPG binding was monitored both by the loss of LFABP/DAUDA fluorescence and by changes in the tryptophan fluorescence emission spectrum. The tryptophan residues were excited at 280 nm and emission fluorescence scan measured between 300-400 nm. LFABP/DAUDA fluorescence was measured at 500 nm following excitation at 350 nm.

5.3.1. Binding to DOPG Vesicles Induces Conformational Changes in F3W LFABP

In order to investigate the effect that the binding of LFABP to a DOPG interface has on the overall structure of the protein, DOPG SUVs were titrated by methanol injection into a solution of either F3W, F18W or C69W LFABP. Fluorescence

emission was measured at 330 nm following excitation at 280 nm as shown in Figure 5.3.1.1.

As can be seen clearly from the graph in Figure 5.3.1.1. there is a significant loss of tryptophan fluorescence from the F3W mutant upon addition of DOPG SUVs to the protein. This loss amounts to approximately 40 % of the initial fluorescence before DOPG vesicles were added into the cuvette. No significant changes were detected in the fluorescence emission intensity of the tryptophan residues in the F18W and C69W mutants. However, scans of the fluorescence emission spectra for the three proteins show a slight red-shift in the maxima for the F18W mutant from 330 nm to 335 nm in the presence of 25 nmoles DOPG SUVs (Figure 5.3.1.2). This red-shift is characteristic of movement of the residue into a more polar environment. The data for the F18W mutant is interesting as one might predict this residue to be the prime candidate for conformational change considering it's location within the α-helical region. For many proteins it is the α-helical regions that are most directly involved in interactions with phospholipid membranes. The fluorescence intensity measurement for the C69W mutant is very unstable and it proved impossible to achieve very consistent data for each point. This may be explained by the previous suggestion that this particular residue exhibits conformational flexibility and no fixed orientation [13].

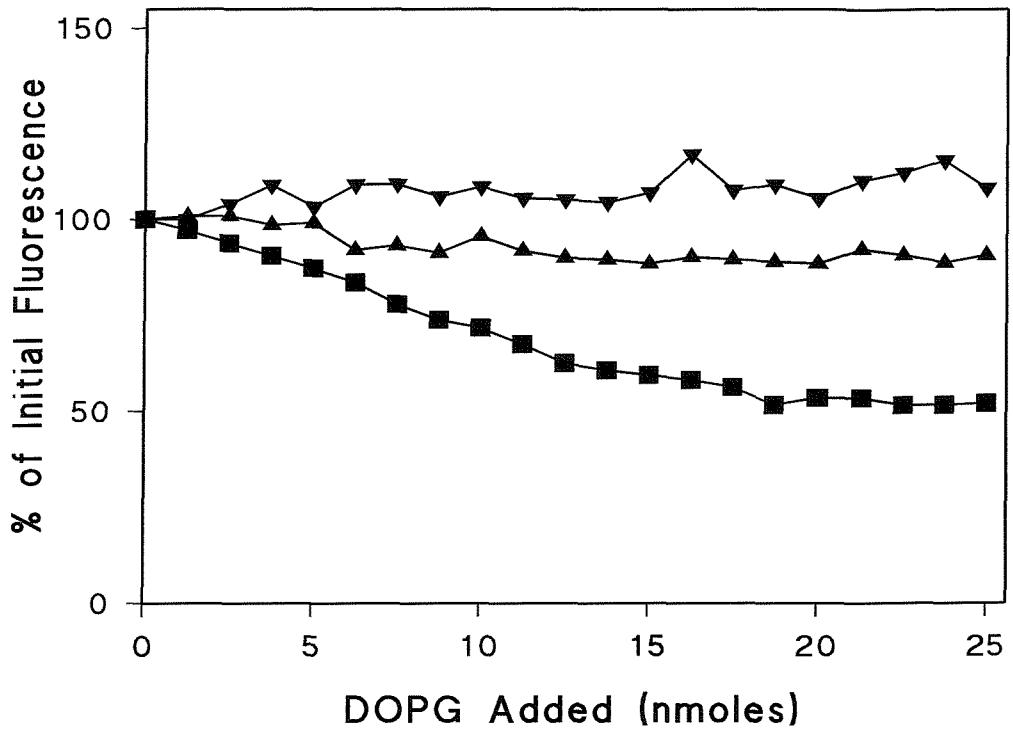

Figure 5.3.1.1. The Effect on the Tryptophan Fluorescence of the Titration of 100 % DOPG SUVs into F3W, F18W and C69W mutants of LFABP

100 % DOPG SUVs were titrated by methanol injection into 10 μg (0.8 nmoles) of either F3W (■), F18W (▲) or C69W (▼) LFABP in 10 mM Hepes. Tryptophan fluorescence was measured at 330 nm following excitation at 280 nm. All data points shown are the mean values of three separate titrations and are corrected for DOPG titration into 10 mM Hepes buffer.

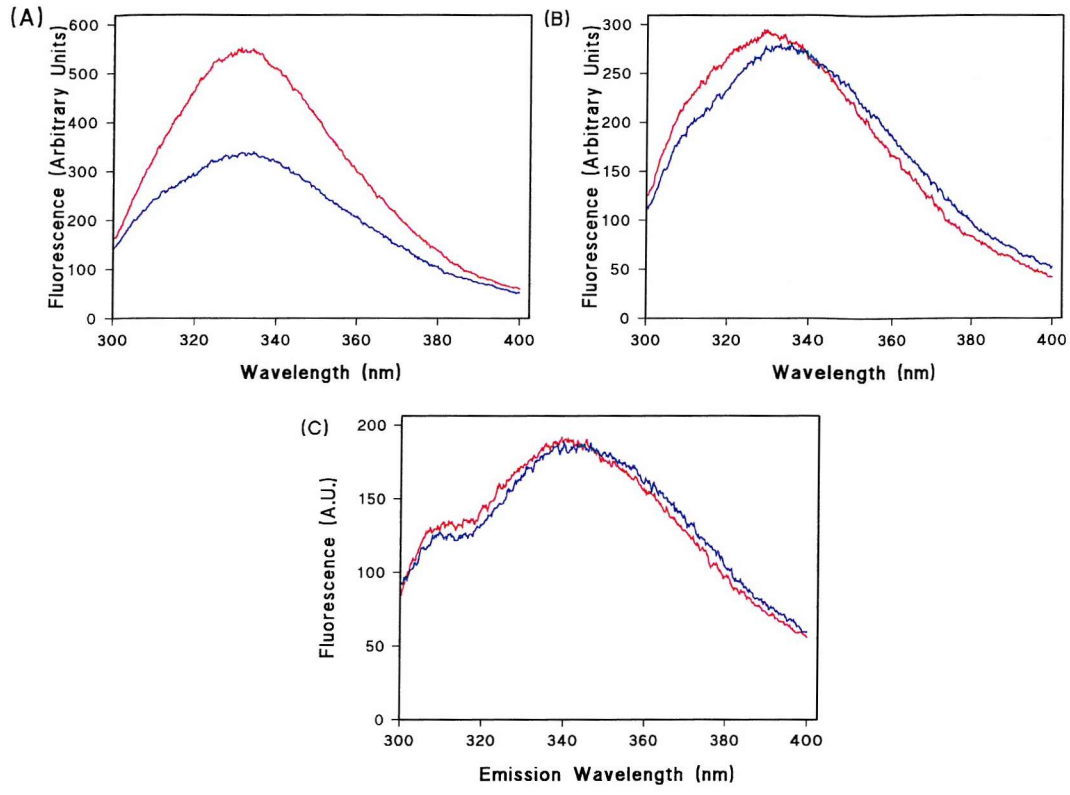

Figure 5.3.1.2. The Effect of 100 % DOPG SUVs on the Tryptophan Emission Maxima of F3W, F18W and C69W LFABP

Tryptophan emission of 10 μg (0.8 nmoles) of either F3W (A), F18W (B) or C69W (C) in 10 mM Hepes was measured at 330 nm following excitation at 280 nm in the absence (red line) or presence (blue line) of 25 nmoles DOPG SUVs. The data presented is representative of three separate titrations.

An important question is whether the presence of ligand within the binding cavity of LFABP had any effect on conformational change when DOPG SUVs were added into solutions of F3W, F18W and C69W LFABP in Hepes buffer. The ligand of choice was oleic acid as it is known to be a high affinity ligand for LFABP that has no intrinsic fluorescence that may affect any tryptophan fluorescence data. Oleic acid was added in a 1:1 ratio as a solution in methanol into 10 μg (0.8 nmoles) of either F3W, F18W or C69W LFABP in 10 mM Hepes buffer. DOPG was titrated into the assay and the fluorescence emission was measured using the assay procedure described in Figure 5.3.1.1. No difference in the tryptophan fluorescence was seen for the mutants when comparing titrations in the presence and absence of oleic acid (data not shown). Thus, the only significant change seen in tryptophan fluorescence upon addition of DOPG vesicles was seen for the F3W LFABP mutant and this change was independent of bound ligand.

5.3.2. Loss of Tryptophan Fluorescence Upon Addition of DOPG Vesicles to F3W LFABP Parallels Exactly the Loss of DAUDA from the Protein

The loss of fluorescence seen from the tryptophan at position 3 was further investigated in order to determine if the fall in fluorescence seen was linked with the release of ligand from the protein. The fluorescent fatty acid analogue, DAUDA, was used as the ligand of choice to enable the monitoring of release of ligand by F3W LFABP. Briefly, DOPG vesicles were titrated into 10 μg (0.8 nmoles) F3W LFABP and changes in DAUDA fluorescence were measured at 500 nm following excitation at 350 nm (Figure 5.3.2).

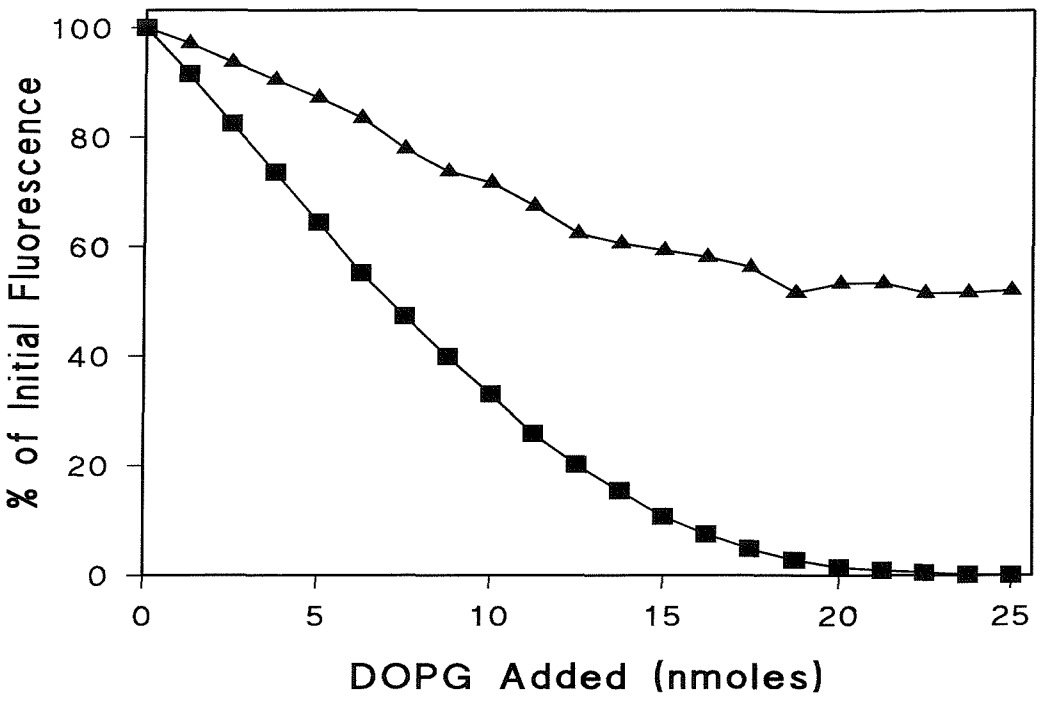

Figure 5.3.2. **Comparison of Loss of Tryptophan Fluorescence and Loss of DAUDA Fluorescence Seen Upon Addition of 100 % DOPG SUVs into F3W LFABP**

Vesicles of 100 % DOPG were titrated by methanol injection into either 10 μg (0.8 nmoles) F3W in 10 mM Hepes and 2 nmoles DAUDA (■) or 10 μg (0.8 nmoles) F3W in 10 mM Hepes (▲). Tryptophan Fluorescence was measured at 330 nm following excitation at 280 nm and DAUDA fluorescence was measured at 500 nm following excitation at 350 nm. All data points are the means values of three separate titrations and are corrected for the titration of 100 % DOPG SUVs into either 10 mM Hepes with 2 nmoles DAUDA (■) or into 10 mM Hepes alone (▲).

The data for loss of F3W tryptophan fluorescence in figure 5.3.2. is taken from the data for figure 5.3.1.1. As can be seen from the graph, the loss of tryptophan fluorescence from F3W LFABP upon addition of DOPG vesicles exactly parallels the loss of DAUDA fluorescence from the protein upon addition of DOPG vesicles. This would suggest that there is indeed a conformational change occurring when DOPG vesicles are added into F3W LFABP and that this conformational change correlates exactly with the release of ligand from the protein.

5.3.3. Loss of Tryptophan Fluorescence from F3W LFABP by DOPG Vesicles is Inhibited by the Presence of 200 mM NaCl

As has previously been demonstrated (Chapter 3), the binding of DOPG vesicles to wild-type LFABP is inhibited by the presence of 200 mM NaCl in the assay buffer. The loss of tryptophan fluorescence from the F3W LFABP mutant is, presumably, the result of a direct interaction between the protein and the phospholipid interface. This interaction induces a conformational change resulting in the re-orientation of the tryptophan at position 3 into a more polar, hence, more quenching environment. In theory, if the binding of DOPG to LFABP is inhibited then there should be no detectable conformational change and it can be concluded that it is the direct interaction of DOPG SUVs with the protein that is responsible for inducing any conformational changes. In order to investigate this the titration of DOPG vesicles into F3W LFABP was repeated in the presence of 200 mM NaCl, as shown in figure 5.3.3. The presence of 200 mM NaCl inhibits the loss of tryptophan fluorescence

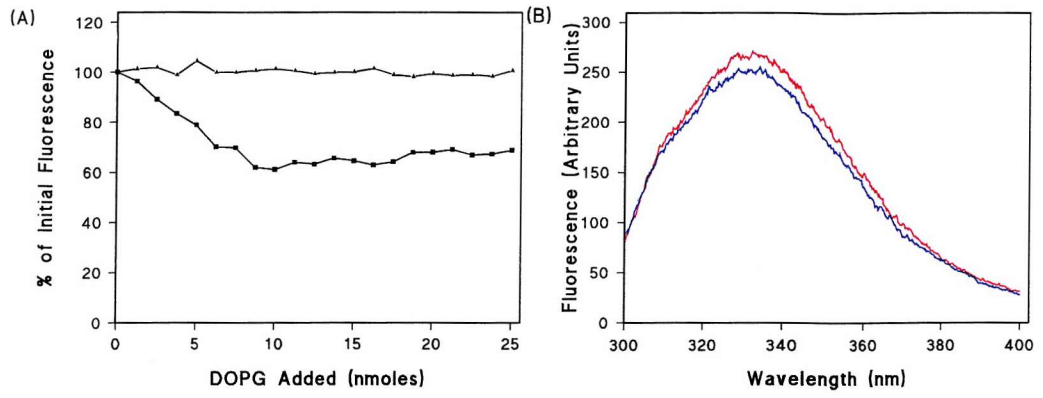

Figure 5.3.3. **The Effect of 200 mM NaCl on Loss of Tryptophan Fluorescence from F3W LFABP by 100 % DOPG SUVs**

Vesicles of 100 % DOPG were titrated by methanol injection into 10 μg (0.8 nmoles) F3W LFABP in 10 mM Hepes, pH 7.5, buffer with 200 mM NaCl (■) and without 200 mM NaCl (▲) in figure (A). Wavelength emission scans were produced of 0.8 nmoles F3W in 10 mM Hepes and 200 mM NaCl with 25 nmoles DOPG (blue line) and without DOPG (red line) in figure (B). In both cases excitation was at 280 nm and the emission wavelength measured for figure (A) was 330 nm. The data points in figure (A) are the mean values of three separate titrations and are corrected for the titration of 100 % DOPG vesicles into 10 mM Hepes (■) and into 10 mM Hepes with 200 mM NaCl (▲). The data in figure (B) is representative of the scans of three separate samples.

seen by the F3W mutant upon addition of DOPG vesicles. From this it can be concluded that the loss of tryptophan fluorescence observed from F3W LFABP is as a result of an initial electrostatic interaction between the protein and anionic phospholipid vesicles.

5.4. Fluorescence Resonance Energy Transfer (FRET) Studies Using Tryptophan Mutants of LFABP

Fluorescence resonance energy transfer (FRET) can be used to provide a more direct measure of the proximity of a tryptophan residue to an appropriate receptor such as a dansyl group. The process is not dependent on conformational changes in the tryptophan donor in order to detect changes in fluorescence intensity of dansyl emission as it is the distance between the tryptophan and the dansyl group that is of primary importance [101]. Therefore the binding of the three mutants F3W, F18W and C69W to phospholipids was determined under a variety of conditions, exciting at 280 nm and monitoring both loss of tryptophan fluorescence at 330 nm and enhanced fluorescence at 500 nm due to dansyl fluorescence as a result of FRET.

5.4.1. F3W LFABP Shows Considerably Enhanced Dansyl Fluorescence Due to FRET That Parallels Loss of Tryptophan Fluorescence

The effect of titrating F3W, F18W and C69W LFABP into DOPG vesicles containing 5 mol% dansyl DHPE is shown in Figure 5.4.1.1(B). The reverse of this titration was also carried out, DOPG containing 5 mol% dansyl DHPE was titrated into 0.8 nmoles of either F3W, F18W or C69W to assess the effect on tryptophan fluorescence

(Figure 5.4.1.1.(A)). As can be seen from the data presented, there was considerably enhanced dansyl fluorescence due to FRET seen for the F3W mutation. This trend was mirrored in the effect of DOPG/dansyl DHPE vesicles on loss of tryptophan fluorescence from the F3W LFABP (Figure 5.4.1.2). The data shown for the F3W mutant would suggest that the N-terminal region of the protein is in close proximity to the dansyl group present at the phospholipid interface.

Figure 5.4.1.1.(A) shows there to be a significant loss of tryptophan fluorescence from the F18W mutant, which is an interesting result as the effect is not mirrored by an increase in dansyl fluorescence as shown in Figure 5.4.1.1.(B). The tryptophan at position 18 has undergone some degree of fluorescence quenching but has not been involved in FRET, which would suggest that α-helix I is in close proximity to the phospholipid interface but that the relationship between the tryptophan and the dansyl group is not optimal for FRET.

Minimal tryptophan fluorescence is lost from the C69W mutant relative to that lost from either the F3W mutant or the F18W mutant. There was no increase seen in the fluorescence of the dansyl DHPE, therefore, no FRET has occurred at this position.

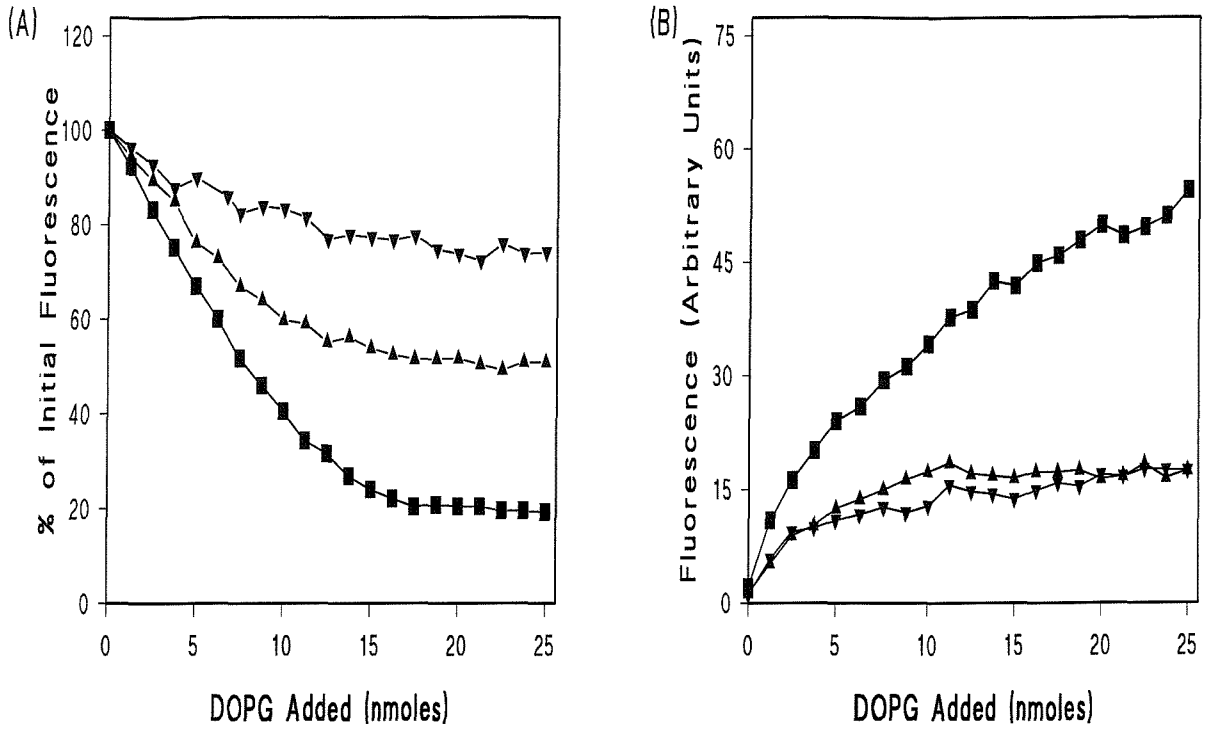

Figure 5.4.1.1. The Effect of DOPG Containing 5 mol% Dansyl DHPE Vesicles on Tryptophan Fluorescence of F3W, F18W and C69W LFABP Mutants

Figure (A), DOPG containing 5 mol% dansyl DHPE vesicles were titrated as a methanol solution into 10 mM Hepes containing 10 μg (0.8 nmoles) of either F3W (■), F18W (▲) or C69W (▼) LFABP. Tryptophan fluorescence was measured at 330 nm following excitation at 280 nm. Figure (B), DOPG containing 5 mol% dansyl DHPE was titrated as described above, dansyl fluorescence was measured at 500 nm following excitation of the tryptophan residues at 280 nm. All data points are the mean values of three separate titrations and are corrected for the titration of vesicles into buffer.

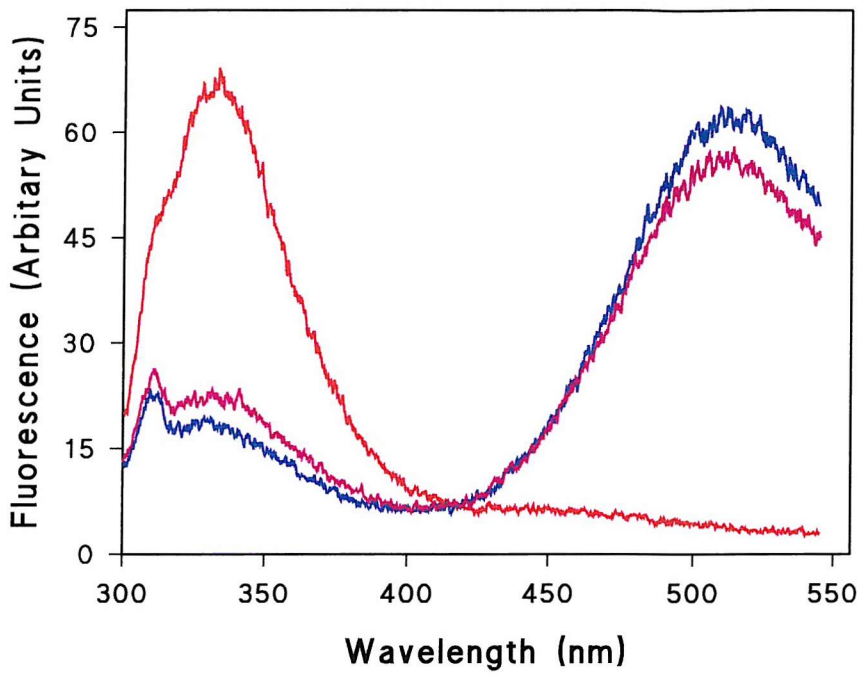

Figure 5.4.1.2. Wavelength Scan of F3W LFABP In The Presence and Absence of DOPG Vesicles Containing Dansyl DHPE

The emission spectrum of F3W LFABP following excitation at 280 nm was measured both in the absence (Red) and presence (Blue and Magenta) of 25 nmoles DOPG vesicles containing 5 mol% dansyl DHPE. The spectra presented are representative of scans on three separate samples.

5.4.2. FRET From F3W LFABP to Dansyl DHPE is Inhibited in the Presence of 200 mM NaCl

As has been previously discussed in Chapter 3, the binding of DOPG-containing vesicles to LFABP is inhibited by the presence of 200 mM NaCl. It has also been shown previously in the present chapter that the presence of 200 mM NaCl prevents the loss of tryptophan fluorescence upon addition of DOPG vesicles to the F3W LFABP mutant (Figure 5.3.3). Therefore, if the FRET observed when the F3W, F18W and C69W mutants are mixed with DOPG containing vesicles requires binding to the phospholipid interface then this FRET should be prevented in the presence of 200 mM NaCl.

The effect of 200 mM NaCl on FRET between F3W, F18W and C69W LFABP and dansyl DHPE-containing vesicles was investigated. DOPG vesicles containing 5 mol% dansyl DHPE were titrated into either F3W, F18W or C69W LFABP in the presence of 200 mM NaCl.

Figure 5.4.2. shows there to be no significant loss of tryptophan fluorescence from either F3W, F18W or C69W upon addition of DOPG/dansyl DHPE vesicles in the presence of 200 mM NaCl. Similarly, no increase in dansyl fluorescence was seen for any of the mutations studied (data not shown). From this it can be concluded that there is no interaction between the protein and the phospholipid interface in the presence of 200 mM NaCl. This reinforces the proposal that electrostatic forces are important for the initial interactions between LFABP and anionic phospholipid vesicles [83].

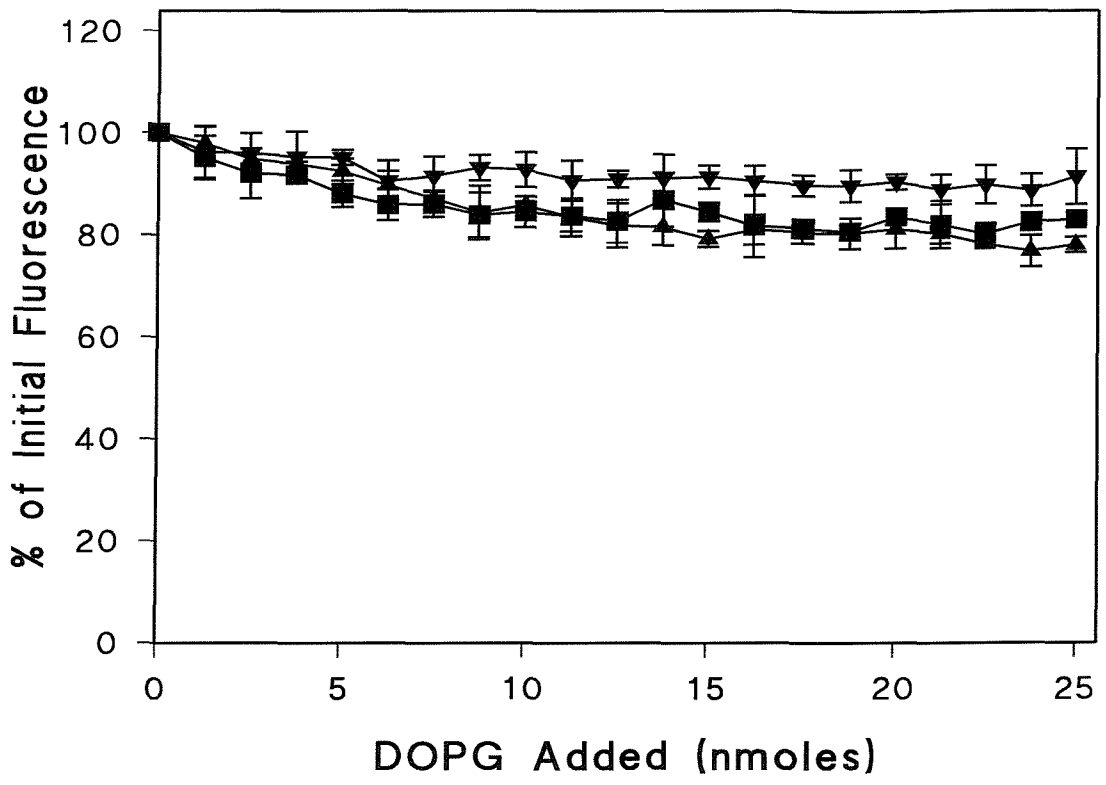

Figure 5.4.2. **The Effect of the Presence of 200 mM NaCl on the Changes in Tryptophan Fluorescence Seen Upon Addition of DOPG Vesicles Containing dansyl DHPE to F3W, F18W and C69W LFABP**

DOPG vesicles containing 5 mol% dansyl DHPE were titrated by methanol injection into 10 mM Hepes, 200 mM NaCl containing 10 μg (0.8 nmoles) of either F3W, F18W or C69W LFABP. Fluorescence emission was measured at 330 nm following excitation at 280 nm. All data points are the mean values of three separate titrations and are corrected for the titration of phospholipid vesicles into the buffer.

5.4.3. No FRET Occurs Between F3W, F18W or C69W LFABP and DOPC Vesicles Containing 5 mol% Dansyl DHPE

It was important to confirm that there is no direct interaction occurring between the tryptophan mutants of LFABP, F3W, F18W and C69W, and DOPC vesicles. Therefore, DOPC vesicles containing 5 mol% dansyl DHPE were titrated into solutions of the mutant proteins in 10 mM Hepes buffer (Figure 5.4.3). As predicted from previous data (Figure 3.2.2), none of the mutants studied show any sign of FRET upon addition of DOPC containing 5 mol% dansyl DHPE vesicles and, therefore, no interaction would appear to be occurring between the proteins and the DOPC vesicle interface.

5.4.4. Succinimide Quenching

Succinimide is a fluorescence quencher that has previously been used to investigate the degree of solvent exposure shown by tryptophan residues in proteins including a related FABP, Sj-FABPc [99]. The more solvent exposed the residue, the greater the degree of fluorescence quenching seen upon addition of succinimide to the protein. Moreover succinimide is larger than the commonly used quencher, acrylamide, and is more sensitive to the structural location of the tryptophan [102].

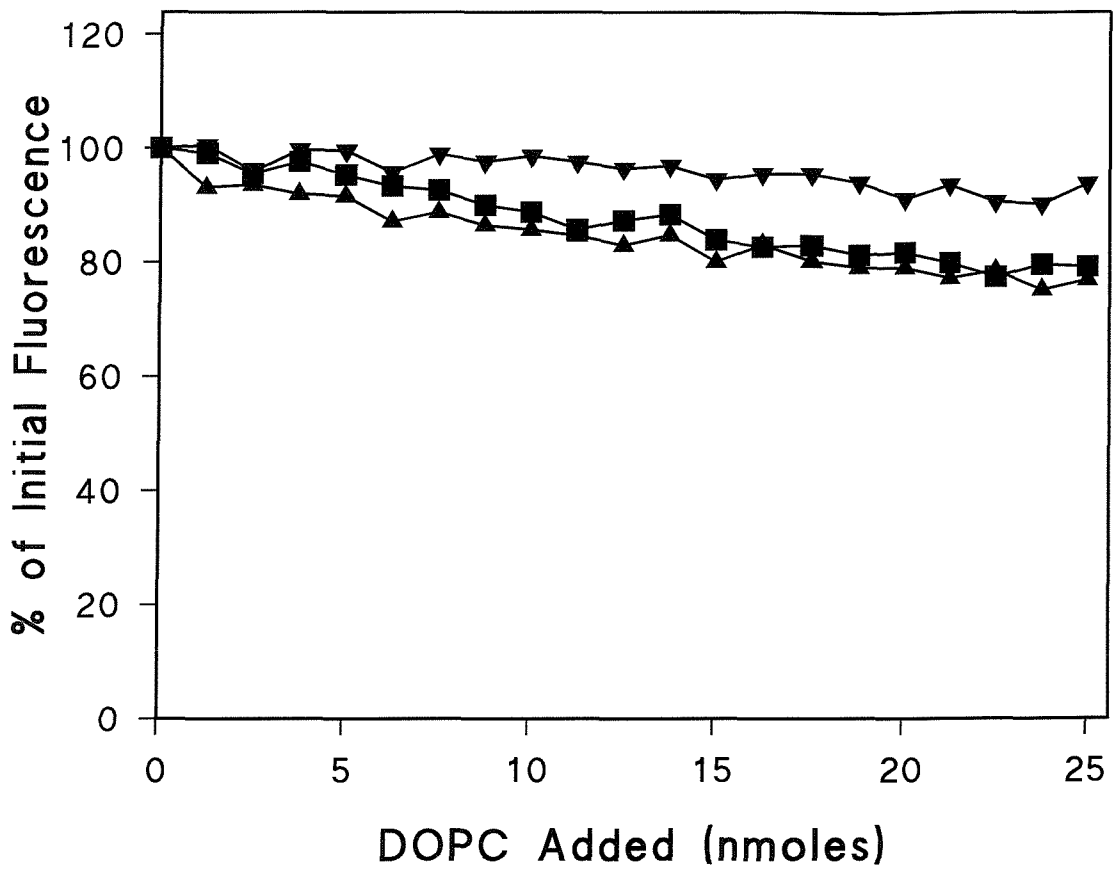

Figure 5.4.3. **Effect of DOPC Vesicles Containing Dansyl DHPE on the Tryptophan Fluorescence of F3W, F18W and C69W LFABP**

DOPC vesicles containing 5 mol% dansyl DHPE were titrated by methanol injection into 10 mM Hepes containing 10 μg (0.8 nmoles) of either F3W, F18W or C69W LFABP. Emission fluorescence was measured at 330 nm following excitation at 280 nm. All data points are the mean values of three separate titrations and are corrected for the titration of phospholipid into the buffer.

Succinimide quenching studies were carried out on 0.8 nmoles protein in 10 mM Hepes buffer in the presence and absence of 25 nmoles DOPG (Figure 5.4.4.1). There was shown to be succinimide quenching of all three tryptophan mutations to varying degrees which, in the case of the F3W mutant, was prevented in the presence of DOPG vesicles. Figure 5.4.4.2. shows a modified Stern-Volmer plot [77] of succinimide quenching for each of the three mutations. The values on the graphs at the Y-intercept are 1.0, 1.13 and 1.15 for F3W, F18W and C69W respectively. This data concludes that the F3W is completely solvent exposed in the absence of ligand and both the F18W and the C69W residues are more than 80 % exposed. Only quenching of the F3W mutation is completely prevented in the presence of DOPG vesicles. There are two possible explanations of this phenomenon, either the F3W mutation is becoming internalised and so no longer solvent exposed or the residue is being shielded by the phospholipid vesicle itself as the N-terminal maybe becomes embedded in the phospholipid membrane.

The degree of quenching of the C69W mutant by succinimide is reduced by approximately 15 % in the presence of DOPG vesicles. An explanation for this is that in the presence of DOPG vesicles the protein undergoes a conformational change that results in the C69W residue becoming less solvent exposed and, therefore, less exposed to the quenching effects of succinimide. It should be noted that there was a small but variable increase in tryptophan fluorescence when the C69W bound to DOPG vesicles (Figure 5.3.1.1). In fact in the crystal structure C69 showed ambiguity that could reflect conformational mobility of this residue [8]. If the reduction of quenching were due to interaction with the phospholipid interface, then this quenching is considerably less than seen with the F3W mutant.

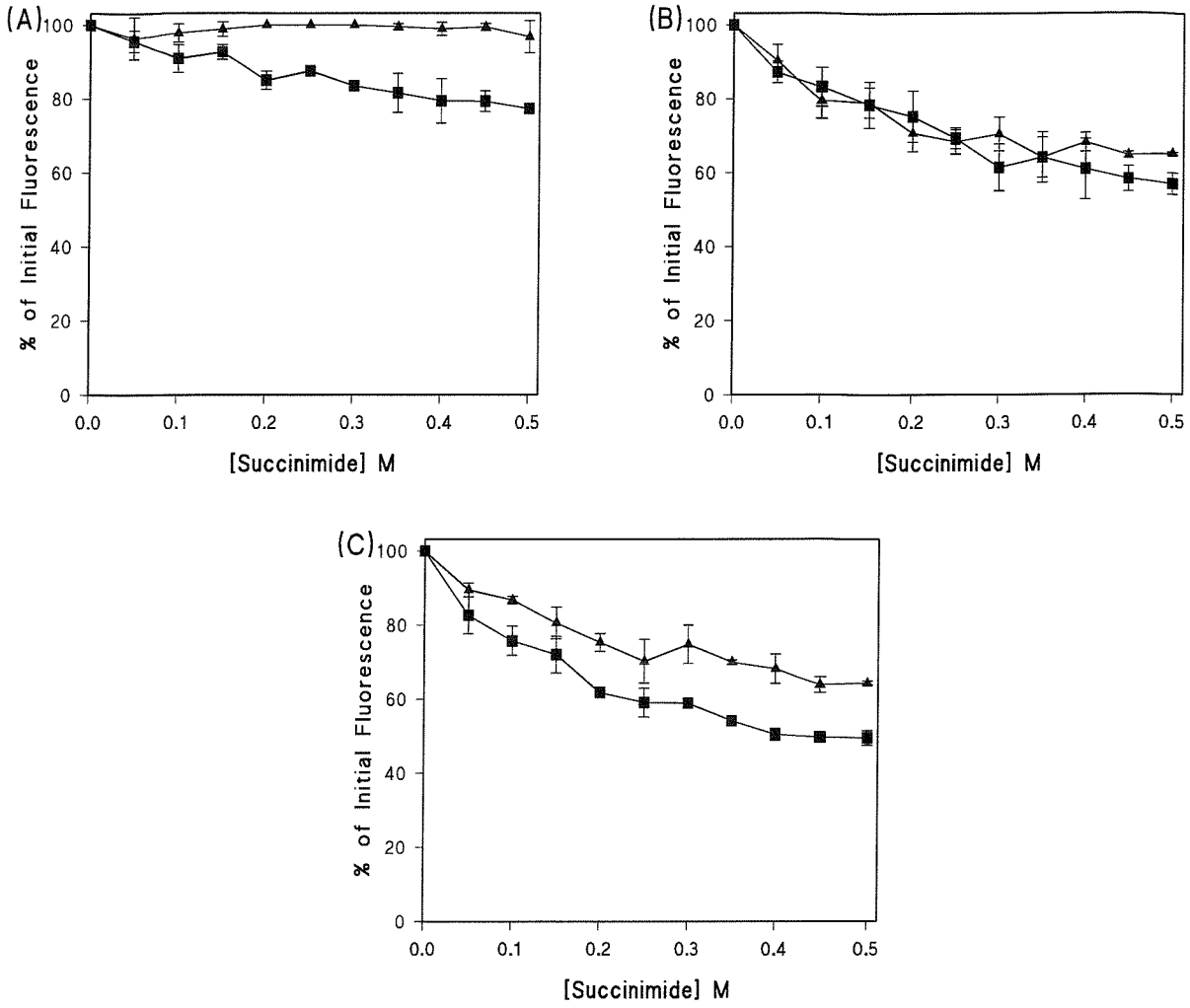

Figure 5.4.4.1. The Effect of Succinimide on the Tryptophan Fluorescence of F3W, F18W and C69W LFABP Mutants in the Presence and Absence of DOPG

Succinimide was titrated as a 3 M stock in H_2O into 10 μg (0.8 nmoles) of either F3W (A), F18W (B), or C69W (C) in 10 mM Hepes in the absence (■) and presence (▲) of 25 nmoles 100 % DOPG vesicles. Tryptophan fluorescence was measured at 330nm following excitation at 280 nm. All data points are the mean values of three separate titrations and are corrected for dilution factors.

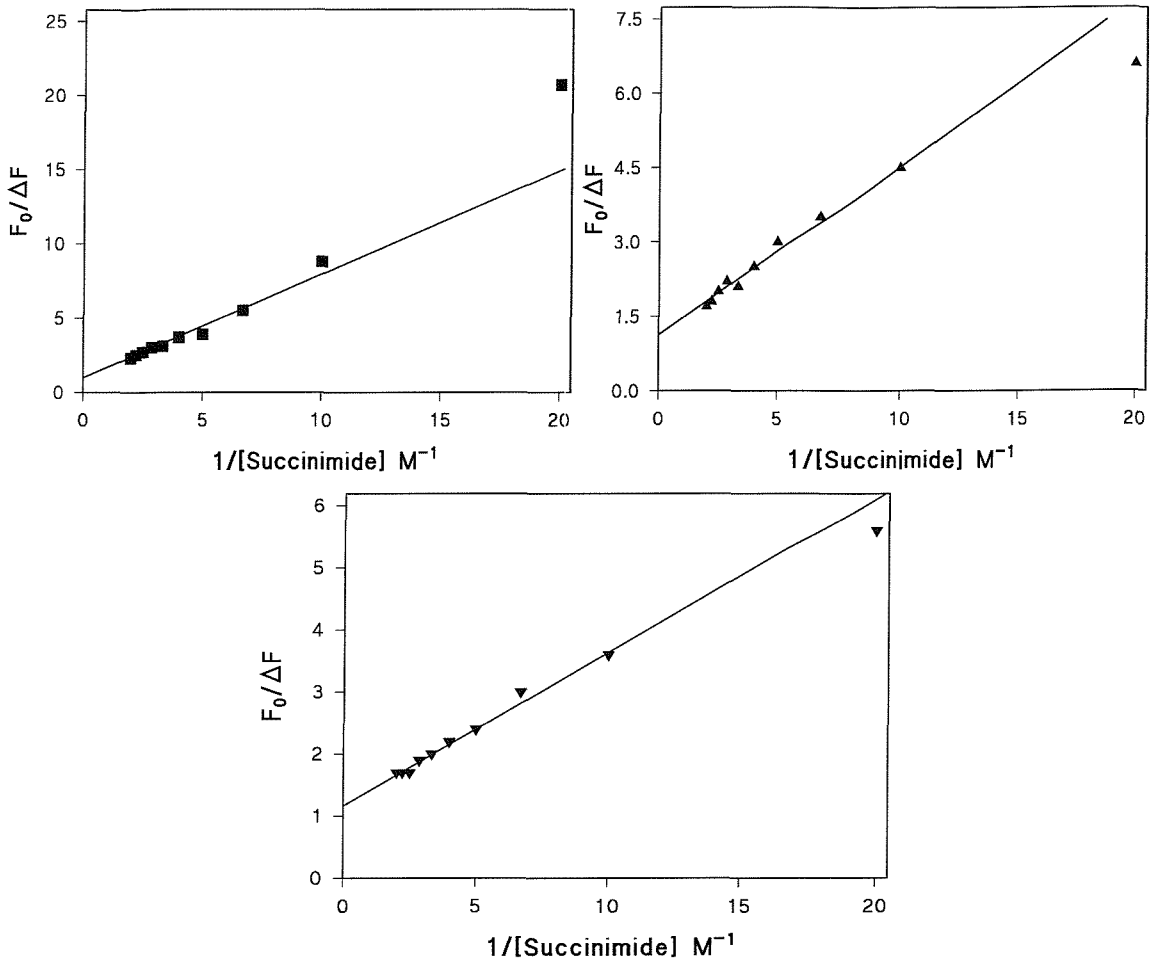

Figure 5.4.4.2. **Modified Stern-Volmer Plots of the Fluorescence Quenching of Mutants F3W, F18W and C69W LFABP by Succinimide**

Modified Stern-Volmer plots were produced using the data in Figure 5.4.4.1. for F3W (■), F18W (▲) and C69W (▼) LFABP.

5.5. Functional Studies on the mutants: K125E and R126E

The α-helical region of the FABP family has been implicated in the proposed ligand portal for this family of proteins. While mutagenic studies on the IFABP, AFABP and HFABP have highlighted the importance of this region in membrane-protein interactions [15, 41] one might expect that if the α-helical region of the protein were important in the transfer of fatty acids to/from the binding cavity to the membrane then a conformational change would be detectable in this region upon addition of the appropriate phospholipid interface. This, however, has been found not to be the case for LFABP. An F18W mutant of α-helix I showed little to no conformational change upon the interaction of LFABP with anionic phospholipid vesicles as discussed earlier in this chapter. In contrast to this, the mutation, F3W, at the 'base' of the structure, the opposite end of the β-barrel to the presumptive ligand entry portal, showed a significant change in conformation that correlated directly with the release of DAUDA from LFABP [83]. This may suggest the presence of a second portal region, the opening up of which would require considerable conformational change [103].

The N-terminal region of the protein is located adjacent to the C-terminal, therefore, an important possibility is that this C-terminal region of LFABP may also interact with the phospholipid surface to produce conformational changes and hence ligand release. The cationic residue within this region that makes a significant contribution to the surface positive potential of LFABP is R126 [8] which is located adjacent to another cationic residue, K125.

It was decided to mutate both Lys-125 and Arg-126 to glutamate, producing the individual mutations K125E and R126E, in order to investigate the possibility that this region of the protein is involved in ligand release from LFABP on interfacial binding. The charge reversal mutants, K125E and R126E, were prepared by the Kunkel method of site-directed mutagenesis [65, 66] and purified by normal procedures. The yield of the two proteins were similar to that for wild-type protein, ~ 10-15 mg per litre bacterial culture.

5.5.1. Comparison of ligand binding properties in wild-type, K125E and R126E LFABP

5.5.1.1. The Binding of DAUDA to Wild-type LFABP and the K125E and R126E Mutants

Firstly, the mutants K125E and R126E LFABP were assayed for their DAUDA binding properties relative to wild-type LFABP. DAUDA binding was assessed by measuring the fluorescence enhancement of the probe upon titration as a methanol solution into a sample of LFABP in 10 mM Hepes buffer. Figure 5.5.1.1. and Table 5.5.1.1.

Table 5.5.1.1. The Binding Affinities and Maxima of the Mutants K125E and R126E for DAUDA with Comparison to Wild-type LFABP

The data presented was generated by the programme FigP using the graph presented in figure 5.5.1.1.

	LFABP WT	LFABP K125E	LFABP R126E
Kd (μM)	0.10 +/- 0.01	0.30 +/- 0.01	0.15 +/- 0.002
Bmax **(Arbitrary Units)**	332 +/- 8.3	384 +/- 6.2	335 +/- 1.4

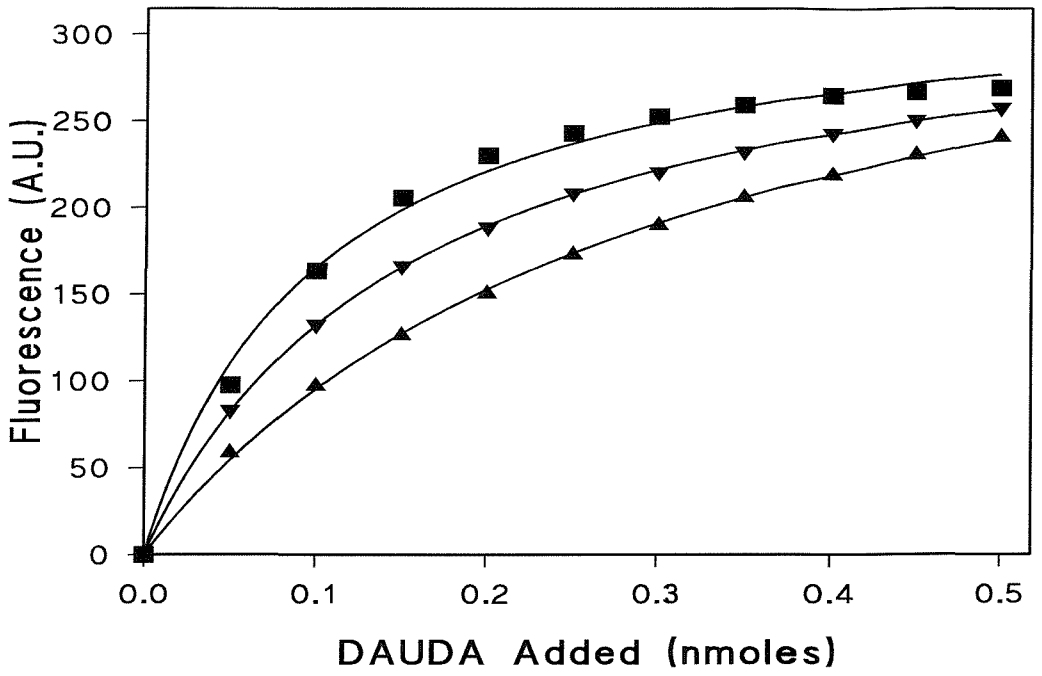

Figure 5.5.1.1. DAUDA Binding Properties of the Mutants K125E and R126E LFABP with Comparison to Wild-type LFABP

DAUDA was titrated by methanol injection into 10 mM Hepes, pH 7.5 buffer containing 5μg (0.4 nmoles) of either wild-type (■), K125E (▲) or R126E (▼) LFABP. Fluorescence emission was measured as Arbitrary Units (A.U.) at 500 nm following excitation at 350 nm. A data points shown are the mean values of three separate titrations and are corrected for the titration of DAUDA into 10 mM Hepes buffer.

As shown in the above data, K125E LFABP has a significantly lower affinity for DAUDA than either the wild-type or R126E LFABP. The Kd of K125E LFABP for DAUDA is shown to be three times that for wild-type LFABP and twice the Kd for R126E LFABP. R122 has previously been highlighted as a residue important in ligand binding within the cavity of the protein [92], although this residue is in close proximity to K125, the side chains of the two residues are located in different environments. R122 is internalised with the side-chain extending into the binding cavity whereas the side-chain of K125 would appear from the crystal structure [13] to be in a more solvent exposed position towards the surface of the protein. From this information, one would not expect the mutation of K125 to affect ligand binding as it is not located within the region of the binding cavity. It may be possible that a charge reversal mutation of the K125 residue affects the conformation of the binding cavity as a result of impairing interactions between this residue and others surrounding it.

5.5.1.2. The Binding of Oleic Acid to Wild-type LFABP, K125E and R126E Measured by DAUDA Displacement

The ability of oleic acid to displace DAUDA from wild-type LFABP, K125E and R126E with loss of fluorescence was measured and the Ki_{app} for oleic acid determined by the method of Kane and Bernlohr [76]. It is clear to see from the data in figure 5.5.1.2. that the loss of fluorescence seen from the R126E/DAUDA complex upon the addition of oleic acid follows almost exactly the loss of fluorescence seen for the wild-type/DAUDA complex, indicating that residue R126

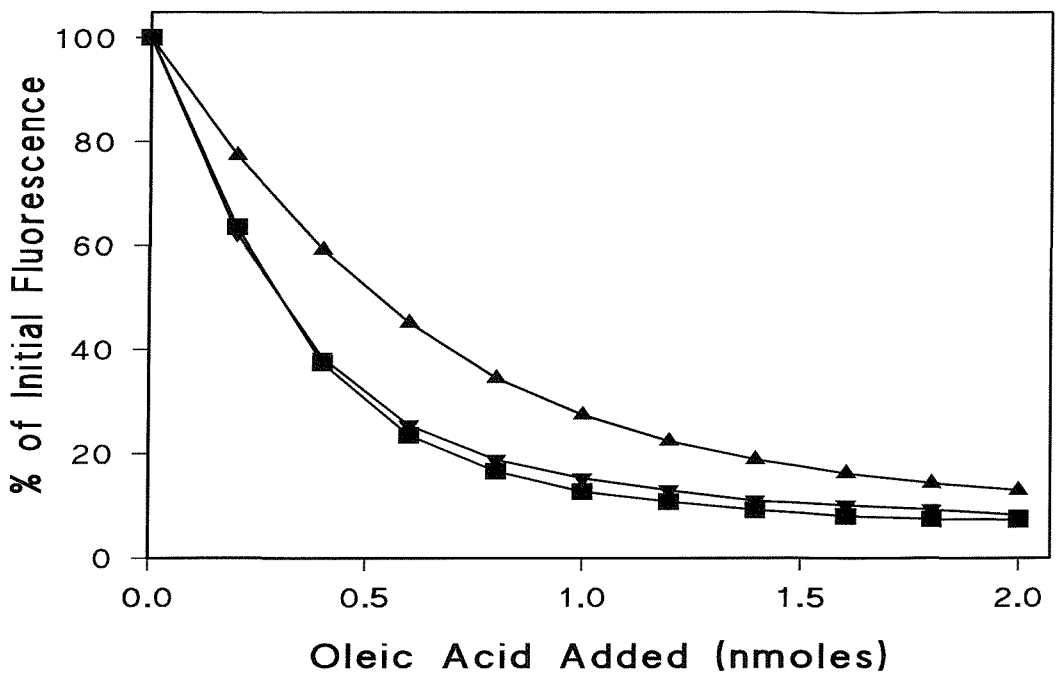

Figure 5.5.1.2. **Ability of the Mutants K125E and R126E LFABP to Bind Oleic Acid with Comparison to Wild-type LFABP as Shown by DAUDA Displacement by Oleic Acid**

Oleic acid was titrated as a methanol solution into 10 mM Hepes, pH 7.5 buffer with 1 μM DAUDA and 5 μg (0.4 nmoles) of either wild-type (■), K125E (▲) or R126E (▼) LFABP. All data points are the mean values of three separate titrations and are corrected for the effect of oleic acid on DAUDA in 10 mM Hepes buffer.

has minimal involvement in the binding of both DAUDA and oleic acid. K125E LFABP, however, shows a significantly reduced loss of LFABP/DAUDA fluorescence upon addition of oleic acid in comparison to wild-type and R126E LFABP. The Ki_{app} values were calculated to be 0.03, 0.15 and 0.05 μM for wild-type, K125E and R126E LFABP respectively. Thus, the K125E mutation must result in a small conformational change that reduces the affinity of this mutant protein for both DAUDA and oleic acid.

We could speculate that a conformational change will involve the part of the cavity involving the site I fatty acid binding site and where we have previously predicted that DAUDA would bind. It is possible that the K125E mutation now allows a new electrostatic interaction with K6 resulting in some protein distortion. If this were the case, binding assays performed under high ionic strength conditions might minimise distortion and effects on affinity.

5.5.1.3. The Binding of Oleoyl CoA to Wild-type LFABP, K125E and R126E is Measured by DAUDA Displacement

The differences between wild-type, K125E and R126E LFABP highlighted by the oleic acid binding data could also be seen for the binding of oleoyl CoA to these proteins. Once again, upon the addition of oleoyl CoA into the LFABP/DAUDA complex, the K125E mutant appeared to show a reduced affinity for oleoyl CoA compared to both the wild-type protein and the R126E mutant. There was also observed to be a slight decrease in the affinity of the R126E mutant for oleoyl CoA

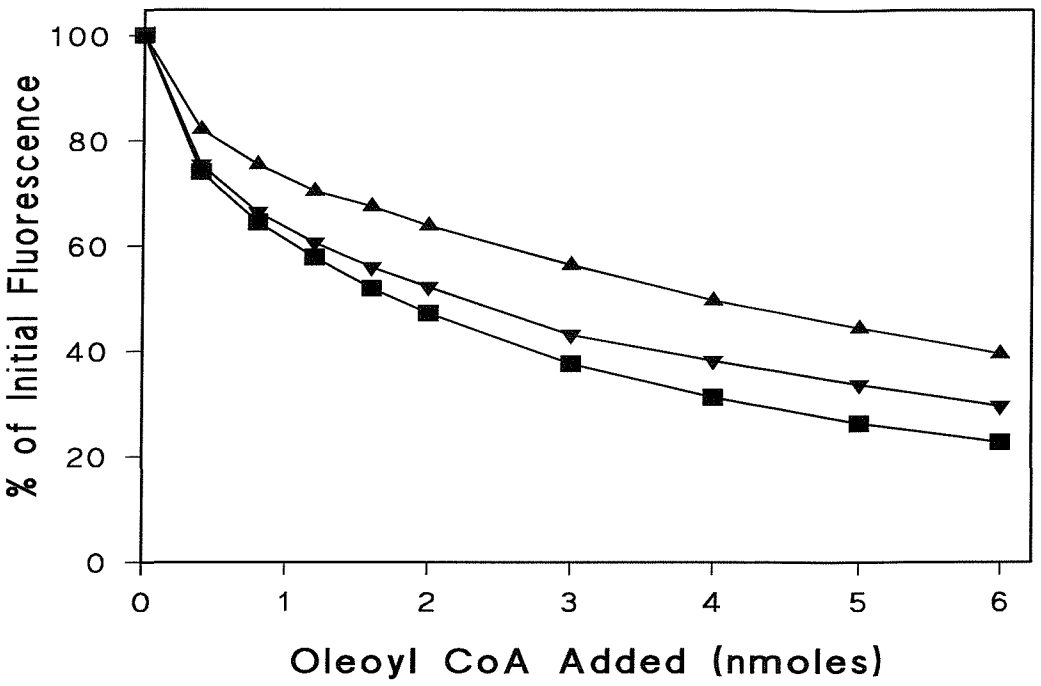

Figure 5.5.1.3. Comparison of Oleoyl CoA Binding by Wild-type LFABP and the K125E and R126E Mutants of LFABP

Oleoyl CoA was titrated as a solution in methanol into 10 mM Hepes, 1 μM DAUDA and 5 μg (0.4 nmoles) of either wild-type (■), K125E (▲) or R126E (▼) LFABP. All data points are the mean values of three separate titrations and are corrected for the effect of oleoyl CoA on DAUDA in 10 mM Hepes.

compared to the wild-type protein but this difference was not as significant as the differences seen for K125E. The Ki_{app} values for wild-type, K125E and R126E LFABP were calculated to be 0.2, 1.1 and 0.36 μM, respectively (Figure 5.5.1.3).

The reason for the reduced affinity of the K125E for oleoyl CoA most probably is the same as that for reduced DAUDA and oleic acid binding. That is to say a small conformational change affects the overall binding of ligand in the cavity that utilises site I.

5.5.1.4. Effects of Lysophospholipids on LFABP/DAUDA Fluorescence

Lysophospholipid binding to the C-terminal mutants was investigated and, once again, the K125E mutant was highlighted as having different binding properties than either the wild-type LFABP or the R126E mutant. In the presence of a 4-fold molar excess of oleoyl lysoPA there was a loss of approximately 15-20 % of LFABP/DAUDA fluorescence for the wild-type and for the R126E mutant. No significant loss of fluorescence was detected from the K125E/DAUDA complex in the presence of a 2-fold excess of oleoyl lysoPA.

This overall binding of lysoPA to the wild-type LFABP and the mutants K125E and R126E closely parallel the binding of DAUDA, oleic acid and oleoyl CoA to these proteins. It is reasonable to assume that a similar explanation must be evoked to explain the reduced affinity of all these ligands.

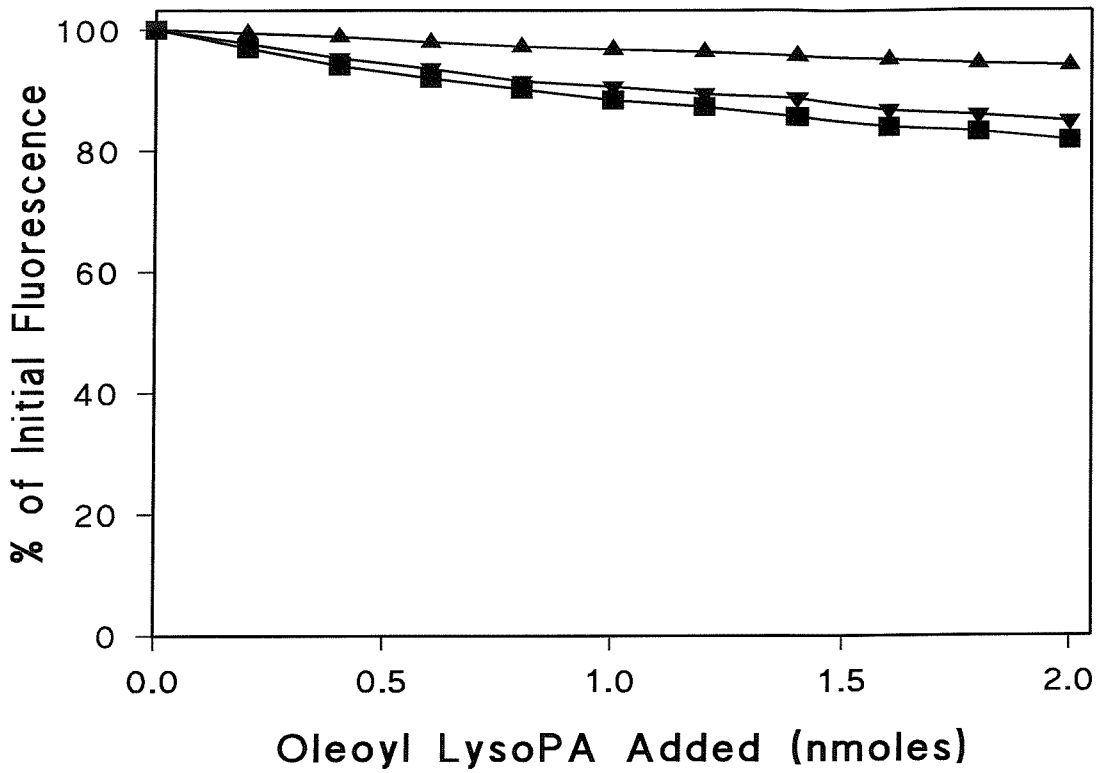

Figure 5.5.1.4. Effect of Lysophosphatidic acid on LFABP/DAUDA Fluorescence

Lysophosphatidic acid was titrated as 0.2 mM stock in methanol into 10 mM Hepes, 1 μM DAUDA and 5 μg (0.4 nmoles) of either wild-type (■), K125E (▲) or R126E (▼) LFABP. Fluorescence emission was measured at 500 nm following excitation at 350 nm. All data points are the mean values of three separate titrations and are corrected for the minimal effect of lysophospholipid on the fluorescence of DAUDA in 10 mM Hepes buffer.

5.5.1.5. Similar Affinities Shown by Wild-type, K125E and R126E LFABP for Vesicles Containing DOPG

Interestingly, no significant difference was observed between the loss of LFABP/DAUDA fluorescence from wild-type, K125E and R126E LFABP by 100 % DOPG vesicles. The amounts of DOPG that produced 50 % loss of LFABP/DAUDA fluorescence were 3.13, 3.75 and 3.75 nmoles for wild-type, K125E and R126E LFABP respectively. In an attempt to highlight any minor differences between the proteins, the effect of 20 mol% DOPG with DOPC vesicles on loss of LFABP/DAUDA fluorescence was investigated. This did not reveal any further differences than the assays using 100 % DOPG vesicles, as can be seen from Figure 5.5.1.5., there were no significant differences seen between the loss of fluorescence from wild-type, K125E and R126E LFABP/DAUDA. The amounts of DOPG that produced 50 % loss of LFABP/DAUDA fluorescence for this particular experiment were 2.5, 4 and 3 nmoles respectively for wild-type, K125E and R126E LFABP.

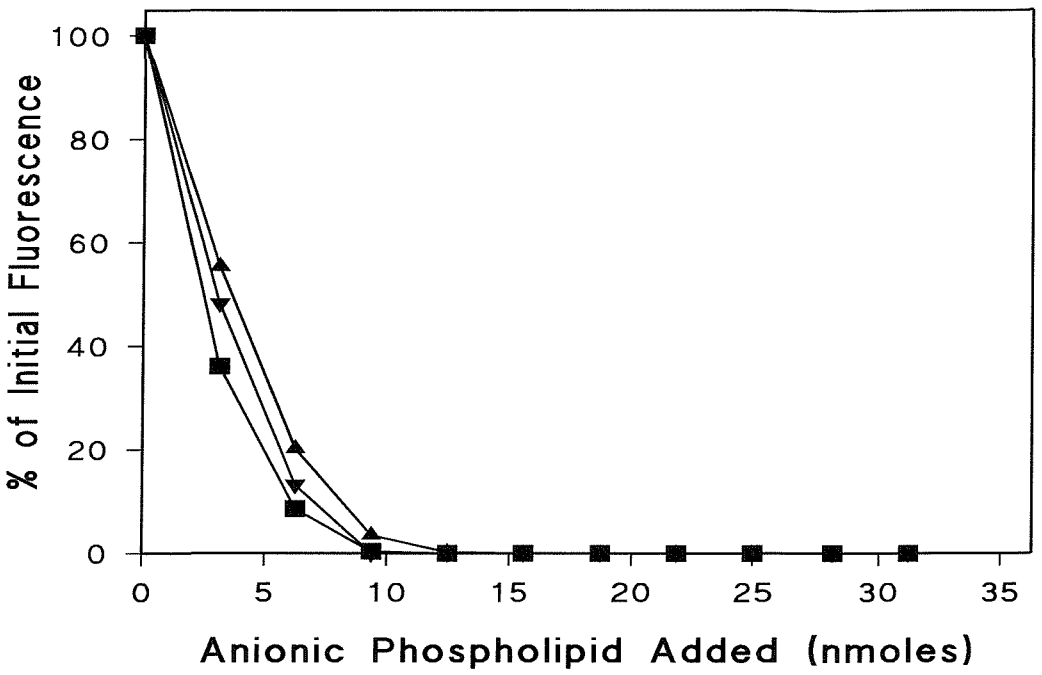

Figure 5.5.1.5. Effect of 20 mol% DOPG with DOPC SUVs on LFABP/DAUDA Fluorescence: A Comparison of Wild-type, K125E and R126E LFABP

20 mol% DOPG with DOPC SUVs were prepared by methanol injection into 10 mM Hepes, 1 μM DAUDA and 5 μg (0.4 nmoles) of either wild-type (■), K125E (▲) or R126E (▼) LFABP. All data points shown are the mean values of three separate titrations are and corrected for the slight increase in fluorescence caused by DAUDA partitioning into the phospholipid vesicles.

5.5.1.6. Titration of DOPC Vesicles into K125E and R126E LFABP

When DOPC vesicles were titrated into the LFABP/DAUDA complex of K125E and R126E an increase in fluorescence was observed (Figure 5.5.1.6.) This increase was approximately 30 % for the K125E complex and 20 % for the R126E complex. It would appear from this data that the DOPC vesicles are either causing K125E LFABP and R126E LFABP to bind DAUDA with a higher affinity or the addition of DOPC vesicles results in an increase in the fluorescence intensity of the bound DAUDA by inducing a conformational change that places the dansyl group of the DAUDA molecule in a less quenched environment resulting in an increase in the fluorescence intensity of the molecule.

5.5.1.7. NaCl Enhances the Increase in Fluorescence Seen Upon Addition of DOPC vesicles into the K125E or R126E/DAUDA Complex

The titration of DOPC vesicles into K125E and R126E LFABP/DAUDA was repeated in the presence of 200 mM NaCl as high salt concentration has previously been demonstrated to inhibit the effects of anionic phospholipid vesicles upon the wild-type LFABP/DAUDA complex [83]. In the presence of NaCl the observations noted for the effect of DOPC on the K125E LFABP/DAUDA complex were further accentuated. There was an increase in the fluorescence of the K125E/DAUDA complex of approximately 40 % upon addition of 100 % DOPC vesicles compared with no change in the fluorescence of wild-type LFABP/DAUDA and an increase in the fluorescence of the R126E/DAUDA complex of approximately 10 % as shown in figure 5.5.1.7. The fact that the presence of 200 mM NaCl accentuates the effect of

DOPC vesicles upon K125E LFABP but inhibits/reduces any effects seen by DOPC vesicles upon either the wild-type or the R126E LFABP would suggest that the increase in fluorescence seen is as a result of a direct interaction between the phospholipid vesicles and the protein. The fact that the effect of DOPC vesicles on K125E LFABP is enhanced by the presence of 200 mM NaCl is suggestive of hydrophobic interactions between DOPC and K125E LFABP which are heightened under conditions of high ionic strength.

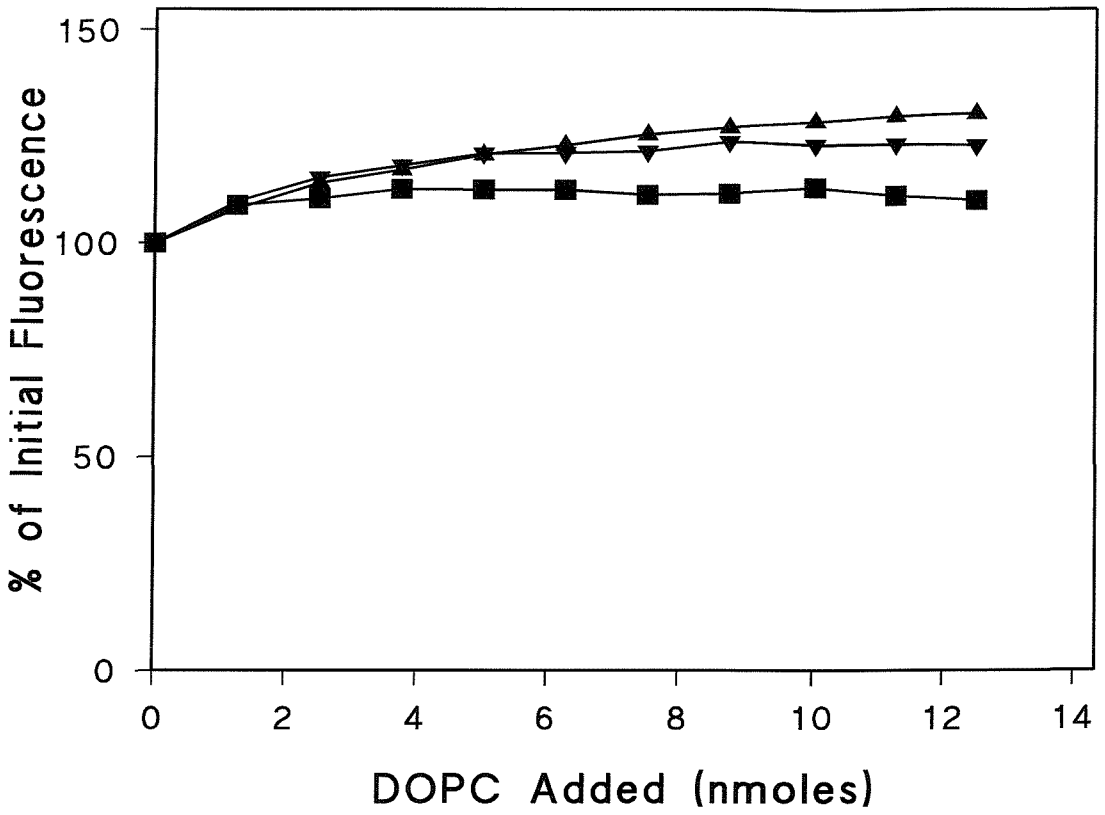

Figure 5.5.1.6. Effect of 100 % DOPC SUVs on Fluorescence of the LFABP/DAUDA Complex

100 % DOPC SUVs were prepared by methanol injection into 10 mM Hepes, 1 μM DAUDA and 5 μg (0.4 nmoles) of either wild-type (■), K125E (▲) or R126E (▼) LFABP. Fluorescence emission was measured at 500 nm following excitation at 350 nm. All data points shown are the mean values of three separate titrations and are corrected for the partitioning of DAUDA into the phospholipid vesicles.

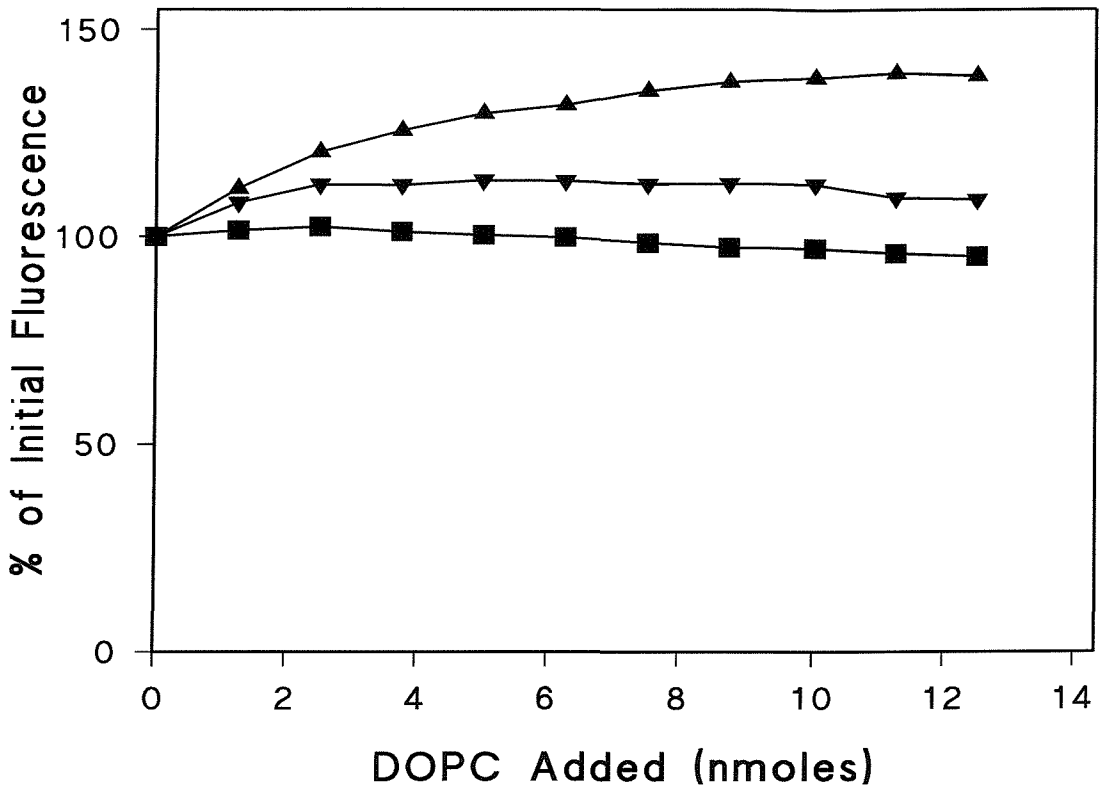

Figure 5.5.1.7. Effect of NaCl on Addition of 100 % DOPC SUVs to the LFABP/DAUDA Complex

100 % DOPC SUVs were titrated by methanol injection into 10 mM Hepes, 200 mM NaCl, 1 μM DAUDA and 5 μg (0.4 nmoles) of either wild-type (■), K125E (▲) or R126E (▼) LFABP. Fluorescence emission was measured at 500 nm following excitation at 350 nm. All data points are the mean values of three separate titrations and are corrected for the partitioning of DAUDA into the phospholipid vesicles.

5.5.1.8. NaCl Inhibits the Binding of K125E and R126E LFABP to 100 % DOPG SUVs

No significant effect on the fluorescence of the LFABP/DAUDA complex was seen when 100 % DOPG vesicles were titrated into the complex in the presence of NaCl. Figure 5.5.1.8. This result is as would be expected if the residues K125 and R126 were not directly involved in interactions with anionic phospholipid, as inhibition of DOPG binding to wild-type LFABP by 200 mM NaCl has previously been demonstrated [83].

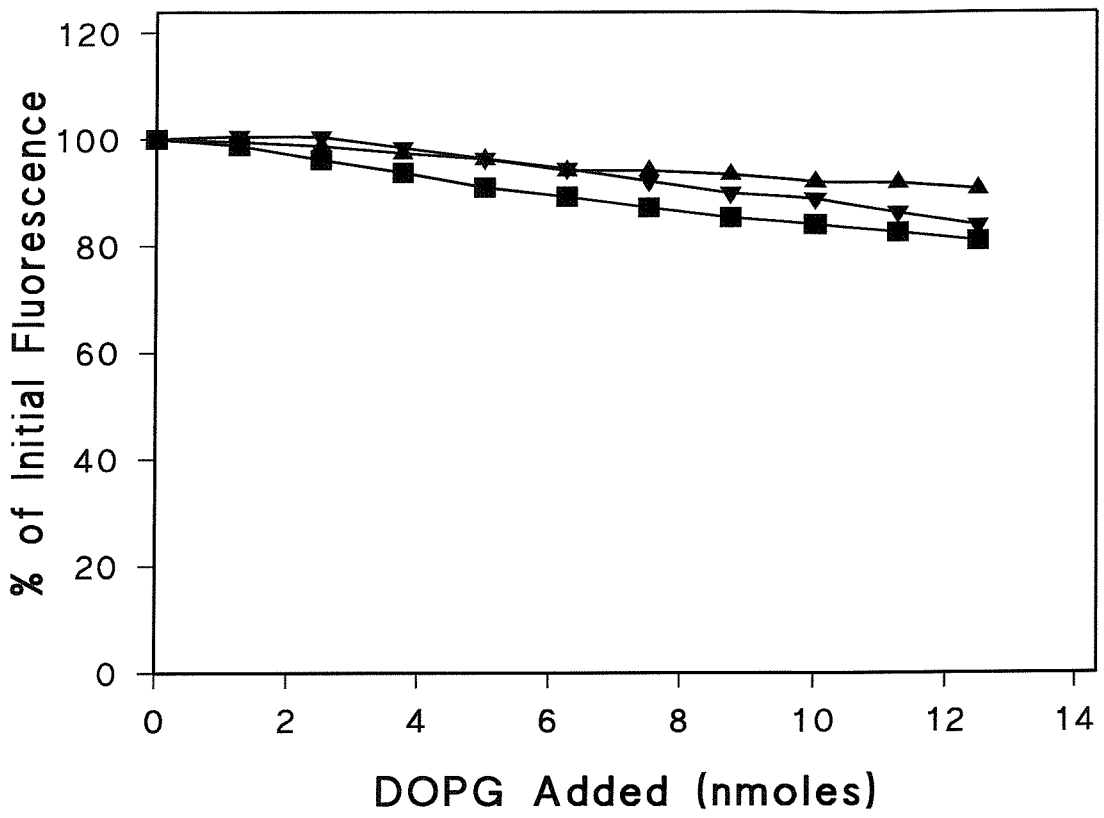

Figure 5.5.1.8. Effect of NaCl on the Loss of Fluorescence of the LFABP/DAUDA Complex by 100 % DOPG SUVs

100 % DOPG SUVs were titrated by methanol injection into 10 mM Hepes, 200 mM NaCl, 1 μM DAUDA and 5 μg (0.4 nmoles) of either wild-type (■), K125E (▲) or R126E (▼) LFABP. All data points shown are the mean values of three separate titrations.

5.5.2. Structural Integrity of the mutants: K125E and R126E

As has already been discussed in Chapter 4, classical unfolding studies cannot be applied to an investigation of the structural stability of LFABP due to the lack of tryptophan residues in the wild-type protein. Owing to this, an investigation of the thermostability of the wild-type, K125E and R126E LFABP with respect to DAUDA binding were carried out under identical conditions to those used for the K20E, K31E and K33E mutants (Figure 4.4.2.2).

The wild-type LFABP, K125E and R126E were incubated at 70°C and aliquots were removed at regular intervals to measure DAUDA binding under normal assay conditions as a reflection of loss of protein structure. The results are shown in Figure 5.5.2.

From the data, the time taken for the DAUDA binding capacity of each protein to be reduced by 50 % could be established. These values were 10 minutes for wild-type LFABP, 10 minutes for LFABP K125E and 7 minutes for LFABP R126E. It would seem that the R126E mutant is significantly less stable at high temperatures than either the wild-type or K125E mutant. This may be due to the fact that this particular residue, R126, plays a role in the surface potential of the protein and so mutating this residue may act to reduce the structural stability of the molecule. However, this result is in marked contrast to the situation with the K31E mutation within α-helix II which showed a considerably enhanced thermal stability (Figure 4.4.2.2).

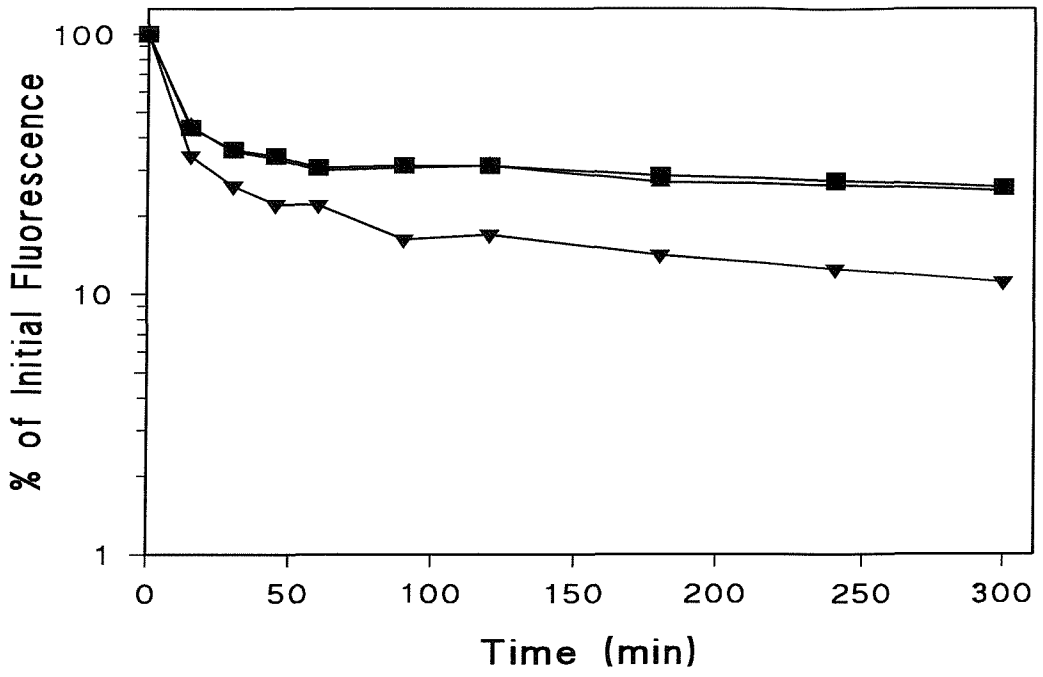

Figure 5.5.2. **Thermostability of Wild-type LFABP and the Mutants K125E and R126E LFABP at 70°C**

The protein samples were incubated at 70°C and samples of each protein were taken at regular time intervals and assayed for DAUDA Binding. A single addition of DAUDA to a final concentration of 1 μM was made to each 5 μg (0.4 nmoles) sample of either wild-type (■), K125E (▲) or R126E (▼) LFABP and the fluorescence emission at 500 nm recorded following excitation of the sample at 350 nm. All data points are the averages of three separate titrations.

5.5.3. K125E and R126E LFABP Bind to Phospholipids with a Similar Affinity to Wild-type LFABP

The use of a polarity sensitive dansyl fluorophore attached to the head group of PE in the previous chapter was used as a method to directly demonstrate the binding of LFABPs to DOPG vesicles. Therefore, it was appropriate to use the same method to directly demonstrate the binding of the K125E and R126E mutants to these anionic vesicles. LFABP was titrated into 50 mM Hepes buffer containing 5 μg DOPG with 5 mol% dansyl DHPE vesicles and the fluorescence emission of the dansyl group measured at 500 nm following excitation at 335 nm, figure 5.5.3. The data shows there to be very little difference between the binding curves of wild-type, K125E and R126E LFABP for DOPG vesicles. Although this method proved problematical as a direct measure of affinity of the proteins for vesicles, the results directly demonstrate the binding of the mutants to these DOPG vesicles that contain 5 mol% dansyl DHPE. Moreover, the similarity of the binding curves indicate that there are not major differences in binding affinity between the wild-type LFABP and the mutants.

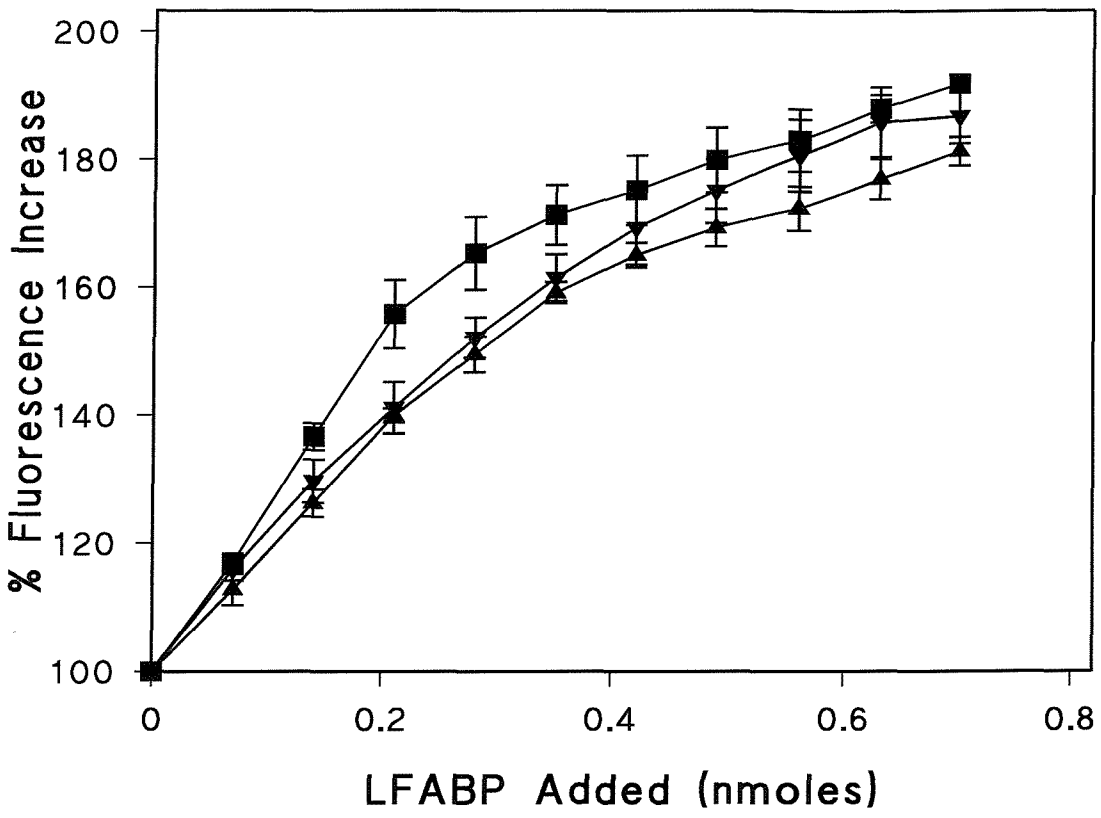

Figure 5.5.3. **No Significant Difference is Seen Between the Affinities of Wild-type, K125E and R126E LFABP for DOPG Vesicles Containing 5 mol% Dansyl DHPE**

Wild-type (■), K125E (▲) and R126E (▼) LFABP were titrated into 50 mM Hepes containing 5 μg (6.25 nmoles) DOPG with 5 mol% dansyl DHPE SUVs. Dansyl fluorescence emission was measured at 500 nm following excitation at 335 nm. All data points shown are the mean values of three separate titrations.

5.6. Discussion

The study of the F3W, F18W and C69W tryptophan mutants of LFABP has revealed a significant conformational change at the N-terminus of the protein upon interaction with anionic phospholipid vesicles, which was found to be independent of bound ligand. The loss of tryptophan fluorescence seen for the F3W mutant upon addition of DOPG vesicles paralleled exactly the loss of DAUDA from the protein suggesting that the conformational change induced correlates with release of ligand. Fluorescence resonance energy transfer studies have shown the tryptophan at position 3 to come in close proximity to the anionic interface. It may be possible that the conformational change induced in LFABP by interaction with anionic phospholipids creates a ligand exit portal, distinct from the proposed ligand entry portal. A second potential portal region in LFABP has been revealed through investigation of the crystal structure, as shown in Figure 5.6.1.

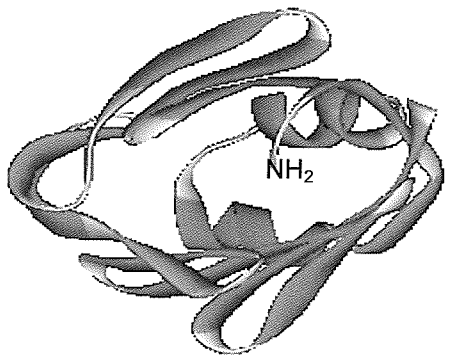

Figure 5.6.1. LFABP showing the Potential Exit Portal

LFABP is shown looking through from the N-terminus at the base of the protein to the α-helices at the top of the protein.

From the structure (Figure 5.6.1.) it is possible to see how a conformational change at the N-terminus of LFABP could open up a secondary portal region in the protein resulting in the release of ligand. Further research is required in order to investigate this as a potential mechanism for the targeting of FABP-bound ligands *in vivo*.

The observations that there was a conformational change at the N-terminal region of the protein on binding to DOPG vesicles highlighted the potential role of this region of the protein in interfacial interactions leading to ligand release. The juxtaposition of the C-terminal in this region focused on the possible role of the cationic C-terminal residues K125 and R126 particularly as R126 makes a significant contribution to the positive surface potential of the region [8].

Analysis of the ligand binding properties of the mutants K125E and R126E highlighted a significant effect of the K125E mutation on ligand binding while a smaller effect was seen with R126E. As both these residues are located on the surface according to the crystal structure and make no direct contribution to the properties of the ligand binding cavity, it is unlikely that such mutations would directly affect ligand binding. The most likely explanation is that charge reversal affects the overall conformation as a result of changed surface interactions. Thus, a new electrostatic interaction between 125E and K6 may be possible causing some distortion of the C and N-terminal regions (Figure 5.6.2.). A more general effect on the ligand binding cavity would be consistent with the fact that the binding of a variety of ligands were adversely affected.

Figure 5.6.2. Structure of LFABP Highlighting Residues K6 and K125

Residue K6 is shown in green and residue K125 is shown in dark blue.

If the mutations were producing a more general structural distortion, then the wild-type neutralisation of 125E at the PC interface by the cationic choline could reverse the process. Although speculative, this proposal could explain the enhanced fluorescence of DAUDA when binding to DOPC due to an enhancement of affinity of the FABP as conformational changes induced by the K125E mutation are reversed. The Kd for DAUDA is 5-fold higher for the K125E mutant while under the conditions of the assay the concentration of DAUDA will not saturate the protein. Therefore, a reduction in Kd would result in increased DAUDA binding and hence greater fluorescence intensity (Figure 5.5.1.6). It would appear that 200 mM NaCl further enhances the effect of adding DOPC vesicles (Figure 5.5.1.7) highlighting that the

nature of the interaction of the mutants with DOPC is not prevented by a higher salt concentration and is not dominated by electrostatic interactions.

Overall these results also highlight the ability of the mutant FABPs to bind to a PC interface but such binding is very different to that seen with DOPG vesicles as there is no major conformational change resulting in ligand release. A simple explanation is that there is not a membrane penetration event, only binding to the PC surface.

Although significant changes in ligand binding were seen with these mutants, the effects on ligand binding to DOPG vesicles were minimal and contrast with the clear difference seen with the K31E mutant. Thus it would appear that the C-terminal region of LFABP does not make a significant contribution to the binding of the protein to DOPG vesicles but it remains to be established if there is a conformational change in this region as a result of interfacial binding.

Chapter Six

General Summary and Future Work

6.1. General Summary and Future Work

The ability of LFABP to bind to phospholipid interfaces with the release of ligand has been studied. The system is sensitive to both the ionic strength of the assay and the proportion of anionic phospholipid contained within the interface, which is suggestive of the involvement of non-specific electrostatic interactions in the binding process. Binding has been found to be inhibited by high salt concentrations but not to be fully reversible using high salt concentrations, thereby suggesting the involvement of secondary hydrophobic interactions. The stoichiometric relationship between LFABP and anionic phospholipid suggests that LFABP coats the surface of the phospholipid vesicle. The displacement of ligand upon addition of anionic phospholipid vesicles points to a conformational change induced by the phospholipid vesicles to enable the release of ligand from the protein. LFABP returns to its native state upon displacement of phospholipid vesicles as shown by its ability to bind fatty acids.

Residue K31 on α-helix II of LFABP has been highlighted as an important residue for the binding of the protein to anionic phospholipid vesicles and also to ligands with bulky charged head groups such as lysophospholipids. Of the other two cationic residues in the helical region of the protein, K33 has no involvement in phospholipid interaction but is involved in interactions with lysophospholipid, whereas, K20 appears to have no contribution to either phospholipid binding or lysphospholipid binding.

Other residues, K36, K47 and K57 have been identified as being important residues contributing to the surface potential of LFABP [8]. Charge reversal mutants have been made mutating K → E thereby producing the individual mutants K36E, K47E and K57E. The effect of these particular mutations on the structural and functional properties of LFABP will be investigated.

It is unlikely that the interactions between LFABP and anionic interfaces involve just a single cationic residue on the protein surface. Therefore, it will be necessary to generate multiple charge reversal mutants to further define surface regions involved in interfacial binding. At this time an α-helical double mutant, K31,33E, has also been produced but has yet to be analysed. Further multiple mutations will depend on the results of the single mutations involving K36, K47 and K57

Preliminary results have suggested a possible interaction occurring between LFABP and microsomal membranes. This work needs investigating further in order to confirm these observations. One method of analysis could be to mix a sample of microsomes and a sample of LFABP and centrifuge in an ultracentrifuge to obtain a microsomal pellet, if LFABP is bound then it will be present in the pellet as, owing to the small size of LFABP (14 kDa), unbound LFABP would remain in the supernatent. Methods commonly used to detect a specific protein in a sample are Western blot analysis or using radiolabelled protein. Western blot analysis was not possible with LFABP as an antibody for this protein was not available. The use of radiolabelled protein would be a more viable option for the detection of LFABP. One possible method of producing C^{14} labelled LFABP is using reductive methylation that modifies lysine residues in the protein [104]. A problem with this particular method is the

possible effect on phospholipid interactions due to the modification of the lysine residues however it should be noted that reductive methylation maintains the positive charge on the protein. Another approach is to transform the plasmid DNA into bacteria that are methionine deficient, i.e. they cannot produce methionine. In this case, C^{14}-methionine can be added into the growth medium and is then incorporated into the protein in the absence of methionine from the bacteria.

Significant conformational changes have been observed in the N-terminal region of the protein upon addition of anionic phospholipid vesicles to the F3W tryptophan mutant of LFABP. No significant conformational changes were observed in the F18W mutant on α-helix I or in the C69W mutant in the β-barrel structure. The conformational change at the N-terminus could be creating a ligand exit portal. Inspection of the crystal structure of LFABP does reveal a potential portal in this region of the protein as seen in Figure 5.6.1.

The significance of the N-terminal region of LFABP could be further investigated by producing a mutant lacking in the first 3 to 4 residues of the protein. In fact the removal of the N-terminal methionine can be achieved by changing the asparagine at position 2 to an alanine. As a result of this mutation the E. coli aminopeptidase will remove the N-terminal methionine during translation.

Further analysis of the conformational changes that occur on binding to anionic vesicles could be achieved by the preparation of other tryptophan-containing mutants. Of particular interest would be the mutations L28W, Y54W and M74W as all these residues are in the vicinity of the ligand portal region.

Mutation of residue K125 of LFABP has been shown to have a significant effect on the ligand binding properties of the protein. The most likely reasoning for this is that charge reversal at this position results in addition interactions with surrounding residues, namely K6, resulting in a structural distortion. In order to investigate this further, K6 could be mutated to either a neutral residue or an anionic residue to assess the effects on ligand binding.

Studies on the α-helical charge reversal mutants suggests that ligands such as oleoyl CoA and lysophospholipids bind in the second fatty acid binding site with the headgroups protruding through the portal region of the protein. In contrast we have proposed that DAUDA is located in the first fatty acid binding site with the head group buried in the binding cavity. This work could be confirmed by the co-crystallisation of LFABP with bound ligand for x-ray crystallographic studies. As the structure with two bound oleate molecules has already been published [13] the optimal conditions for crystallisation of LFABP have already been determined.

Overall, LFABP provides another important example of proteins that bind to anionic phospholipid interfaces and the conformational changes that result. These changes are not only of general importance in understanding interfacial binding but also provide a possible mechanism for targeting fatty acids to membrane enzymes that require fatty acids as substrates.

References

[1] Berk, P.D. and Stump, D.D. Mechanisms of uptake of long chain free fatty acids. (1999) Mol. Cell. Biochemistry **192**, 17-31

[2] McArthur, M.J., Atshaves, B.P., Frolov, A., Foxworth, W.D., Kier, A.B., and Schroeder, F. Cellular uptake and trafficking of long chain fatty acids. (1999) J. Lipid Res. **40**, 1371-1383

[3] Buckland, A.G. and Wilton, D.C. Anionic phospholipids, interfacial binding and the regulation of cell functions. (2000) Biochim. Biophys. Acta **1483**, 199-216

[4] Ockner, R.K., Manning, J.A., Poppenhausen, R.B., and Ho, W.K. A binding protein for fatty acids in cytosol of intestinal mucosa, liver, myocardium and other tissues. (1972) Science **177**, 56-58

[5] Ockner, R.K., Manning, J.A., and Kane, J.P. Fatty acid binding protein – isolation from rat liver, characterisation and immunochemical quantitation. (1982) J. Biol. Chem. **257**, 7872-7878

[6] Storch, J., and Thumser, A.A. The fatty acid transport function of fatty acid binding proteins. (2000) Biochim. Biophys. Acta – Mol. And Cell Biol. Lipids **1486**, 28-44

[7] Banaszak, L., Winter, N., Xu, Z., Bernlohr, D.A., Cowan, S., and Jones, T.A. Lipid binding proteins: a family of fatty acid and retinoid transport proteins. (1994) Adv. Prot. Chem. 89-151

[8] Thompson, J., Reese-Wagoner, A., and Banaszak, L. Liver fatty acid binding protein: Species variation and the accommodation of different ligands. (1999) Biochim. Biophys. Acta – Mol. Cell Biol. Lipids **1441**, 117-130

[9] Zimmerman, A.W., Rademacher, M., Ruterjans, H., Lucke, C., and Veerkamp, J.H. Functional and conformational characterisation of new mutants of heart fatty acid binding protein. (1999) Biochem. J. **344**, 495-501

[10] Coe, N.R., and Bernlohr, D.A. Physiological properties and functions of intracellular fatty acid-binding proteins. (1998) Biochim. Biophys. Acta **1391**, 287-306

[11] Cistola, D.P., Sacchettini, J.C., Banaszak, L.J., Walsh, M.T., and Gordon, J.I. Fatty acid interactions with rat intestinal and liver fatty acid-binding proteins expressed in *Escherichia coli*. (1989) J. Biol. Chem. **264**, 2700-2710

[12] Zhu, L.Y., Kurian, E., Prendergast, F.G., and Kemple, M.D. Dynamics of palmitic acid complexed with rat intestinal fatty acid binding protein. (1999) Biochemistry **38**, 1554-1561

[13] Thompson, J., Winter, N., Terwey, D., Bratt, J., and Banaszak, L. The crystal structure of the liver fatty acid binding protein (a complex with 2 bound oleates). (1997) J. Biol. Chem. **272**, 7140-7150

[14] Hodsdon, M.E., and Cistola, D.P. Discrete backbone disorder in the nuclear magnetic resonance structure of apo intestinal fatty acid binding protein: Implications for the mechanism of ligand entry. (1997) Biochemistry **36**, 1450-1460

[15] Richieri, G.V., Low, P.J., Ogata, R.T., and Kleinfeld, A.M. Binding linetics of engineered mutants provide insight about the pathway for entering intestinal fatty acid binding protein. (1999) Biochemistry **38**, 5888-5895

[16] Wilkinson, T.C.I, and Wilton, D.C. Studies on fatty acid binding proteins: The binding properties of rat liver fatty acid binding protein. (1987) Biochem. J. **247**, 485-488

[17] Richieri, G.V., Ogata, R.T., Zimmerman, A.W., Veerkamp, J.H., and Kleinfeld, A.M. Fatty acid binding proteins from different tissues show distinct patterns of fatty acid interactions. (2000) Biochemistry **39**, 7197-7204

[18] Richieri, G.V., Ogata, R.T., and Kleinfeld, A.M. Equilibrium constants for the binding of fatty acids with fatty acid binding proteins from adipocyte, intestine, heart and liver measured with the fluorescent probe ADIFAB. (1994) J. Biol. Chem. **269**, 23918-23930

[19] Hubbell, T., Behnke, W.D., Woodford, J.K., and Schroeder, F. Recombinant liver fatty acid binding protein interacts with fatty acyl coenzyme A. (1994) Biochemistry **33**, 3327-3334

[20] Thumser, A.E.A., and Wilton, D.C. Thebinding of natural and fluorescent lysophospholipids to wild-type and mutant rat liver fatty acid binding protein and albumin. (1995) Biochem. J. **307**, 305-311

[21] Rolf, B., OudenampsenKruger, E., Borchers, T., Faergeman, N.J., Knudsen, J., Lezius, A., and Spener, F. Analysis of the ligand binding properties of recombinant bovine liver-type binding protein. (1995) Biochim. Biophys. Acta – Lipids and Lipid Metabolism **1259**, 245-253

[22] Dietrich, A., Dieminger, W., Fuchte, K., Stoll, G.H., Schlitz, E., Gerok, W., and Kurz, G. Functional significance of interaction of H-FABP with sulphated and non-sulfated taurine-conjugated bile salts in rat liver. (1995) J. Lipid Res. **36**, 1745-1755

[23] Thumser, A.E., and Storch, J. Liver and intestinal fatty acid-binding proteins obtain fatty acids from phospholipid membranes by different mechanisms (2000) J. Lipid Res. **41**, 647-656

[24] Storch, J. Diversity of fatty acid binding protein structure and function – studies with fluorescent ligands. (1993) Mol. Cell. Biochem. **123**, 45-53

[25] Storch, J., and Bass, N.M. Transfer of fluorescent fatty acids from liver and heart fatty acid binding proteins to model membranes. (1990) J. Biol. Chem. **265**, 7827-7831

[26] Hsu, K.T., and Storch, J. Fatty acid transfer from liver and intestinal fatty acid binding proteins occurs by different mechanisms. (1996) J. Biol. Chem. **271**, 13317-13323

[27] Kim, H.K., and Storch, J. Mechanism of free fatty acid transfer from rat heart fatty acid binding protein to phopsholipid membranes – evidence for a collisional process. (1992) J.Biol. Chem. **267**, 20051-20056

[28] Herr, F.M., Matarese, V., Bernlohr, D.A., and Storch, J. Surface lysine residues modulate the collisional transfer of fatty acids from adipocyte fatty acid binding protein to membranes. (1995) Biochemistry **34**, 11840-11845

[29] Gericke, A., Smith, E.R., Moore, D.J., Mendelsohn, R., and Storch, J. Adipocyte fatty acid binding protein: Interaction with phospholipid membranes and thermal stability studied by FTIR spectroscopy. (1997) Biochemistry **36**, 8311-8317

[30] Herr, F.M., Aronson, J., and Storch, J. Role of portal region lysine residues in electrostatic interactions between heart fatty acid binding protein and phopsholipid membranes. (1996) Biochemistry **35**, 1296-1303

[31] Spender, L., Storch, J., Davies, A., and Cook, R.M. Production of IL-4, IL-5 and IFN-gamma by human T-cells. (1994) Clin. Exper. Allergy **24**, 181-181

[32] Wootan, M.G., Bernlohr, D.A. and Storch, J. Mechanism of fluorescent fatty acid transfer from adipocyte fatty acid binding protein to membranes. (1993) Biochemistry **32**, 8622-8627

[33] Vancura, A., and Haldar, D. Regulation of mitochondrial and microsomal phospholipid synthesis by liver fatty acid binding protein. (1992) J. Biol. Chem. **267**, 14353-14359

[34] Khan, S.H., and Sorof, S. Liver fatty acid binding protein – specific mediator of the mitogenesis induced by 2 classes of carcinogenic peroxisome proliferators. (1994) Proc. Natl. Acad. Sci. **91**, 848-852

[35] Sorof, S. Motdulation of mitogenesis by liver fatty acid binding protein. (1994) Cancer Metastasis Reviews **13**, 317-336

[36] Gervois, P., Torra, I.P., Fruchart, J.C., and Staels, B. Regulation of lipid and lipoprotein metabolism by PPAR activators. (2000) Clin. Chem. Lab. Med. **38**, 3-11

[37] Wolfrum, C., Borchers, T., Sacchettini, J.C., and Spener, F. Binding of fatty acids and peroxisome proliferators to orthologous fatty acid binding proteins from human, murine and bovine liver. (2000) Biochemistry **39**, 1469-1474

[38] Pelton, P.D., Zhou, L.B., Demarest, K.T., and Burris, T.P. PPAR gamma activation induces the expression of the adipocyte fatty acid binding protein gene in human monocytes. (1999) Biochem. Biophys. Res. Comm. **261**, 456-458

[39] Kim, H.K., and Storch, J. Free fatty acid transfer from rat liver fatty acid binding protein to phopsholipid vesicles – effect of ligand and solution properties. (1992) J. Biol. Chem. **267**, 77-82

[40] Herr, F.M., Aronson, J., and Storch, J. Role of portal region lysine residues in electrostatic interactions between heart fatty acid binding protein and phopsholipid membranes. (1996) Biochemistry **35**, 1296-1303

[41] Corsico, B., Cistola, D.P., Frieden, C., and Storch, J. The helical domain of intestinal fatty acid binding protein is critical for collisional transfer of fatty acids to phospholipid membranes. (1998) Proc. Natl. Acad. Sci. **95**, 12174-12178

[42] Wolfrum, C., Borrman, C.M., Borchers, T., and Spener, F. Fatty acid and hypolipidemic drugs regulate peroxisome proliferator-activated receptors α- and γ-mediated gene expression via liver fatty acid binding protein: A signalling path to the nucleus. (2001) Proc. Natl. Acad. Sci. **98**, 2323-2328

[43] Shen, W.J., Sridhar, K., Bernlohr, D.A., and Kraemer, F.B. Interaction of rat hormone sensitive lipase with adipocyte lipid binding protein. (1999) Proc. Natl. Acad. Sci. – USA **96**, 5528-5532

[44] Watts, A. Protein conformational distortions induced by membrane interfacial interactions. (1997) Biochem. Soc. Trans. **25**, 1119-1124

[45] Kennedy, M.W., Garside, L.H., Goodrick, L.E., McDermott, L., Brass, A., Price, N.C., Kelly, S.M., Cooper, A., and Bradley, J.E. The OV20 protein of the parasitic nematode *Onchocerca volvulus*. (1997) J. Biol. Chem. **272**, 29442-29448

[46] Kennedy, M.W., Britton, C., Price, N.C., Kelly, S.M., and Cooper, A. The DvA-1 polyprotein of the parasitic nematode *Dictyocaulus viviparous.* (1995) J. Biol. Chem. **33**, 19277-19281

[47] Dalton, K.A., Pilot, J.D., Mall, S., East, J.M., and Lee, A.G. Anionic phospholipids decrease the rate of slippage on the Ca2+ATPase of sarcoplasmic reticulum. (1999) Biochem. J. **342**, 431-438

[48] Cornell, R.B. How cytidylyltransferase uses an amphipathic helix to sense membrane phospholipid composition. (1998) Biochem. Soc. Trans. **26**, 539-544

[49] Johnson, J.E., and Cornell, R.B. Membrane-binding amphipathic alpha-helical peptide derived from CTP: phospholcholine cytidylyltransferase (1994) Biochemistry **33**, 4327-4335

[50] Arnold, R.S., and Cornell, R.B. Lipid regulation of CTP: phospholcholine cytidylyltransferase: electrostatic, hydrophobic and synergistic interactions of anionic phospholipid and diacylglycerol. (1996) Biochemistry **35**, 9917-9924

[51] Clement, J.M., and Kent, C. CTP: phospholcholine cytidylyltransferase: insights into regulatory mechanisms and novel functions. (1999) Biochem. Biophys. Res. Comm. **257**, 643-650

[52] Arnold, R.S., DePaoliRoach, A.A., and Cornell, R.B. Binding of CTP: phospholcholine cytidylyltransferase to lipid vesicles: diacylglycerol and enzyme dephosphorylation increases the affinity for negatively charged membranes. (1997) Biochemistry **36**, 6149-6156

[53] Kitchen, J.L., Li, Z.Y., and Crooke, E. Electrostatic interactions during acidic phopsholipid reactivation of DnaA protein, the *Escherichia coli* initiator of chromosomal replication. (1999) Biochemistry **38**, 6213-6221

[54] Garner, J., Durrer, P., Kitchen, J., Brunner, J., and Crooke, E. Membrane-mediated release of nucleotides from initiator of chromosomal replication, *Escherichia coli* DnaA, occurs with insertion of a distinct region of the protein into the lipid bilayer. (1998) J. Biol. Chem. **273**, 5167-5173

[55] Yamaguchi, Y., Hase, M., Makise, M., Mima, S., Yoshimi, T., Ishikawa, Y., Tsuchiya, T., and Mizushima, T. Involvement of Arg-328, Arg-334, and Arg-342 of DnaA protein in the functional interaction with acidic phospholipids. (1999) Biochem. J. **340**, 433-438

[56] Cajal, Y., Svendsen, A., Girona, V., Patkar, S.A., and Alsina, M.A. Interfacial control of lid opening in *Thermomyces lanuginose* lipase. (2000) Biochemistry **39**, 413-423

[57] Wojtasek, H., and Leal, W.S. Conformational change in the pheromone-binding protein from Bombyx mori induced by pH and by interaction with membranes. (1999) J. Biol. Chem. **274**, 30950-30956

[58] Wang, S.X., Sun, Y.T., and Sui, S.F. Membrane-induced conformational changes in human apolipoprotein H. (2000) Biochem. J. **348**, 103-106

[59] Huang, H., Ball, J.M., Billheimer, J.T., and Schroeder, F. Interaction of the N-terminus of sterol carrier protein-2 with membranes: Role of membrane curvature. (1999) Biochem. J. **344**, 593-603

[60] Silvestro,L. and Axelsen, P.H. Fourier transform infrared linked analysis of conformational changes in annexin V upon membrane binding. (1999) Biochemistry **38**, 113-121

[61] Ahn, T., Guengerich, F.P., and Yun, C.H. Membrane insertion of cytochrome P450 1A2 promoted by anionic phospholipids. (1998) Biochemistry **37**, 12860-12866

[62] Oldenburg, K.R., Epand, R.F., D'Orfani, A., Vo, K., Selick, H., and Epand, R.M. Conformational studies on analogs of human recombinant parathyroid hormone and their interactions with phospholipids. (1996) J. Biol. Chem. **271**, 17582-17591

[63] SkorkoGlonek, J., Lipinska, B., Krzewski, K., Zolese, G., Bertoli, E., and Tanfani, F. HtrA heat shock protease interacts with phopsholipid membranes and undergoes conformational changes. (1997) J. Biol. Chem. **272**, 8974-8982

[64] Rilfors, L., Niemi, A., Haraldson, S., Edwards, K., Andersson, A-S., and Dowhan, W. Reconstituted phosphatidylserine synthase from *Escherichia coli* is activated by anionic phospholipids and micelle-forming amphiphiles. (1999) Biochim. Biophys. Acta. **1438**, 281-294

[65] Kunkel, T.A. Rapid and efficient site-specific mutagenesis without phenotypic selection. (1985) Proc. Natl. Acad. Sci. **82**, 488-492

[66] Kunkel, T.A., Roberts, J.D., and Zakour, R.A. Rapid and efficient site-specific mutagenesis without phenotypic selection. (1987) Methods in Enzymology **154**, 367-382

[67] Higuchi, R., Krummel, B., and Saiki, R.K. A general method of *in vitro* preparation and specific mutagenesis of DNA fragments: study of protein and DNA interactions. (1988) Nucleic Acids Res. **16**, 7351-7367

[68] Wilton, D.C. Studies on fatty acid binding proteins: The purification of rat liver fatty acid binding protein and the role of cysteine-69 in fatty acid binding. (1989) Biochem. J. **261**, 273-276

[69] Sheridan, M., and Wilton, D.C. Dansylaminodecyl agarose – A novel affinity column for rat liver fatty acid binding protein. (1988) Biochem. Soc. Trans. **16**, 719

[70] Laemmli, U.K. Cleavage of structural proteins during the assembly of the head of bacteriophage T4. (1970) Nature **227**, 680-685

[71] Smith, P.K., Krohn, R.I., Hermanson, G.T., Mallia, A.K., Gartner, F.H., Provenzano, M.D., Fujimoto, E.K., Goeke, N.M., Olson, B.J., and Klenk, D.C. Measurement of protein using bicinchoninic acid. (1985) Anal. Biochem. **150**, 76-85

[72] Perkins, S.J. Protein volumes and hydration effects. (1986) Eur. J. Biochem. **157**, 169-180

[73] Hogeboom, G.H. Fractionation of cell components of animal tissues: General method for the isolation of liver cell components. (1962) Methods in Enzymology **1**, 16-19

[74] Bustamante, E., Soper, J.W., and Pedersen, P.L. A high yield preparative method for the isolation of rat liver mitochondria. (1977) Anal. Biochem. **80**, 401-408

[75] Bartlett, G.R. Phosphorus assay in column chromatography. (1958) J. Biol. Chem. **234**, 466-468

[76] Kane, C.D., and Bernlohr, D.A. A simple assay for intracellular lipid binding proteins using displacement of 1-anilinonphthalene 8-sulfonic acid. (1996) Anal. Biochem. **233**, 197-204

[77] Lehrer, S.S. Solute perturbation of protein fluorescence. The quenching of the tryptophyl fluorescence of model compounds and of lysozyme by iodide ion. (1971) Biochemistry **10**, 3254-3263

[78] Kim, H.K., and Storch, J. Free fatty acid transfer from rat liver fatty acid binding protein to phopsholipid vesicles – effect of ligand and solution properties. (1992) J. Biol. Chem. **267**, 77-82

[79] Jain, M.K., and Berg, O.G. PLA2. (1989) Biochim. Biophys. Acta. **1002**, 127-156

[80] Denisov, G., Wanasaki, S., Luan, P., Glaser, M., and McLaughlin, S. Binding of basic peptides to membranes produces lateral domains enriched in the acidic lipids phosphatidyl serine and phosphatidylinositol 4,5-bisphosphate: An electrostatic model and experimental results. (1998) Biophys. J. **74**, 731-744

[81] BenTal, N., Honig, B., Miller, C., and McLaughlin, S. Electrostatic binding of proteins to membranes. Theoretical predictions and experimental results with charybdotoxin and phospholipid vesicles. (1997) Biophys. J. **73**, 1717, 1727

[82] Huang, H., Ball, J.M., Billheimer, J.T., and Schroeder, F. Interaction of the N-terminus of sterol carrier protein-2 with membranes: Role of membrane curvature. (1999) Biochem. J. **344**, 593-603

[83] Davies, J.K., Thumser, A.E.A., and Wilton, D.C. Binding of recombinant rat liver fatty acid binding protein to small anionic phospholipid vesicles results in ligand release: A model of interfacial binding and fatty acid targeting. (1999) Biochemistry **38**, 16932-16940

[84] Schroeder, F., Myers-Payne, S.C., Billheimer, J.T., and Wood, W.G. Probing the ligand binding sites of fatty acid and sterol carrier proteins: effects of ethanol. (1995) Biochemistry **34**, 11919-11927

[85] Wilkinson, T.C.I., and Wilton, D.C. Studies on fatty acid binding proteins: The detection and quantification of the protein from rat liver using a fluorescent fatty acid analogue. (1987) Biochem. J. **247**, 485-488

[86] Pinheiro, T.J.T., Elove, G.A., Watts, A., and Roder, H. Structural and kinetic description of cytochrome C unfolding induced by the interaction with lipid vesicles. (1997) Biochemistry **36**, 13122-13132

[87] Buckland, A.G., and Wilton, D.C. The antibacterial properties of secreted phospholipases A(2). (2000) Biochim. Biophys. Acta – Mol. Cell Biol. Lipids **1488**, 71-82

[88] Huang, H., Ball, J.M., Billheimer, J.T., and Schroeder, F. The sterol carrier protein-2 amino terminus: A membrane interaction domain. (1999) Biochemistry **38**, 13231-13243

[89] Snitko, Y., Koduri, R.S., Han, S.K., Othman, R., Baker, S.F., Molini, B.J., Wilton, D.C., Gelb, M.H., and Cho, W.H. Mapping the interfacial binding surface of human secretory group IIa phospholipase A2. (1997) Biochemistry **36**, 14325-14333

[90] Wilton, D.C. A continuous fluorescent displacement assay for the measurement of phospholipase A2 and other lipases that release long chain fatty acids. (1990) Biochem. J. **266**, 435-439

[91] Thumser, A.E., Evans, C., Worrall, A.F., and Wilton, D.C. Effect on ligand binding of arginine mutations in recombinant rat liver fatty acid-binding protein. (1994) Biochem. J. **297**, 103-107

[92] Thumser, A.E.A., Voysey, J., and Wilton, D.C. Mutations of recombinant rat liver fatty acid binding protein at residues 102 and 122 alter its structural integrity and affinity for physiological ligands. (1996) Biochem. J. **314**, 943-949

[93] Thumser, A.E.A, Voysey, J.E., and Wilton, D.C. The binding of lysophospholipids to rat liver fatty acid binding protein and albumin. (1994) Biochem. J. **301**, 801-806

[94] Kramer, W., Sauber, K., Baringhaus, K.H., Kurz, M., Stengelin, S., Lange, O., Corsiero, D., Girbig, F., Konig, W., and Weyland, C. Identification of the bile acid binding site of the ileal lipid binding protein (ILBP) by photoaffinity labelling, MALDI mass sprectrometry and NMR structure. (2001) J. Biol. Chem. **276**, 7291-7301

[95] Smith, E.R., and Storch, J. The adipocyte fatty acid binding protein binds to membranes by electrostatic interactions. (1999) J. Biol. Chem. **274**, 35325-35330

[96] Jain, M.K., and Vaz, W.L. Dehydration of the lipid-protein microinterface on binding of phospholipase A2 to lipid bilayers. (1987) Biochim. Biophys. Acta **905**, 1-8

[97] Bayburt, T., Yu, B.Z., Lin, H.K., Browning, J., Jain, M.K., and Gelb, M.H. Human nonpancreatic secreted phospholipase A2: interfacial parameters, substrate specificities and competitive inhibitors. (1993) Biochemistry **32**, 573-582

[98] Othman, R., Baker, S.F., Li, Y., Worrall, A.F., and Wilton, D.C. Human non-pancreatic (group II) secreted phospholipase A2 expressed from a synthetic gene in *Escherichia coli*: characterisation of N-terminal mutants. (1996) Biochim. Biophys. Acta – Lipids and Lipid Metabolism **1303**, 92-102

[99] Kennedy, M.W., Scott, J.C., Lo, S., Beauchamp, J., and McManus, D.P. Sj-FABPc fatty acid binding protein of the human blood fluke *Schistosoma japonicum*: structural and functional characterisation and unusual solvent exposure of a portal-proxmial tryptophan residue. (2000) Biochem. J. **349**, 377-384

[100] Thumser, A.E.A., and Wilton, D.C. Characterisation of binding and structural properties of rat liver fatty acid binding protein using tryptophan mutants. (1994) Biochem. J. **300**, 827-833

[101] Selvin, P.R. Fluorescence Resonance Energy-Transfer (1995) Methods Enzymol. **246**, 300-334

[102] Eftink, M.R., and Ghiron, C.A. Does the fluorescence quencher acrylamide bind to proteins? (1987) Biochim. Biophys. Acta. **916**, 343-349

[103] Woolf, T.B., and Tychko, M. The third leg: Molecular dynamics stimulations of lipid binding proteins. (1999) Mol. Cell. Biochem. **192**, 9305-9311

[104] Rypniewski, W.R., Holden, H.M., and Rayment, I. Structural consequences of reductive methylation of lysine residues in hen egg-white lysozyme – an x-ray analysis at 1.8-Angstrom resolution. (1993) Biochemistry **32**, 9851-9858